TABLE 2.10.1-1A (CONTINUED)

INDIVIDUAL LOAD CASES FOR TN-FSV CASK BODY ANALYSIS

LOAD CASE NUMBER	INDIVIDUAL LOAD DESCRIPTION	STRESS RESULT TABLES
15	30 FT 15° SLAP DOWN	2.10.1-15A (CONTACT SIDE) 2.10.1-15B (OPP. CONTACT SIDE)
16	30 FT 45° DROP	2.10.1-16A (CONTACT SIDE) 2.10.1-16B (OPP. CONTACT SIDE)
17	30 FT 70° DROP	2.10.1-17A, 17C (CONTACT SIDE) 2.10.1-17B, 17D (OPP. CONTACT SIDE)
18	THERMAL ACCIDENT (t = 0.53 hrs.)	2.10.1-18
18A	THERMAL ACCIDENT (t = 1.0 hrs.)	2.10.1-18A

TABLE 2.10.1-1B

CONSTRAINT REACTIONS

LOAD CASE	REACTION FORCE (LBS)	
	NODE #1	NODE #552
SIDE DROP	F_x = 1734	F_x = 4973 F_y = 0
15° SLAP DOWN	F_x = 389	F_x = 1932 F_y = 792
45° DROP	F_x = -642	F_x = 1514 F_y = 693
70° DROP	F_x = -736	F_x = 933 F_y = 1017
C.G. OVER CORNER DROP	F_x = -1354	F_x = -572 F_y = 1241
90° BOTTOM DROP	F_x = 0	F_x = -212 F_y = 1023
90° LID END DROP	F_x = 0 F_y = 188	F_x = 13

TABLE 2.10.1-1

CASK BODY STRESSES UNDER BOLT PRELOAD

LOCATION		MEMBRANE STRESSES (PSI)		BENDING STRESSES (PSI)	
		MERIDIONAL SM	HOOP SH	MERIDIONAL SBM	HOOP SBH
C O N T A I N M E N T	1	-1	-1	-60	-60
	2	-1	-1	196	29
	3	-8	-4	17	5
	4	-8	0	0	0
	5	-8	0	0	0
	6	-8	0	0	0
	7	-8	0	0	0
	8	-8	0	0	0
	9	-9	0	0	0
NON-C O N T A I N M E N T	10	-6	-1	1	1
	11	-6	0	0	0
	12	-6	0	0	0
	13	-6	0	0	0
	14	-6	0	0	0
	15	-6	0	0	0
	16	-6	0	0	0
	17	-8	6	-20	-6

TABLE 2.10.1-2

CASK BODY STRESSES UNDER HOT ENVIRONMENT CONDITION

LOCATION		MEMBRANE STRESSES (PSI)		BENDING STRESSES (PSI)	
		MERIDIONAL SM	HOOP SH	MERIDIONAL SBM	HOOP SBH
C	1	-18	-18	-60	-60
O	2	-18	-18	7	-37
N	3	36	16	-44	-13
T	4	37	0	0	0
A	5	37	0	0	0
I	6	37	0	0	0
N	7	37	0	0	0
M	8	37	0	0	0
E	9	37	0	-11	-3
N					
T					
NON-					
C	10	132	203	56	17
O	11	130	334	-1	-1
N	12	130	334	0	0
T	13	130	334	0	0
A	14	130	334	0	0
I	15	130	334	0	0
N	16	130	341	1	1
M	17	72	23	190	57
E					
N					
T					

TABLE 2.10.1-3

CASK BODY STRESSES UNDER -20°F UNIFORM TEMPERATURE

LOCATION		MEMBRANE STRESSES (PSI)		BENDING STRESSES (PSI)	
		MERIDIONAL SM	HOOP SH	MERIDIONAL SBM	HOOP SBH
C O N T A I N M E N T	1	19	19	52	52
	2	19	19	-9	31
	3	-11	-35	19	6
	4	-11	-51	0	0
	5	-11	-50	0	0
	6	-11	-50	0	0
	7	-11	-51	0	0
	8	-11	-51	0	0
	9	-13	-12	-31	-9
NON-C O N T A I N M E N T	10	5	8	1	1
	11	5	0	0	0
	12	5	0	0	0
	13	5	0	0	0
	14	5	0	0	0
	15	5	0	0	0
	16	5	0	0	0
	17	6	-3	10	3

TABLE 2.10.1-4

CASK BODY STRESSES UNDER -40°F UNIFORM TEMPERATURE

LOCATION		MEMBRANE STRESSES (PSI)		BENDING STRESSES (PSI)	
		MERIDIONAL SM	HOOP SH	MERIDIONAL SBM	HOOP SBH
CONTAINMENT	1	23	23	63	63
	2	23	23	-11	38
	3	-14	-43	23	7
	4	-14	-62	0	0
	5	-14	-62	0	0
	6	-14	-62	0	0
	7	-14	-62	0	0
	8	-14	-62	0	0
	9	-16	-15	-38	-11
NON-CONTAINMENT	10	6	10	2	1
	11	6	0	0	0
	12	6	0	0	0
	13	6	0	0	0
	14	6	0	0	0
	15	6	0	0	0
	16	6	0	0	0
	17	7	-3	13	4

TABLE 2.10.1-5

CASK BODY STRESSES UNDER 30 PSIG INTERNAL PRESSURE

LOCATION		MEMBRANE STRESSES (PSI)		BENDING STRESSES (PSI)	
		MERIDIONAL SM	HOOP SH	MERIDIONAL SBM	HOOP SBH
CONTAINMENT	1	47	47	-349	-354
	2	47	47	230	27
	3	102	214	-100	-26
	4	104	233	6	6
	5	104	233	6	6
	6	104	233	6	6
	7	104	233	6	6
	8	104	233	6	6
	9	117	-26	259	82
NON-CONTAINMENT					
	10	36	-2	2	1
	11	36	5	0	0
	12	36	5	0	0
	13	36	5	0	0
	14	36	5	0	0
	15	36	5	0	0
	16	36	5	1	1
	17	45	-21	96	29

TABLE 2.10.1-6

CASK BODY STRESSES UNDER 14.7 PSI EXTERNAL PRESSURE

LOCATION		MEMBRANE STRESSES (PSI)		BENDING STRESSES (PSI)	
		MERIDIONAL SM	HOOP SH	MERIDIONAL SBM	HOOP SBH
	1	-39	-39	168	170
O	2	-39	-39	-113	-16
N	3	-27	-15	27	8
T	4	-28	-5	0	0
A	5	-28	-5	0	0
I	6	-28	-5	0	0
N	7	-28	-5	0	0
M	8	-28	-5	0	0
E	9	-30	9	-50	-15
N					
T					
NON-					
C	10	-59	-85	-24	-7
O	11	-58	-125	0	0
N	12	-58	-125	0	0
T	13	-58	-125	0	0
A	14	-58	-125	0	0
I	15	-58	-125	0	0
N	16	-58	-127	-1	0
M	17	-72	-17	-127	-40
E					
N					
T					

TABLE 2.10.1-7

CASK BODY STRESSES UNDER 1 G VERTICAL LOAD

LOCATION		MEMBRANE STRESSES (PSI)		BENDING STRESSES (PSI)	
		MERIDIONAL SM	HOOP SH	MERIDIONAL SBM	HOOP SBH
CONTAINMENT	1	9	4	-3	-6
	2	-2	27	9	-6
	3	-51	-19	57	15
	4	51	-3	-14	-28
	5	158	8	-22	-36
	6	234	12	-27	-39
	7	182	10	-22	-36
	8	52	-3	-8	-26
	9	-44	-2	17	6
NON-CONTAINMENT					
	10	-30	27	-8	-3
	11	91	42	-10	-13
	12	257	26	-22	-20
	13	346	22	-28	-23
	14	288	24	-25	-22
	15	101	40	-16	-15
	16	-101	121	83	20
	17	5	33	-22	-6

TABLE 2.10.1-8

CASK BODY STRESSES UNDER VIBRATION LOAD

LOCATION		MEMBRANE STRESSES (PSI)		BENDING STRESSES (PSI)	
		MERIDIONAL SM	HOOP SH	MERIDIONAL SBM	HOOP SBH
CONTAINMENT	1	9	5	-71	-74
	2	1	21	47	-1
	3	-6	3	3	-1
	4	65	22	-12	-20
	5	139	46	-17	-25
	6	194	73	-21	-27
	7	161	92	-17	-25
	8	77	105	-8	-18
	9	19	43	71	22
NON-CONTAINMENT	10	-12	15	-9	-3
	11	71	7	-6	-9
	12	185	-18	-14	-13
	13	247	-42	-18	-15
	14	211	-60	-16	-14
	15	88	-67	-10	-10
	16	-45	-11	65	17
	17	-80	10	-184	-55

TABLE 2.10.1-9
CASK BODY STRESSES UNDER SHOCK LOAD

LOCATION		MEMBRANE STRESSES (PSI)		BENDING STRESSES (PSI)	
		MERIDIONAL SM	HOOP SH	MERIDIONAL SBM	HOOP SBH
C	1	56	36	-543	-558
O	2	14	130	349	7
N	3	20	51	-48	-24
T	4	436	172	-73	-114
A	5	865	340	-105	-144
I	6	1184	547	-123	-155
N	7	1003	696	-105	-145
M	8	522	806	-52	-107
E	9	205	330	523	160
N					
T					
NON-					
C	10	-57	79	-60	-19
O	11	426	-1	-31	-48
N	12	1083	-174	-78	-77
T	13	1448	-354	-99	-88
A	14	1247	-488	-87	-81
I	15	545	-565	-53	-54
N	16	-217	-239	395	101
M	17	-618	36	-1379	-412
E					
N					
T					

TABLE 2.10.1-10

CASK BODY STRESSES UNDER TIE DOWN LOAD

LOCATION		MEMBRANE STRESSES (PSI)		BENDING STRESSES (PSI)	
		MERIDIONAL SM	HOOP SH	MERIDIONAL SBM	HOOP SBH
CONTAINMENT	1	141	114	-2320	-2364
	2	87	260	1413	96
	3	668	440	-858	-271
	4	1318	783	-164	-178
	5	1966	1393	-208	-219
	6	2485	2243	-234	-235
	7	2292	2920	-208	-222
	8	1682	3540	-135	-169
	9	1395	1461	2085	629
NON-CONTAINMENT	10	87	37	-173	-53
	11	815	-477	-17	-60
	12	1782	-1048	-82	-99
	13	2365	-1794	-112	-115
	14	2144	-2393	-95	-105
	15	1244	-2911	-50	-68
	16	199	-2415	778	209
	17	-2742	-213	-5747	-1721

TABLE 2.10.1-11

CASK BODY STRESSES UNDER 30 FOOT BOTTOM END DROP - 54G

LOCATION		MEMBRANE STRESSES (PSI)		BENDING STRESSES (PSI)	
		MERIDIONAL SM	HOOP SH	MERIDIONAL SBM	HOOP SBH
C O N T A I N M E N T	1	362	362	2741	2782
	2	362	362	-2279	-502
	3	-5716	-3193	5969	1791
	4	-6258	-4351	490	147
	5	-6645	-7330	490	147
	6	-7225	-11799	490	147
	7	-7709	-15522	490	147
	8	-8193	-19246	490	147
	9	-10148	210	-25815	-7744
NON-C O N T A I N M E N T	10	803	456	672	202
	11	388	3857	-213	-64
	12	1	6478	-213	-64
	13	-579	10410	-213	-64
	14	-1063	13687	-213	-64
	15	-1547	16963	-213	-64
	16	-1838	18938	-237	-71
	17	-1999	3600	15299	4590

TABLE 2.10.1-11A

CASK BODY STRESSES UNDER 30 FOOT BOTTOM END DROP - 54G

ADDITIONAL REPORTING LOCATIONS

LOCATION		STRESS COMPONENTS (PSI)				STRESS INTENSITY
		SX	SY	SZ	SXY	SI(PSI)
CONTAINMENT	18	-1213	-1566	-535	646	1524
	19	-1292	-5382	-1678	753	4359
	20	-2213	-8011	-1554	1272	6723
	21	-1107	-470	984	510	2374

LOCATION		MEMBRANE STRESSES (PSI)		BENDING STRESSES (PSI)	
		MERIDIONAL	HOOP	MERIDIONAL	HOOP
CONTAINMENT	22	-5801	-2886	1993	598
	23	-5903	-1225	-529	-159
	24	-8256	-21256	1927	578
	25	-8499	-23040	3262	978
NON-CONTAINMENT	26	767	1184	-364	-109
	27	678	1899	-234	-70
	28	-1943	19355	-571	-171
	29	-2216	18852	-5963	-1789

TABLE 2.10.1-12

CASK BODY STRESSES UNDER 30 FOOT LID END DROP - 54G

LOCATION		MEMBRANE STRESSES (PSI)		BENDING STRESSES (PSI)	
		MERIDIONAL SM	HOOP SH	MERIDIONAL SBM	HOOP SBH
C	1	-1324	-1324	27265	27660
O	2	-1292	-1200	-14683	294
N	3	-8168	-31071	24931	7479
T	4	-8234	-19450	-481	-144
A	5	-7847	-16470	-490	-147
I	6	-7267	-12001	-490	-147
N	7	-6783	-8277	-490	-147
M	8	-6300	-4554	-490	-147
E	9	-5597	-2234	1767	530
N					
T					
NON-					
C	10	-1844	19095	5067	1520
O	11	-1596	17071	212	64
N	12	-1209	14449	213	64
T	13	-629	10517	213	64
A	14	-145	7241	213	64
I	15	339	3964	213	64
N	16	629	2001	213	64
M	17	1128	-140	2182	655
E					
N					
T					

TABLE 2.10.1-12A

CASK BODY STRESSES UNDER 30 FOOT LID END DROP - 54G

ADDITIONAL REPORTING LOCATIONS

LOCATION		STRESS COMPONENTS (PSI)				STRESS INTENSITY
		SX	SY	SZ	SXY	SI(PSI)
CONTAINMENT	18	-11251	-40706	-1564	-3873	52532
	19	18681	10302	16389	-3282	10644
	20	3247	3467	-10982	-2429	16770
	21	995	-18697	-16343	-1621	19957

LOCATION		MEMBRANE STRESSES (PSI)		BENDING STRESSES (PSI)	
		MERIDIONAL	HOOP	MERIDIONAL	HOOP
CONTAINMENT	22	-8140	-29128	26215	7865
	23	-8404	-21817	682	205
	24	-5909	-1537	-391	-117
	25	-5830	-717	-856	-257
NON-CONTAINMENT	26	-2080	19304	-1817	-545
	27	-1880	19192	118	36
	28	724	1319	153	46
	29	823	420	57	17

TABLE 2.10.1-13A

CASK BODY STRESSES UNDER 30 FOOT SIDE DROP

(71 G) - CONTACT SIDE

LOCATION		MEMBRANE STRESSES (PSI)		BENDING STRESSES (PSI)	
		MERIDIONAL SM	HOOP SH	MERIDIONAL SBM	HOOP SBH
C	1	-5444	-10	-718	-1676
O	2	-8121	-7142	3708	-162
N	3	754	1871	-3694	677
T	4	19978	799	-1657	-1256
A	5	28920	785	-2531	-2479
I	6	33763	727	-2965	-3042
N	7	30305	744	-2633	-2579
M	8	19876	759	-1508	-987
E	9	-942	-7390	9910	3522
N					
T					
NON-					
C	10	5538	-3937	-2657	536
O	11	30100	1913	-2013	-561
N	12	41625	1726	-2931	-1615
T	13	47748	1678	-3376	-2080
A	14	43158	1675	-3037	-1710
I	15	29481	1740	-1933	-420
N	16	16388	2504	-469	823
M	17	984	-10930	-2090	-893
E					
N					
T					

TABLE 2.10.1-13B
CASK BODY STRESSES UNDER 30 FOOT SIDE DROP
(71 G) - SIDE OPPOSITE CONTACT

LOCATION		MEMBRANE STRESSES (PSI)		BENDING STRESSES (PSI)	
		MERIDIONAL SM	HOOP SH	MERIDIONAL SBM	HOOP SBH
C	1	-7327	1322	-444	-1519
O	2	-4650	2954	-9624	-4278
N	3	-623	255	2848	2622
T	4	-19147	-219	1063	-457
A	5	-28210	-237	1332	-1338
I	6	-33133	-201	1518	-1715
N	7	-29587	-193	1407	-1384
M	8	-19350	-126	1166	-202
E	9	442	4151	-4961	-958
N					
T					
NON-					
C	10	-9534	-425	-333	1234
O	11	-30235	-1718	1939	625
N	12	-41358	-1713	2322	-38
T	13	-47617	-1734	2599	-288
A	14	-42904	-1679	2389	-82
I	15	-29711	-1523	1937	741
N	16	-18428	-1485	1574	1436
M	17	-4451	4414	-14083	-3722
E					
N					
T					

TABLE 2.10.1-13C

CASK BODY STRESSES UNDER 30 FOOT SIDE DROP - CONTACT SIDE

ADDITIONAL REPORTING LOCATIONS

LOCATION		STRESS COMPONENTS (PSI)				STRESS INTENSITY
		SX	SY	SZ	SXY	SI(PSI)
CONTAINMENT	18	-6891	19389	-8790	1103	28225
	19	-9052	-17025	-21876	2444	13514
	20	-3136	-4312	-8937	1862	7165
	21	-2518	273	-9414	1454	10307

LOCATION		MEMBRANE STRESSES (PSI)		BENDING STRESSES (PSI)	
		MERIDIONAL	HOOP	MERIDIONAL	HOOP
CONTAINMENT	22	1957	2099	-805	1449
	23	6378	940	596	1220
	24	6508	533	169	704
	25	2253	29	-624	566
NON-CONTAINMENT	26	11412	2305	-3545	15
	27	16906	2273	-490	706
	28	10795	2054	-6101	-613
	29	5113	-18961	1458	2110

TABLE 2.10.1-13D

CASK BODY STRESSES UNDER 30 FOOT SIDE DROP - SIDE OPPOSITE CONTACT

ADDITIONAL REPORTING LOCATIONS

LOCATION		STRESS COMPONENTS (PSI)				STRESS INTENSITY
		SX	SY	SZ	SXY	SI(PSI)
CONTAINMENT	18	2208	-4346	6540	-474	10920
	19	1305	5035	7151	-1721	6519
	20	1985	3442	4391	-894	2831
	21	1212	-1442	-87	-468	2796

LOCATION		MEMBRANE STRESSES (PSI)		BENDING STRESSES (PSI)	
		MERIDIONAL	HOOP	MERIDIONAL	HOOP
CONTAINMENT	22	-1640	-160	1724	2190
	23	-5596	-96	449	1158
	24	-6807	-7	773	868
	25	-2742	224	1033	1046
NON-CONTAINMENT	26	-14127	-1458	2660	1876
	27	-18616	-1768	1710	1366
	28	-14202	-1689	1969	1808
	29	-9149	444	5221	3238

TABLE 2.10.1-14A

CASK BODY STRESSES UNDER 30 FOOT C.G. OVER CORNER DROP

CONTACT SIDE

LOCATION		MEMBRANE STRESSES (PSI)		BENDING STRESSES (PSI)	
		MERIDIONAL SM	HOOP SH	MERIDIONAL SBM	HOOP SBH
C	1	-3368	-962	26622	26987
O	2	-2578	-1957	-14963	73
N	3	-7617	-30294	24573	8611
T	4	-6607	-19264	316	2654
A	5	-5651	-16332	1	1881
I	6	-5327	-11961	-676	-349
N	7	-5522	-8314	-1202	-2202
M	8	-5573	-4663	-1487	-3143
E	9	-5802	-2889	3168	819
N					
T					
NON-					
C	10	-1535	18742	4866	2286
O	11	494	17365	717	1913
N	12	1652	14690	477	1402
T	13	2106	10610	20	-71
A	14	1903	7208	-330	-1290
I	15	1727	3880	-525	-1852
N	16	1536	1956	-387	-1405
M	17	1175	-565	3803	1036
E					
N					
T					

TABLE 2.10.1-14B

CASK BODY STRESSES UNDER 30 FOOT C.G. OVER CORNER DROP

SIDE OPPOSITE CONTACT

LOCATION		MEMBRANE STRESSES (PSI)		BENDING STRESSES (PSI)	
		MERIDIONAL SM	HOOP SH	MERIDIONAL SBM	HOOP SBH
CONTAINMENT	1	-1394	-901	26671	27015
	2	-2011	-1020	-15647	-67
	3	-7484	-30624	25060	8756
	4	-10381	-19522	579	2731
	5	-10210	-16482	308	1972
	6	-9109	-12015	-426	-275
	7	-7750	-8298	-1064	-2161
	8	-6216	-4521	-1478	-3142
	9	-6221	-2942	3797	1007
NON-CONTAINMENT	10	-3145	18878	5228	2395
	11	-4679	16822	1075	2020
	12	-4499	14278	876	1521
	13	-3290	10418	348	28
	14	-1707	7204	-126	-1229
	15	81	4031	-449	-1829
	16	866	2176	-376	-1401
	17	1299	-270	3828	1050

TABLE 2.10.1-14C

CASK BODY STRESSES UNDER 30 FOOT C.G. OVER CORNER DROP-CONTACT SIDE

ADDITIONAL REPORTING LOCATIONS

LOCATION		STRESS COMPONENTS (PSI)				STRESS INTENSITY
		SX	SY	SZ	SXY	SI(PSI)
CONTAINMENT	18	10821	-39183	-1781	-3882	50604
	19	17982	9161	14710	-3216	10916
	20	3412	3916	-11381	-2471	17529
	21	944	-18967	-18240	-1526	20143

LOCATION		MEMBRANE STRESSES (PSI)		BENDING STRESSES (PSI)	
		MERIDIONAL	HOOP	MERIDIONAL	HOOP
CONTAINMENT	22	-7520	-28590	26638	9357
	23	-7675	-21679	1373	2206
	24	-5537	-1573	-1026	-1886
	25	-5788	-716	-1283	-1274
NON-CONTAINMENT	26	-1380	19615	-1623	679
	27	-800	19490	693	1632
	28	1391	1301	-371	-1107
	29	1151	209	-452	-703

TABLE 2.10.1-14D

CASK BODY STRESSES UNDER 30 FOOT C.G. OVER CORNER DROP

SIDE OPPOSITE CONTACT

ADDITIONAL REPORTING LOCATIONS

LOCATION		STRESS COMPONENTS (PSI)				STRESS INTENSITY
		SX	SY	SZ	SXY	SI(PSI)
CONTAINMENT	18	11912	-41719	-347	-4098	54254
	19	19304	12042	17768	-3701	10370
	20	4127	5281	-10050	-2862	17673
	21	1410	-19079	-17521	-1796	20801

LOCATION		MEMBRANE STRESSES (PSI)		BENDING STRESSES (PSI)	
		MERIDIONAL	HOOP	MERIDIONAL	HOOP
CONTAINMENT	22	-7663	-29007	27102	9495
	23	-8863	-22091	1492	2241
	24	-5698	-1310	-1076	-1902
	25	-6058	-420	-1377	-1303
NON-CONTAINMENT	26	-3938	18929	-916	891
	27	-4197	18822	902	1695
	28	987	1558	-328	-1094
	29	981	698	-527	-725

TABLE 2.10.1-15A

CASK BODY STRESSES UNDER 30 FOOT 15° SLAP DOWN

CONTACT SIDE

LOCATION		MEMBRANE STRESSES (PSI)		BENDING STRESSES (PSI)	
		MERIDIONAL SM	HOOP SH	MERIDIONAL SBM	HOOP SBH
C O N T A I N M E N T	1	-7204	268	-722	-1822
	2	-9229	-7059	116	-1668
	3	-1313	2673	-1957	1343
	4	19444	1761	-1780	-1597
	5	22629	803	-2066	-2171
	6	18151	326	-1796	-1750
	7	10086	-33	-842	-881
	8	2239	-776	-95	-408
	9	2732	446	-3609	-1057
NON-C O N T A I N M E N T	10	6158	-2976	-3272	499
	11	25528	2912	-1853	-544
	12	30194	2134	-2229	-1315
	13	25764	947	-1766	-1143
	14	16706	-48	-1029	-646
	15	7327	-830	-366	-262
	16	2901	-1147	-51	-55
	17	-676	-1514	504	180

TABLE 2.10.1-15B

CASK BODY STRESSES UNDER 30 FOOT 15° SLAP DOWN

SIDE OPPOSITE CONTACT

LOCATION		MEMBRANE STRESSES (PSI)		BENDING STRESSES (PSI)	
		MERIDIONAL SM	HOOP SH	MERIDIONAL SBM	HOOP SBH
CONTAINMENT	1	-7334	1219	-490	-1687
	2	-5311	2311	-6955	-3437
	3	874	-671	1596	2383
	4	-18606	-1129	875	-825
	5	-22287	-575	973	-1274
	6	-17955	-180	796	-987
	7	-10011	86	444	-500
	8	-2114	808	-132	-415
	9	-2898	-944	4952	-1520
NON-CONTAINMENT	10	-10438	-1824	-97	1451
	11	-25294	-2465	1686	517
	12	-29645	-1951	1656	-149
	13	-25688	-863	1346	-210
	14	-16820	103	829	-89
	15	-7380	882	261	-74
	16	-3017	1268	31	-31
	17	457	965	-1475	-473

TABLE 2.10.1-16A

CASK BODY STRESSES UNDER 30 FOOT 45° IMPACT ON LID END

CONTACT SIDE

LOCATION		MEMBRANE STRESSES (PSI)		BENDING STRESSES (PSI)	
		MERIDIONAL SM	HOOP SH	MERIDIONAL SBM	HOOP SBH
C	1	-4671	-522	16744	17087
O	2	-5554	-5507	-11084	225
N	3	-8257	-14941	16804	6541
T	4	3033	-8476	-757	-208
A	5	5430	-7502	-1045	-815
I	6	4237	-5610	-1021	-864
N	7	1105	-4003	-612	-502
M	8	-2040	-2577	-243	-217
E	9	-1368	-857	-836	-235
N					
T					
NON-					
C	10	-2420	7875	892	1251
O	11	8233	9593	-466	232
N	12	11423	7967	-778	-373
T	13	10546	5525	-662	-478
A	14	7134	3497	-355	-275
I	15	3374	1566	-56	-76
N	16	1570	467	88	26
M	17	234	-768	1285	402
E					
N					
T					

TABLE 2.10.1-16B

CASK BODY STRESSES UNDER 30 FOOT 45° IMPACT ON LID END

SIDE OPPOSITE CONTACT

LOCATION		MEMBRANE STRESSES (PSI)		BENDING STRESSES (PSI)	
		MERIDIONAL SM	HOOP SH	MERIDIONAL SBM	HOOP SBH
CONTAINMENT	1	-3594	-62	-6325	11233
	2	-2890	1205	-7518	-1548
	3	-672	-13695	9052	4205
	4	-10579	-9922	220	74
	5	-12730	-8213	191	-451
	6	-11071	-5858	83	-540
	7	-7546	-3928	-65	-340
	8	-3951	-1818	-295	-231
	9	-4012	-1511	3067	939
NON-CONTAINMENT	10	-2913	8209	2589	1760
	11	-9898	7101	864	631
	12	-12250	6039	797	100
	13	-11030	4625	659	-82
	14	-7282	3490	453	33
	15	-3072	2268	225	8
	16	-1037	1509	131	39
	17	742	349	- 326	85

TABLE 2.10.1-17A

CASK BODY STRESSES UNDER 30 FOOT 70° IMPACT ON LID END

CONTACT SIDE

LOCATION		MEMBRANE STRESSES (PSI)		BENDING STRESSES (PSI)	
		MERIDIONAL SM	HOOP SH	MERIDIONAL SBM	HOOP SBH
C	1	-2762	-1071	28792	30081
O	2	-3334	-4718	-18796	1479
N	3	-13177	-27040	29774	10175
T	4	-7445	-15467	-169	562
A	5	-5498	-13228	-453	-55
I	6	-4610	-9703	-580	-379
N	7	-4725	-6729	-502	-316
M	8	-4981	-3816	-395	-183
E	9	-4060	-1753	964	296
N					
T					
NON-					
C	10	-8054	15276	3654	1778
O	11	-2632	14352	395	692
N	12	-285	12105	119	178
T	13	1083	8743	22	-92
A	14	1170	5948	66	-66
I	15	910	3185	134	10
N	16	752	1542	172	53
M	17	820	-319	1882	571
E					
N					
T					

TABLE 2.10.1-17B

CASK BODY STRESSES UNDER 30 FOOT 70° IMPACT ON LID END

SIDE OPPOSITE CONTACT

LOCATION		MEMBRANE STRESSES (PSI)		BENDING STRESSES (PSI)	
		MERIDIONAL SM	HOOP SH	MERIDIONAL SBM	HOOP SBH
C	1	-1718	-895	10993	20079
O	2	-1449	552	-8168	-384
N	3	1692	-22755	14246	5513
T	4	-5820	-16059	-236	538
A	5	-7068	-13525	-334	-22
I	6	-7068	-9802	-391	-324
N	7	-6213	-6724	-408	-289
M	8	-5199	-3603	-432	-194
E	9	-4973	-2024	2191	665
N					
T					
NON-					
C	10	1853	15092	4438	2013
O	11	-295	13629	349	678
N	12	-1449	11493	259	221
T	13	-1492	8391	233	-29
A	14	-1338	5845	219	-20
I	15	-331	3274	196	29
N	16	269	1733	187	58
M	17	1013	-54	1589	472
E					
N					
T					

TABLE 2.10.1-17C

CASK BODY STRESSES UNDER 70° IMPACT LID END - CONTACT SIDE

ADDITIONAL REPORTING LOCATIONS

LOCATION		STRESS COMPONENTS (PSI)				STRESS INTENSITY
		SX	SY	SZ	SXY	SI(PSI)
CONTAINMENT	18	8879	-40597	-1142	-2621	49752
	19	13763	3462	13600	-2787	11713
	20	345	-7472	-9102	-836	9535
	21	-245	-16194	-11195	-771	16023

LOCATION		MEMBRANE STRESSES (PSI)		BENDING STRESSES (PSI)	
		MERIDIONAL	HOOP	MERIDIONAL	HOOP
CONTAINMENT	22	-12981	-25525	-24637	8708
	23	-11704	-17058	-227	1186
	24	-4667	-1442	-289	-89
	25	-4434	-797	-632	-184
NON-CONTAINMENT	26	-6890	16360	-1044	490
	27	-5562	16161	761	1060
	28	713	962	135	50
	29	686	161	74	43

TABLE 2.10.1-17D

CASK BODY STRESSES UNDER 70° IMPACT LID END-SIDE OPPOSITE CONTACT

ADDITIONAL REPORTING LOCATIONS

LOCATION		STRESS COMPONENTS (PSI)				STRESS INTENSITY
		SX	SY	SZ	SXY	SI(PSI)
CONTAINMENT	18	9053	-27262	-1126	-3614	37027
	19	15488	10191	11913	-2609	7435
	20	4590	10456	-8924	-2919	20584
	21	1570	-15505	-17112	-1520	18816

LOCATION		MEMBRANE STRESSES (PSI)		BENDING STRESSES (PSI)	
		MERIDIONAL	HOOP	MERIDIONAL	HOOP
CONTAINMENT	22	-1723	-21571	20422	7440
	23	-2811	-18140	2049	1866
	24	-4884	-1054	-338	-104
	25	-4991	-369	-780	-228
NON-CONTAINMENT	26	1143	15412	-1230	434
	27	825	15346	393	950
	28	444	1193	48	24
	29	625	227	93	49

TABLE 2.10.1-18

CASK BODY STRESSES UNDER THERMAL ACCIDENT (t = 0.53 HRS.)

LOCATION		MEMBRANE STRESSES (PSI)		BENDING STRESSES (PSI)	
		MERIDIONAL SM	HOOP SH	MERIDIONAL SBM	HOOP SBH
C	1	-2228	-2228	1521	1521
O	2	-2228	-2228	-393	857
N	3	8624	3380	-5139	-1542
T	4	8729	0	0	0
A	5	8729	0	0	0
I	6	8729	0	0	0
N	7	8729	0	0	0
M	8	8729	0	0	0
E	9	8668	8384	214	64
N					
T					
NON-					
C	10	-3521	270	-1057	-317
O	11	-3493	544	1	0
N	12	-3493	544	0	0
T	13	-3493	544	0	0
A	14	-3493	544	0	0
I	15	-3493	544	0	0
N	16	-3492	553	31	9
M	17	-4195	-3379	1978	593
E					
N					
T					

TABLE 2.10.1-18A

CASK BODY STRESSES UNDER THERMAL ACCIDENT (t = 1.0 HRS.)

LOCATION		MEMBRANE STRESSES (PSI)		BENDING STRESSES (PSI)	
		MERIDIONAL SM	HOOP SH	MERIDIONAL SBM	HOOP SBH
CONTAINMENT	1	-31	-31	-101	-101
	2	-31	-31	12	-62
	3	61	28	-75	-22
	4	62	0	0	0
	5	62	0	0	0
	6	62	0	0	0
	7	62	0	0	0
	8	62	0	0	0
	9	61	16	-19	-6
NON-CONTAINMENT	10	225	345	96	29
	11	221	568	-1	0
	12	221	568	0	0
	13	221	568	0	0
	14	221	568	0	0
	15	221	568	0	0
	16	221	580	2	1
	17	122	39	324	97

2.10.1.2 TRUNNION ANALYSIS

This section discusses the analysis performed to calculate the local stresses in the cask body outer shell at the trunnion locations due to the loadings applied through the trunnions. These local effects are not included in the ANSYS stress results tables reported above in Section 2.10.1.1. The local stresses must be superimposed on the above stress results for the cases where the inertial loadings are reacted at the trunnions. The local stresses are calculated in accordance with the methodology of Reference WRC-107* which is based on the "Bijlaard" analysis for local stresses in cylindrical shells due to external loadings.

Loading

The Bijlaard analysis was performed for several different trunnion loading conditions to support various structural evaluation cases. A summary of the load cases considered is provided in Table 2.10.1-19A.

Section 2.5 of Chapter Two provides the analyses of the trunnions under the limiting 2/5/10 g tiedown loading (cask horizontal). That analyses was performed to demonstrate that the trunnions satisfy the performance requirements of 10CFR71.45. The Bijlaard analysis for this load case was performed to verify that the trunnion induced stresses in the cask body outer shell are also acceptable.

* Welding Research Council Bulletin No. 107
Local Stresses in Spherical and Cylindrical Shell Due to External Loading, March 1979 Revision

Three additional load cases were analyzed to support the normal condition of transport load combinations described in Section 2.6 of Chapter Two. A 1g-vertical (cask horizontal) load case is applicable for load combinations as identified in Table 2.6-1A in Section 2.6 of Chapter 2.0. The vibration and shock loading cases pertain to load combinations involving specific transport loadings (see Table 2.6-1A). The shock/vibration inertia values used for vibration and shock conditions were obtained from truck bed accelerations in ANSI N14.23*.

Loads used for the "Bijlaard" analysis are obtained from the packaging inertial loadings and are listed in Table 2.10.1-19B. The loads are based on a transport weight of 50,000 lb. which is larger than the calculated weight of 47,000 lb.

Method of Analysis

The local stresses induced in the outer shell cylinder by the trunnions are calculated using "Bijlaard's" method. The trunnion is approximated by an equivalent attachment so that the curves of the Reference WRC-107 can be used to obtain the necessary coefficients. These resulting coefficients are inserted into blanks in the column entitled "Read Curves For," in a standard computation form, a sample of which is attached as Table 2.10.1-19C. The stresses are calculated by performing the indicated multiplication in the column entitled "Compute Absolute Values of Stress and Enter Result". The resulting stress is inserted into the stress table at the eight stress locations, i.e., AU, AL, BU, BL, etc. Note that the sign convention for this table is defined on the figure as if the load directions are as shown. The membrane plus bending stresses are calculated by completing Table 2.10.1-19C.

* Draft American National Standard Design Basis for Resistance to Shock and Vibration, ANSI N14.23, May, 1980.

Model, Boundary Conditions and Assumptions

The cylindrical body is assumed to be a hollow cylinder of infinite length. Since the trunnions are located away from the ends of the cylinder, this assumption is acceptable because the local effects are not significantly affected by the end restraints, i.e., lid and bottom. This is conservative since end restraints would reduce the local bending effects.

Results of Analysis

The attachment parameter, β, is obtained by using an attachment radius, r_o, equal to the radius of the trunnion base plate. For the "Bijlaard" parameter computations, an equivalent cylinder thickness is employed. The equivalent thickness has the same bending stiffness as the layered wall consisting of the outer shell, lead and inner shell. The equivalent thickness is determined assuming the layers can slide relative to each other (unbonded lead).

Tables 2.10.1-19 to 22 summarize the resulting local membrane stresses and bending stresses for the various loading conditions. These local stresses are combined with the finite element results at the same locations from Section 2.10.1.1 above and compared with allowables in Section 2.6.

Table 2.10.1-23 lists the total stresses at all locations which includes the Section 2.10.1.1 finite element results and the local stresses at the trunnion locations from this section for the tie down load cases. Note that the stresses do not exceed the 30,000 psi yield strength of the 304 stainless steel at any location.

TABLE 2.10.1-19A

LOAD CASES FOR TN-FSV CASK BODY LOCAL STRESS ANALYSIS USING BIJLAARD METHOD

LOAD CASE NUMBER	INDIVIDUAL LOAD DESCRIPTION	STRESS RESULT TABLES
19	Local Stresses at Trunnion/Cask Body Interface Cask Horizontal With 1 G Vertical Loading	2.10.1-19
20	Local Stresses at Trunnion/Cask Body Interface With Vibration Loading	2.10.1-20
21	Local Stresses at Trunnion/Cask Body Interface Cask Horizontal With Shock Loading	2.10.1-21
22	Local Stresses at Trunnion/Cask Body Interface With Tie Down Loading	2.10.1-22
23	Stresses Due to Tie Down Load Including Local Stresses at Trunnion/Cask Body Interface	2.10.1-23

TABLE 2.10.1-19B

TRUNNION LOADING

LOADING DESCRIPTION	INERTIAL LOAD	MAX. TRUNNION LOAD REAR TRUNNION
GRAVITY (Cask Horizontal)	1 G (Vertical)	V_C = 12.5 KIPS M_C = 25 IN-KIPS
SHOCK (Cask Horizontal)	2.3 G (Longitudinal)	V_L = 57.5 KIPS V_C = 43.75 KIPS
	1.6 G (Lateral)	P = 40 KIPS M_L = 115 KIPS
	3.5 G (Vertical)	M_C = 87.5 In-KIPS
VIBRATION (Cask Horizontal)	0.3 G (Longitudinal)	V_L = 7.5 KIPS V_C = 7.5 KIPS
	0.3 G (Lateral)	P = 7.5 KIPS M_L = 15 IN-KIPS
	0.6 G (Vertical)	M_C = 15 IN-KIPS
TIE-DOWN (Cask Horizontal)	10 G (Longitudinal)	V_L = 250 KIPS V_C = 25 KIPS
	5 G (Lateral)	P = 125 KIPS M_L = 500 IN-KIPS
	2 G (Vertical)	M_C = 50 IN-KIPS

TABLE 2.10.1-19C
BIJLAARD COMPUTATION SHEET

* 1. APPLIED LOADS

RADIAL LOAD P * ± _____ LB

CIRC. MOMENT Mc * ± _____ IN-LB

LONG. MOMENT Ml * ± _____ IN-LB

TORSION MOMENT Mt * ± _____ IN-LB

SHEAR LOAD Vc * ± _____ LB

SHEAR LOAD Vl * ± _____ LB

* NOTE: ENTER ALL FORCE VALUES IN ACCORDANCE WITH SIGN CONVENTION

2. GEOMETRY

VESSEL THICKNESS T ± _____ IN.

ATTACHMENT RADIUS r_o ± _____ IN.

VESSEL RADIUS Rm ± _____ IN.

3. GEOMETRIC PARAMETERS

$\gamma = \frac{Rm}{T}$ = _____

$\beta = (0.875)\frac{r_o}{Rm}$ = _____

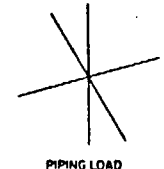

PIPING LOAD COORDINATE SYSTEM

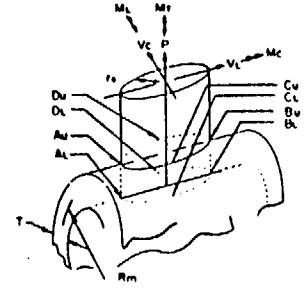

FROM FIG.	READ CURVES FOR	COMPUTE ABSOLUTE VALUES OF STRESS AND ENTER RESULT	STRESSES – IF LOAD IS OPPOSITE THAT SHOWN, REVERSE SIGNS SHOWN Au	Al	Bu	Bl	Cu	Cl	Du	Dl
3C AND 4C	$\frac{N\phi}{P/Rm}$ *	$\left(\frac{N\phi}{P/Rm}\right)\frac{P}{RmT}$ *	+	+	+	+	+	+	+	+
1C AND 2C-1	$\frac{M\phi}{P}$ *	$\left(\frac{M\phi}{P}\right)\frac{6P}{T^2}$ *	+	–	+	–	+	–	+	–
3A	$\frac{N\phi}{Mc/Rm^2\beta}$ *	$\left(\frac{N\phi}{Mc/Rm^2\beta}\right)\frac{Mc}{Rm^2\beta T}$ *					–	–	+	+
1A	$\frac{M\phi}{Mc/Rm\beta}$ *	$\left(\frac{M\phi}{Mc/Rm\beta}\right)\frac{6Mc}{Rm\beta T^2}$ *					–	+	+	–
3B	$\frac{N\phi}{Ml/Rm^2\beta}$ *	$\left(\frac{N\phi}{Ml/Rm^2\beta}\right)\frac{Ml}{Rm^2\beta T}$ *	–	–	+	+				
1B OR 1B-1	$\frac{M\phi}{Ml/Rm\beta}$ *	$\left(\frac{M\phi}{Ml/Rm\beta}\right)\frac{6Ml}{Rm\beta T^2}$ *	–	+	+	–				
ADD ALGEBRAICALLY FOR SUMMATION OF ϕ STRESSES $\sigma\phi$ *										
3C AND 4C	$\frac{Ns}{P/Rm}$ *	$\left(\frac{Ns}{P/Rm}\right)\frac{P}{RmT}$ *	+	+	+	+	+	+	+	+
1C-1 AND 2C	$\frac{Ms}{P}$ *	$\left(\frac{Ms}{P}\right)\frac{6P}{T^2}$ *	+	–	+	–	+	–	+	–
4A	$\frac{Ns}{Mc/Rm^2\beta}$ *	$\left(\frac{Ns}{Mc/Rm^2\beta}\right)\frac{Mc}{Rm^2\beta T}$ *					–	–	+	+
2A	$\frac{Ms}{Mc/Rm\beta}$ *	$\left(\frac{Ms}{Mc/Rm\beta}\right)\frac{6Mc}{Rm\beta T^2}$ *					–	+	+	–
4B	$\frac{Ns}{Ml/Rm^2\beta}$ *	$\left(\frac{Ns}{Ml/Rm^2\beta}\right)\frac{Ml}{Rm^2\beta T}$ *	–	–	+	+				
2B OR 2B-1	$\frac{Ms}{Ml/Rm\beta}$ *	$\left(\frac{Ms}{Ml/Rm\beta}\right)\frac{6Ml}{Rm\beta T^2}$ *	–	+	+	–				
ADD ALGEBRAICALLY FOR SUMMATION OF s STRESSES σs *										
SHEAR STRESS DUE TO TORSION Mt		$\tau\phi s = \tau s\phi = \frac{Mt}{2\pi r_o^2 T}$	+	+	+	+	+	+	+	+
SHEAR STRESS DUE TO LOAD Vc		$\tau s\phi = \frac{Vc}{\pi r_o T}$	+	+	–	–				
SHEAR STRESS DUE TO LOAD Vl		$\tau\phi s = \frac{Vl}{\pi r_o T}$					+	+	–	–
ADD ALGEBRAICALLY FOR SUMMATION OF SHEAR STRESSES τ *										

	LONGITUDINAL σs	CIRCUMFERENTIAL $\sigma\phi$
PRESSURE STRESS	$\frac{PR-0.4PT}{2T}$ * = * _____	$\frac{PR+0.6PT}{ET}$ * = * _____
LONGITUDINAL BENDING STRESS	* _____	
TOTAL MEMBRANE STRESS	* _____ ≤ _____	* _____ ≤ _____
TOTAL SURFACE STRESS	* _____ ≤ _____	* _____ ≤ _____

NOZZLE NO. _____

PIPING LOAD CODE _____

ANALYSIS POINT _____

COMPUTATION SHEET FOR LOCAL STRESSES IN CYLINDRICAL SHELLS

SERVICE:

ITEM NO.

JOB NO

DATE BY SHEET

TABLE 2.10.1-19

LOCAL STRESSES AT TRUNNION/CASK BODY INTERFACE -
CASK HORIZONTAL WITH 1G VERTICAL LOADING

LOCATION		MEMBRANE STRESSES (PSI)		BENDING STRESSES (PSI)	
		MERIDIONAL SM	HOOP SH	MERIDIONAL SBM	HOOP SBH
CONTAINMENT	1				
	2				
	3				
	4				
	5				
	6				
	7				
	8				
	9				
NON-CONTAINMENT	10				
	11				
	12				
	13				
	14				
	15				
	16	-170	-87	-356	-679
	17				

TABLE 2.10.1-20

LOCAL STRESSES AT TRUNNION/CASK BODY INTERFACE

WITH VIBRATION LOADING

LOCATION		MEMBRANE STRESSES (PSI)		BENDING STRESSES (PSI)	
		MERIDIONAL SM	HOOP SH	MERIDIONAL SBM	HOOP SBH
C	1				
O	2				
N	3				
T	4				
A	5				
I	6				
N	7				
M	8				
E	9				
N					
T					
NON-					
C	10				
O	11				
N	12				
T	13				
A	14				
I	15				
N	16	-546	-358	-671	1145
M	17				
E					
N					
T					

TABLE 2.10.1-21

LOCAL STRESSES AT TRUNNION/CASK BODY INTERFACE

WITH SHOCK LOADING

LOCATION		MEMBRANE STRESSES (PSI)		BENDING STRESSES (PSI)	
		MERIDIONAL SM	HOOP SH	MERIDIONAL SBM	HOOP SBH
C	1				
O	2				
N	3				
T	4				
A	5				
I	6				
N	7				
M	8				
E	9				
N					
T					
NON-					
C	10				
O	11				
N	12				
T	13				
A	14				
I	15				
N	16	-2972	-1938	-3688	-6314
M	17				
E					
N					
T					

TABLE 2.10.1-22

LOCAL STRESSES AT TRUNNION/CASK BODY INTERFACE

WITH TIE DOWN LOADING

LOCATION		MEMBRANE STRESSES (PSI)		BENDING STRESSES (PSI)	
		MERIDIONAL SM	HOOP SH	MERIDIONAL SBM	HOOP SBH
C	1				
O	2				
N	3				
T	4				
A	5				
I	6				
N	7				
M	8				
E	9				
N					
T					
NON-					
C	10				
O	11				
N	12				
T	13				
A	14				
I	15				
N	16	-7771	-5283	-8350	-13665
M	17				
E					
N					
T					

TABLE 2.10.1-23

STRESSES DUE TO TIE DOWN LOAD INCLUDING LOCAL STRESSES AT TRUNNION/CASK BODY INTERFACE

LOCATION		MEMBRANE STRESSES (PSI)		BENDING STRESSES (PSI)	
		MERIDIONAL SM	HOOP SH	MERIDIONAL SBM	HOOP SBH
CONTACT	1	141	114	-2320	-2364
CONTACT	2	87	260	1413	96
CONTACT	3	668	440	-858	-271
CONTACT	4	1318	783	-164	-178
CONTACT	5	1966	1393	-208	-219
CONTACT	6	2485	2243	-234	-235
CONTACT	7	2292	2920	-208	-222
CONTACT	8	1682	3540	-135	-169
CONTACT	9	1395	1461	2085	629
NON-CONTACT	10	87	37	-173	-53
NON-CONTACT	11	815	-477	-17	-60
NON-CONTACT	12	1782	-1048	-82	-99
NON-CONTACT	13	2365	-1794	-112	-115
NON-CONTACT	14	2144	-2393	-95	-105
NON-CONTACT	15	-1224	-2911	-50	-68
NON-CONTACT	16	-7572	-7698	-7572	-13456
NON-CONTACT	17	-2742	-213	-5747	-1721

2.10.1.3 Lid Bolt Analysis

The TN-FSV lid closure arrangement is shown in Figure 2.10.1-19. The 2.5 inch thick lid is bolted directly to the end of the containment vessel body by 12 high strength 1.0 inch diameter bolts. Close fitting alignment pins ensure that the lid is centered in the vessel.

The lid bolt is shown in Figure 2.10.1-20. Note that the material is ASME SA-540, GR B24, Class 1 which has a minimum yield strength of 150,000 psi at room temperature. The lid closure flange and bolt arrangement is shown in Figure 2.10.1-21. The bolts are designed to be preloaded at assembly to seat the seals against the 30 psi maximum design pressure and to withstand all normal and accident loadings without yielding. The lid bolt analysis performed below is in accordance with NUREG/CR-6007 stress analysis of Closure Bolts for Shipping Casks.

Normal Conditions

The loadings considered for normal conditions include operating preload, pressure loads, temperature, impact loads and the vibration loads.

The non-prying tensile bolt force due to the applied preload is given by the formula

$$Fa = \frac{Q}{KD_b}$$

where Q is the applied torque for preload, 1540 in. lbs.

K is the nut factor for empirical relation between the applied torque and the achieved preload, 0.1 to 0.2
This value is based on lubricating the bolts with Neolube having a coefficient of friction of 0.03 -0.09.

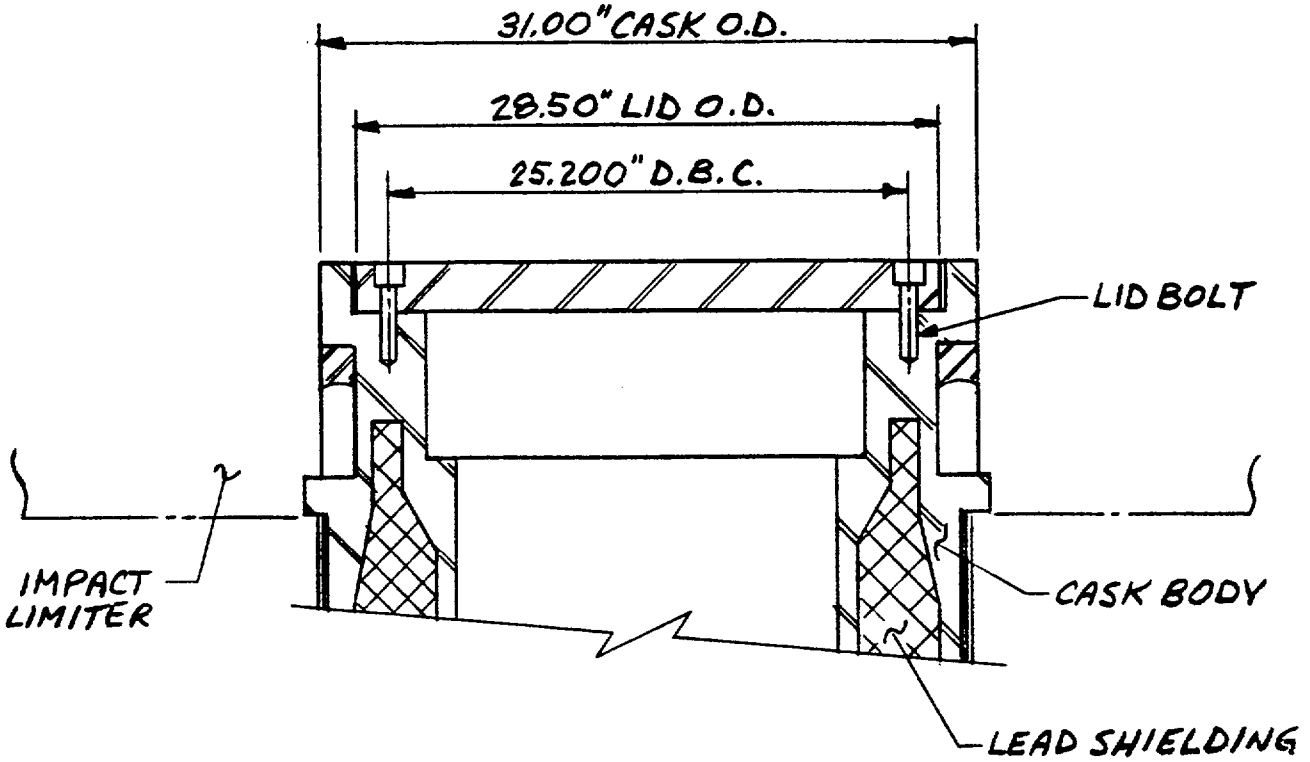

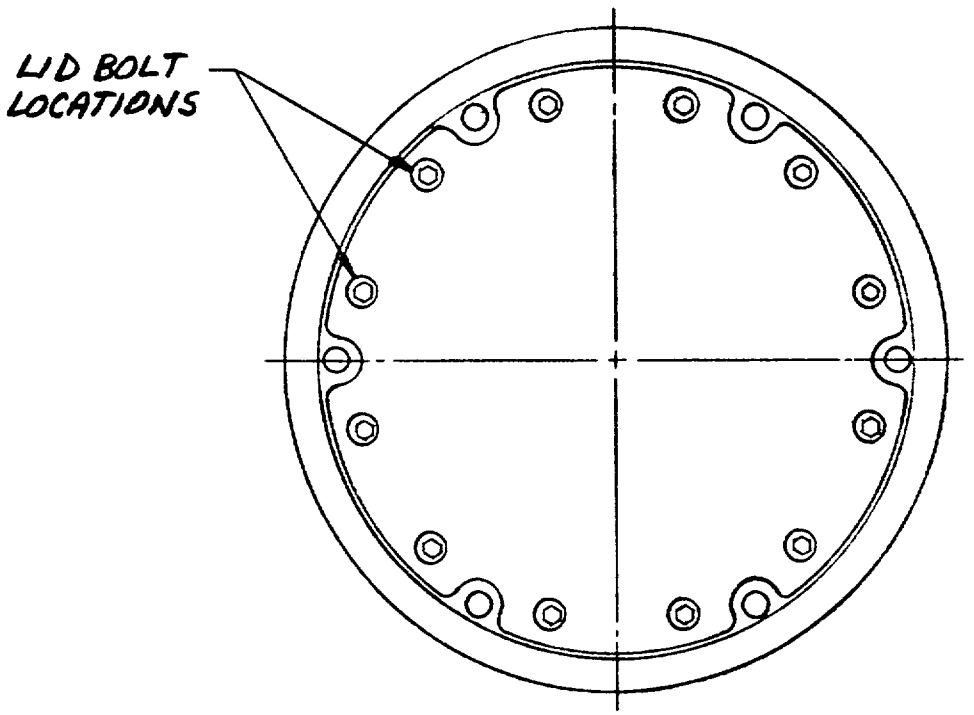

FIGURE 2.10.1-19
TN-FSV LID CLOSURE

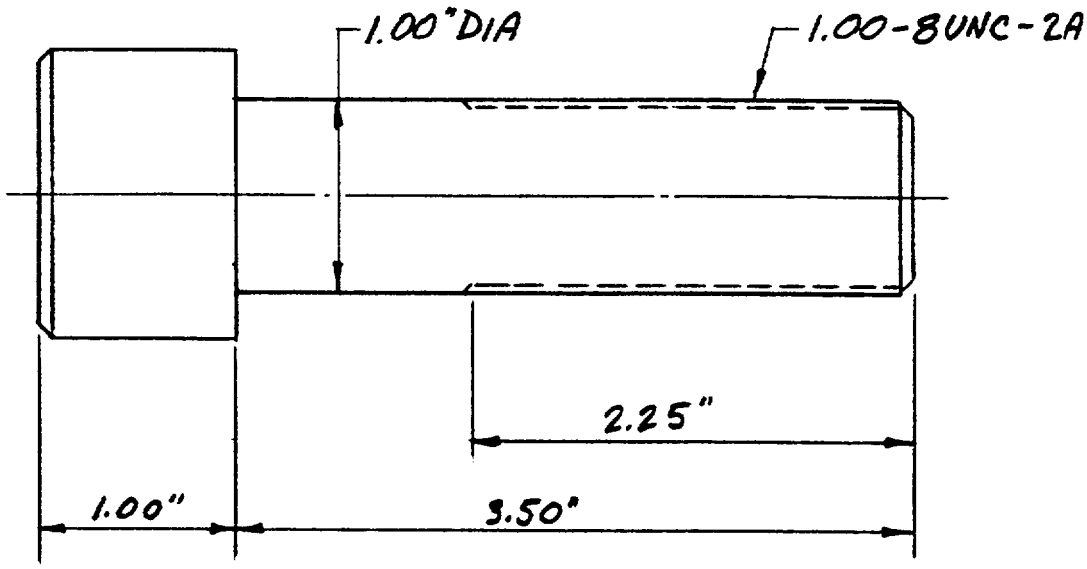

FIGURE 2.10.1-20
TN-FSV LID BOLT

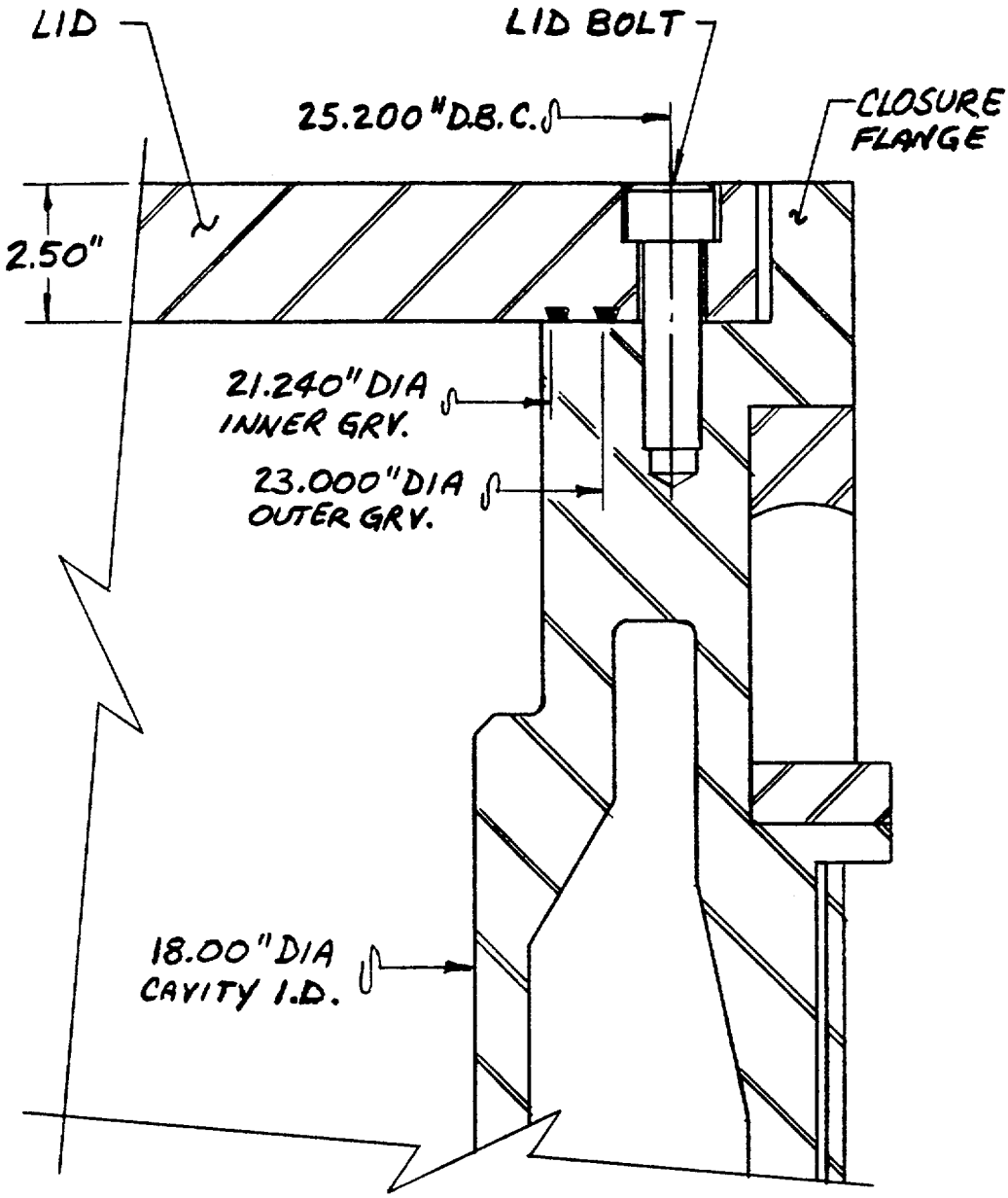

FIGURE 2.10.1-21

TN-FSV LID BOLT ARRANGEMENT

and D_b is the nominal diameter of the closure bolt, 1.0 inch.

$$F_a = \frac{1540}{(0.1)(1.0)} = 15,400 \text{ lbs. } (K=0.1) \text{ or } F_a = 7,700 \text{ lbs } (K=0.2)$$

The torsional bolt moment per bolt is

$$M_t = 0.5Q$$
$$= 0.5\ (1540) = 770 \text{ in-lbs.}$$

The maximum residual tensile bolt force after preload is

$F_{ar} = F_a = 15,400$ lbs. (K=0.1) and $F_{ar} = 7,700$ lbs.(K=0.2)

The maximum residual torsional bolt moment is

Mtr = 0.5Q = 770 in-lbs.

The gasket seating load is negligible since o-rings are used.

The loads caused by the pressure difference between the interior and the exterior of the closure components are calculated below. The non-prying tensile bolt force is

$$F_a = \frac{\pi\ Dlg^2\ (Pli-Plo)}{4N_b}$$

where Dlg is the closure lid diameter at the inner seal, 21.24 in.
Pli is the pressure inside the closure lid and
Plo is the pressure outside the closure lid.
N_b is the number of bolts, 12

The maximum differential pressure for both normal and accident conditions is 30 psi.

$$F_a = \frac{\pi\ (21.24)^2 (30)}{4(12)}$$
$$= 886 \text{ lbs.}$$

The increased external pressure combined with no internal pressure results is a force of $F_a = -591$ lbs.

The shear bolt force due to 30 psi differential pressure is

$$F_S = \frac{\pi \, El\,tl\,(Pci-Pco)\,Dlb^2}{2Nb\,Ectc\,(1-NUl)}$$

where

El is Young's Modulus of the closure lid material, 28.3×10^6 psi

tl is the lid thickness, 2.5 inches

Pci-Pco is the differential pressure on the cask wall, 30 psi

Dlb is the closure lid diameter at the bolt circle, 25.2 inches

Ec is the Young's Modulus of the cask wall material, 28.3×10^6 psi

tc is the thickness of the cask wall. Since the cask is a composite material, a conservative value of 3.0 inches is used.

NUl is Poisson's ratio of the closure lid material, 0.3.

$$F_S = \frac{\pi\,(28.3 \times 10^6)(2.5)(25.2)^2(30)}{2(12)(28.3 \times 10^6)(3.0)(1-.3)}$$

$$= 2969 \text{ lbs.}$$

The fixed edge closure lid force (Ff) and Moment (Mf) for the calculation of prying tensile bolt force and bending bolt moment are given by the formulas below.

$$Ff = \frac{Dlb\,(Pli-Plo)}{4}$$

$$= \frac{25.2\,(30)}{4} = 189 \text{ lbs}$$

$$Mf = \frac{(Pli-Plo)\,Dlb^2}{32}$$

$$= \frac{(30)\,(25.2)^2}{32} = 595 \text{ in-lbs.}$$

The load caused by differential thermal expansion of the closure lid and bolt is calculated below.

$$F_a = 0.25\,\pi Db^2\,Eb\,(alTl-abTb)$$

where Eb is the Young's Modulus of the bolt material, 29.7×10^6 psi

al is the thermal expansion coefficient of the lid material, 8.79×10^{-6} in/in°F

Tl is the temperature change of the lid. The lid can get as hot as 170°F at an ambient temperature of 100°F with maximum insolation. The lid can get as cold as -40°F in the cold environment. Assuming the lid is bolted to the cask inside at a room temperature of 70°F, Tl is 100°F for the hot environment and -110°F for the cold environment.

ab is the thermal expansion coefficient of the bolt material, 6.5×10^{-6} in/in°F

Tb is the temperature change of the bolt material. This is the same as Tl.

$$F_a = 0.25\pi\ (1.0)^2\ (29.7 \times 10^6)(8.79 \times 10^{-6} - 6.5 \times 10^{-6})(100°F)$$
$$= 5342 \text{ lbs for the hot environment}$$
$$F_a = -5876 \text{ lbs for the cold environment}$$

There is no load caused by the thermal expansion difference between the closure lid and cask wall since they are made of the same material, and the lid and flange are insulated by the impact limiter so that temperature changes are gradual and the temperature of the lid and flange are equal.

There is also no load caused by the temperature gradient between the inner and outer surfaces of the closure lid since $\Delta T=0$.

The worst loading on the bolts due to a 1 foot drop is during an end drop. The lip on the cask protects the closure lid during the side drop. The non prying tensile bolt force due to a one foot end drop is

$$F_a = \frac{1.34\ (DLF)(Wl+Wc)(ai)}{Nb}$$

where DLF is the dynamic load factor, 1.2
Wl is the weight of the lid, 500 lbs.
Wc is the maximum weight of the cargo, 5000 lbs.
ai is the maximum rigid body impact acceleration of the cask, 14 g's

$$F_a = \frac{1.34\ (1.2)(5500)(14)}{12} = 10{,}318 \text{ lbs.}$$

The shear bolt force is maximum for the 1 foot side drop having a g loading of 17.

$$F_s = \frac{\cos(xi)ai\ Wl}{Nb}$$

$$= \frac{(17)(500)}{12} = 708 \text{ lbs.}$$

The fixed edge closure lid force (Ff) and moment (Mf) is calculated below for the 1 ft end drop. Ff and Mf are 0 for the 1 ft side drop.

$$F_f = \frac{1.34\ DLF\ ai\ (Wl+Wc)}{\pi\ Dlb}$$

$$F_f = \frac{(1.34)(1.2)(14)(5500)}{\pi(25.2)}$$

$$= 1564 \text{ lbs.}$$

$$M_f = \frac{1.34DLF\ ai\ (Wl+Wc)}{8\pi}$$

$$= \frac{(1.34)(1.2)(14)(5500)}{8\pi}$$

$$= 4926 \text{ lbs.}$$

Vibration loads are insignificant on the bolts.

The load combinations are calculated using the methodology outlined in Table 4.9 of NUREG/CR-6007.

The sum of the tensile bolt forces for operating preload and temperature is

Fa_pt = 15400 + 5342 = 20,742 lbs. (K=0.1)
or Fa_pt = 7700 + 5342 = 13,024 lbs. for K=0.2

The sum of the tensile forces for the remainder of the loads is

Fa_al = 10318 + 886 = 11,204 lbs.

This is based on the 1 foot impact and internal pressure. The combined non-prying tensile bolt force is the larger of the two forces calculated above, 20,717 lbs.

Combination of Prying Tensile Bolt Forces

The maximum combined prying fixed-edge force Ff_c is 1564 + 189 = 1753 lbs and the maximum combined prying moment Mf-c is 595 + 4926 = 5521 in-lbs.

The prying tensile bolt force for the combined load is

$$Fap = \left[\frac{(\pi\ Dlb)}{Nb}\right]\left[\frac{\frac{2Mf}{(Dlo-Dlb)} - C1\ (B-Ff) - C2\ (B-P)}{C1 + C2}\right]$$

where

Mf = 5521 in-lbs

Ff = 1753 lbs

P = the bolt preload per unit length of the bolt circle

$$= \frac{Fa\text{-}pt\ Nb}{\pi Dlb}$$

$$= \frac{(20742)(12)}{\pi(25.2)} = 3144 \text{ lbs } (K=0.1) \text{ or } \frac{(13024)(12)}{\pi(25.2)} = 1974 \text{ lbs } (K=0.2)$$

B = P since P>Ff

Dlo = the closure lid diameter at the outer edge

= 28.5 inches

C1 = 1

$$C2 = \left[\frac{8}{3(Dlo-Dlb)^2}\right]\left[\frac{Eltl^3}{1-Nul} + \frac{(Dlo-Dli)\ El\ tlf^3}{Dlb}\right]\left[\frac{Lb}{NbDb^2\ Eb}\right]$$

where Tlf is the thickness of the flange of the closure lid, 2.5 inches

Dli is the closure lid diameter at the inner edge, 20.83 in.

Eb is the Young's Modulus of the Closure bolt material, 29.7 x 10^6 psi

Lb is the bolt length between the top and bottom surfaces of the closure lid at the bolt circles.

Since the flange is counterbored to extend the length of the bolt, Lb is 2.5 inches.

$$C2 = \left[\frac{8}{3(28.5-25.2)^2}\right]\left[\frac{(28.3\times10^6)(2.5)^3}{(1-.3)} + \frac{(28.5-20.83)(28.3\times10^6)(2.5)^3}{25.2}\right] * \left[\frac{2.5}{12(1)^2(29.7\times10^6))}\right]$$

$$C2 = 1.3162$$

$$Fap = \left[\frac{\pi(25.2)}{12}\right]\left[\frac{\frac{2(5521)}{(28.5-25.2)} - 1(3144-1753) - 1.3162(0)}{1 + 1.3162}\right]$$

= 5569 lbs. for K=0.1 or Fap=8901 lbs. for K=0.2.

Combining the non-prying and prying tensile bolt force

Fa-c = 5569 + 20742 = 26,311 lbs. for K=0.1 and

Fa-c = 8901 + 13024 = 21,925 lbs. for K=0.2.

The maximum average tensile stress in a lid bolt is

$$S_{ba} = Fa\text{-}c/A_t$$

where A_t is the tensile area of the bolt, 0.606 $in.^2$

$$S_{ba} = 26311/0.606 = 43,417 \text{ psi}$$

The allowable tensile stress is 2/3 of the yield strength at the operating temperature of 170°F, or 2/3 (150,000) or 100,000 psi. S_{ba} is much less than the allowable stress.

The shear bolt force is not evaluated since the bolts and closure lid are protected during an impact by the lip of the cask flange. The bolts are not relied upon to resist transverse shear load. The bending bolt moment is calculated below.

$$M_{bb} = \left[\frac{\pi D1b}{Nb}\right]\left[\frac{Kb}{Kb+K1}\right] Mf$$

where

$$K_b = \left[\frac{Nb}{Lb}\right]\left[\frac{Eb}{D1b}\right]\left[\frac{Db^4}{64}\right]$$

$$= \left[\frac{12}{2.5}\right]\left[\frac{29.7\times10^{6}}{25.2}\right]\left[\frac{(1)^{4}}{64}\right]$$

$K_b = 88,393$

$$Kl = \frac{El\ tl^{3}}{3[(1-NUl^{2}) + (1-NUl)^{2}\quad (Dlb/Dlo)^{2}]\ Dlb}$$

$$= \frac{(28.3\times10^{6})\ (2.5)^{3}}{3[(1-(.3)^{2}) + (1-.3)^{2}\quad (25.2/28.5)^{2}]\ (25.2)}$$

$Kl = 4.523 \times 10^{6}$

$Mf = 5521$ in-lbs.

$$M_{bb} = \left[\frac{\pi(25.2)}{12}\right]\left[\frac{88393}{(4.523\times10^{6} + 88393)}\right](5521)$$

$M_{bb} = 698$ in. lbs.

The maximum bending stress caused by the bending bolt moment is

$$S_{bb} = 10.186\ M_{bb}/D^{3}$$

The minimum bolt diameter is equal to

$$D_{ba} = 1.0 - 0.9743\ p$$

where $p = 1/8$

$D_{ba} = 0.8782$ in.

$$S_{bb} = \frac{(10.186)(698)}{(.8782)^{3}} = 10,494 \text{ psi}$$

The maximum shear stress caused by the torsional bolt moment (M_t) is

$$S_{bt} = 5.093\ M_t/D^{3}$$

$$= 5.093\ (1540)/(.8782)^{3}$$

$= 10,170$ psi

This is much less than the allowable stress of 0.6 S_m = 60,000 psi.

The maximum stress intensity caused by tension plus shear plus bending plus torsion is

$$S_{bi} = [(Sba + Sbb)^2 + 4\ (Sbt)^2]^{0.5}$$

$$= [(43417 + 10494)^2 + 4\ (10170)^2]^{0.5}$$

$$S_{bi} = 57,620 \text{ psi}$$

This is much less than the allowable maximum stress intensity of 1.35 S_m = 135,000 psi.

Bolt Fatigue Analysis

The purpose of the fatigue analysis is to show quantitatively that the fatigue damage to the bolts during normal transport conditions is acceptable. This is done by determining the fatigue usage factor for each normal transport event. For this analysis it is assumed that the bolts are replaced after 350 round trip shipments. The total cumulative damage or fatigue usage for all events was conservatively determined by adding the usage factors for the individual events. The sum of the individual usage factors was checked to make certain that, for the 350 round trip shipments of the TN-FSV, the total usage factor is less than one. The following sequence of events was assumed for the fatigue evaluation.

1. Operating Preload
2. Pressure Fluctuations
3. Road Vibration
4. Shock
5. Test Pressure
6. Impact (1 Ft) End Drop

Number of Load/Stress Cycles for Each Loading
(2 Round Trips Per Week)

A. Test Pressure:

Proof Test: 1.5 x MNOP = 45 psig. This occurs once during the TN-FSV lifetime. (See Table 2.10.1.24 for stress calculation).

B. Preload

Assuming the bolts are replaced after 350 round trips between INEL and Fort St. Vrain. The number of preload cycles is two times the number of trips, or 700. (See Table 2.10.1.24 for stress calculation).

C. Shock and Vibration

Shock and vibration input was obtained from ANSI N14.23. This standard specifies shock loads that correspond to normal transport over rough roads or minor accidents such as backing into a loading dock. Since the TN-FSV will be transported on interstate highways and/or major good roads, the shock loads will not be applied continuously to the normal transport mode for the package. The fatigue calculation assumes an average trip of 600 miles in 12 hours.

Assuming the driver stops and leaves the interstate every 4 hours and assuming that one shock loading could be experienced on each of these stops, the following cycles are added to the histogram. The return trip package behavior is assumed to be the same as the "loaded" trip even though the cargo is no longer present. Therefore shock loading occurs 3 (shocks per trip) x 2 (round trip) x 350 shipments = 2100 cycles.

Assuming a peak shock loading of 1.8 g's in the longitudinal direction, this results in a bolt tensile stress of (5500 lbs)(1.8 g's)/12(.606) = 1361 psi. According to ANSI N14.23, the peak vibration load at the bed of a truck in the longitudinal direction is 0.3 g's. This results in a stress of 227 psi in the bolt. This stress is negligible for a high strength bolt.

D. 1 Foot Drop:

Assume this occurs twice. The stress intensity of 21,414 psi (see Table 2.10.1.24 for stress derivation) is a combination of the non prying and prying tensile stress due to the one foot end drop, with a zero preload.

E. Pressure and Temperature Fluctuations:

The full internal equilibrium temperature of 170°F is not reached during a typical trip. However, for conservatism we assume that the temperature increases from 70°F to 170°F during each trip. This results in a load due to differential thermal expansion coefficients, and also due to pressure changes. The pressure increase is composed of:

6 psi - partial pressure of water at 170°F
2 psi - pressure increase of the air when heated from 70°F to 170°F

NOTE: The TN-FSV is quite rigid and is attached relatively rigidly to its trailer. Therefore, the vibration frequency of concern in determining the number of cycles of vibration is that of the trailer. It is expected that the actual trailer frequency will be less than 10 cps.

Combining the stress due to a hot environment and 8 psi internal pressure results in a stress intensity of 9,347 psi (see Table 2.10.1.24 for stress derivation). Conservatively assuming this cycle occurs each shipment, this results in 700 cycles. This is very conservative since it takes roughly 6 hours to reach the maximum temperature.

Fatigue Evaluation - Usage Factor Calculations

Based on the stresses and cyclic histories described above, stress histograms are plotted in Figure 2.10.1-22. In each histogram, a fatigue strength reduction factor (K) of 4.0 has been assumed in the evaluation. The stress range for each combination of events and the corresponding alternating stress are shown in Table 2.10.1-24. The damage factors are computed using the fatigue curve shown in Table I-9.4 of ASME Section III Appendices. The cumulative fatigue damage factors in this case is 0.9367 which is less than the limit of 1.0. Therefore, the TN-FSV satisfies the fatigue requirements.

TABLE 2.10.1.24

FORCES, MOMENTS AND STRESSES CALCULATED FOR FATIGUE EVALUATION

EVENT/ LOAD	F_A (LBS)	F_f (LBS)	M_f (IN-LBS)	F_{AP} (LBS)	F_c (LBS)	τ (PSI)	σ (PSI)
TEST PRESSURE	1,328	284	893	480	1,808	--	2,983
PRELOAD	30,800	--	M_t =1,540	--	30,800	10,170	54,744 (S.I.)
ONE FOOT DROP	10,318	1,564	4,926	2,659	12,977	--	21,414
PRESSURE + TEMPERATURE	5,578	50	158	86	5,664	--	9,347
SHOCK	825	--	--	--	825	--	1,361
VIBRATION	138	--	--	--	138	--	227

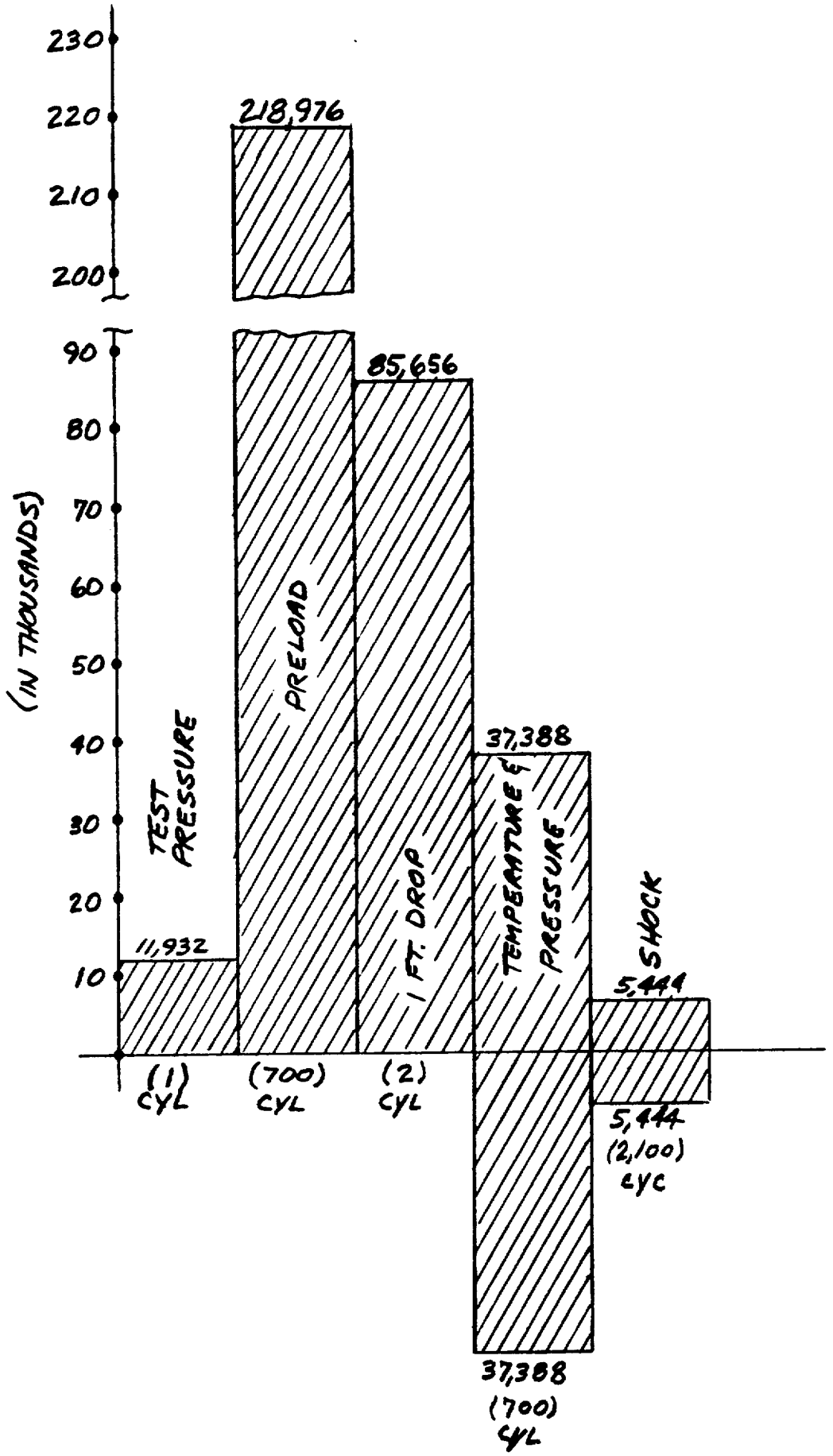

FIGURE 2.10.1-22
SCHEMATIC OF STRESS HISTOGRAM AT BOLTS (K = 4)

TABLE 2.10.1.25

BOLT DAMAGE FACTORS

EVENT COMBINATIONS	STRESS RANGE (PSI)	Sa (PSI)	FATIGUE CURVE	CYCLES n	CYCLES N	DAMAGE FACTOR n/N
Test Pressure	11,932	5,966	I-9.4	1	$1x10^6$	0.0000
Preload	218,976	109,488	I-9.4	700	839	0.8343
1 Foot Drop	85,656	42,828	I-9.4	2	6,000	0.0003
Shock	5,444	5,444	I-9.4	2,100	$1x10^6$	0.0021
Temp. & Pressure	37,388	37,388	I-9.4	700	7,000	.1000
TOTAL						0.9367

Accident Conditions

The hypothetical accident conditions considered for the bolt analysis are: impact, puncture, fire and submersion.

The worst loading due to the 30 foot impact occurs at an angle just slightly offset from 90 degrees. This results in a g loading of 54.

The nonprying tensile bolt force due to impact is:

$$F_a = \frac{(1.34)(DLF)(W1+Wc)(ai)}{N_b}$$

$$= \frac{(1.34)(1.2)(5500)(54)}{12} = 39,798 \text{ lbs.}$$

There is no shear bolt force due to impact, since the load is taken by the lip of the cask flange. The fixed edge closure lid force (Ff) and moment (Mf) are

$$F_f = \frac{1.34(DLF)ai(W1+Wc)}{\pi D1b}$$

$$= \frac{(1.34)(1.2)(54)(5500)}{\pi(25.2)}$$

$$= 6033 \text{ lbs.}$$

$$Mf = \frac{1.34DLFai\ (W1+Wc)}{8\pi}$$

$$= \frac{(1.34)(1.2)(54)(5500)}{8\pi} = 19,002 \text{ in-lbs.}$$

The puncture accident results in an inward load on the bolts which relaxes the tensile force due to preload.

The fire accident results in a maximum bolt and lid temperature of 193°F. The load caused by differential thermal expansion of the closure lid and bolt is

$$F_a = 0.25\pi D_b^2 Eb (alTl - abTb)$$
$$= 0.25\pi(1.0)^2(29.7x10^6)(8.79x10^{-6} - 6.5x10^{-6})(123°F)$$
$$F_a = 6570 \text{ lbs.}$$

Submersion of the cask under 200 meters of water results in an external pressure on the cask which acts to reduce preload on the bolts.

Therefore the worst accident condition for the bolts is the 30 foot end drop. This must be combined with preload, internal pressure and thermal expansion loads.

The sum of the tensile bolt forces for operating preload and temperature is 20,742 lbs. or 13024 lbs. depending on the friction factor as in the normal load cases.

The sum of the non prying tensile forces from internal pressure and 30 foot drop accident is 39798 + 886 or 40,684 lbs.

The combined non-prying tensile bolt force is the larger of the two forces calculated above, 40,684 lbs.

The maximum combined prying fixed edge force Ff-c is 6033 + 189 = 6222 lbs. The combined prying moment Mf-c is 19002 + 595 = 19597 in. lbs.

The prying tensile bolt force for the combined load is

$$F_{a\text{-}pt} = \left[\frac{\pi D_{1b}}{N_b}\right]\left[\frac{\frac{2M_f}{(D_{1o}-D_{1b})} - C_1(B-F_f) - C_2(B-P)}{C_1 + C_2}\right]$$

where Mf = 19597 in lbs.

Ff = 6222 lbs.

P = 3144 lbs.

B = Ff since Ff>P

and the remainder of the variables are the same as those given for the normal conditions.

$$F_{a\text{-}pt} = \left[\frac{\pi(25.2)}{12}\right]\left[\frac{\frac{2(19597)}{3.3} - 1.3162\ (6222-3144)}{2.3162}\right]$$

Fa-pt = 22,290 lbs. for K=0.1 and

$$F_{a\text{-}pt} = \left[\frac{\pi(25.2)}{12}\right]\left[\frac{\frac{2(19597)}{3.3} - 1.3162\ (6222-1974)}{2.3162}\right]$$

Fa-pt = 17,904 lbs for K=0.2

Combining the non-prying and prying tensile bolt force

Fa-C = 40684 + 22290 = 62974 lbs. for K=0.1 and

Fa-C = 40684 + 17904 = 58,588 lbs. for K=0.2

The maximum average tensile stress in a lid bolt is

S_{ba} = 62974/.606 = 103,917 psi

This is less than the smaller of 0.7 Su or Sy which is 115,000 psi.

The average shear stress is due to torsion from preloading the bolts. The maximum shear stress is 10,170 psi. This is much less than the allowable stress 0.42 Sy or 69,300 psi.

The stress ratio for average tensile stress is

$\frac{103917}{115500}$ or 0.90. The stress ratio for

average shear stress is 10170/69300 or 0.1468.

The combined tensile and shear ratios must meet the following criterion:

$$Rt^2 + Rs^2 \leq 1$$

where Rt is the stress ratio for average tensile stress and Rs is the stress ratio for average shear stress ratio

$$(.90)^2 + (.1468)^2 = .811 \leq 1$$

which is acceptable.

Closure Flange Shoulder Analysis

Transverse lid deceleration loads are resisted by the closure flange shoulder during all normal and accident conditions. The shoulder thickness at the base has a shear area equal to

$$\text{Shear Area} = \frac{(31.00)^2-(28.56)^2}{4}\pi = 641 \text{ in}^2$$

For conservatism, it is assumed that only a 120° arc of the shoulder is effective. Effective shear is:

$$\text{Effective Shear} = \frac{120}{360}(641) = 214 \text{ in}^2$$

Normal Conditions of Transport

Maximum transverse deceleration loads during normal conditions occurs during the hypothetical one foot horizontal drop. Maximum deceleration is 17.0 g's. (Table 2.10.2-18 of Appendix 2.10.2)

Total Force = 17.0 x wt of lid = 17.0 (480) = 8,160 lbs.

$$\text{Average Shear Stress} = \frac{8,160}{214} = 38 \text{ psi}$$

$$\text{Allowable Average Shear} = S_y/2 = 30,000/2 = 15,000 \text{ psi}$$

$$\text{Factor of Safety} = \frac{15,000}{38} = 393$$

Hypothetical Accident Conditions of Transport

The maximum transverse deceleration load during accident conditions is 1.777 kips for the near horizontal 30 foot drop (i.e. 10°). The average shear stress across the shoulder is

$$\text{Average shear stress across shoulder} = \frac{1,777,000}{214} = 8,304 \text{ psi}$$

Allowable average shear = Ultimate stress of closure flange material/2

$$= \frac{75,000}{2} = 37,500 \text{ psi}$$

$$\text{Factor of Safety} = \frac{37,500}{8,304} = 4.52$$

Conclusions

The maximum average tensile stress in the lid bolts during normal conditions is 43,417 psi which is less than the allowable tensile stress of 2/3 yield, or 100,000 psi. The maximum stress intensity for the bolts during normal conditions is 57,620 psi which is much less than the allowable maximum stress intensity of 135,000 psi.

The fatigue analysis performed shows that for 350 round trip shipments, the bolts will not fail due to fatigue. They should be replaced after 350 shipments.

The maximum average tensile stress due to the accident conditions is 103,917 psi, which is less than the allowable stress of 115,000 psi. The average shear stress of 10,170 psi is much less than the allowable stress of 69,300 psi. The combined shear and tensile stress is also acceptable.

Lid shoulder stresses during both normal and accident conditions provide large margins of safety of resisting transverse lid deceleration loads.

CHAPTER TWO
APPENDIX 2.10.2
LIST OF FIGURES

CHAPTER TWO
APPENDIX 2.10.2
LIST OF TABLES

CHAPTER TWO
APPENDIX 2.10.2
LIST OF TABLES

APPENDIX 2.10.2
STRUCTURAL ANALYSIS OF IMPACT LIMITERS

2.10.2.1 INTRODUCTION

This appendix presents the details of the structural analysis of the TN-FSV impact limiters. The impact limiters are designed to absorb the kinetic energy resulting from the one (1) foot and thirty (30) foot normal and hypothetical accident free drop events specified by 10 CFR 71. Redwood and balsa wood are used as the primary energy absorption material(s) in the impact limiters. A sketch of the impact limiter is shown in Figure 2.10.2-1. A functional description of the impact limiters is given in Section 2.10.2.2. The impact limiter design criteria are described in Section 2.10.2.3.

A computer model of the TN-FSV Packaging was developed to perform a system dynamic analysis during the impact after the 30 foot drop accident. The model was developed for use with the ADOC (Acceleration Due To Drop On Covers) computer code described in detail in Section 2.10.2.5 which determines the deformation of the impact limiters, the forces on the containment and the packaging deceleration due to impact on an unyielding surface. Numerous cases were run to determine the effects of the wood properties and initial drop angle. A description of the computer model, input data, the ADOC computer code, analysis results and conclusions are given in Sections 2.10.2.4 through 2.10.2.5. The forces and decelerations calculated by ADOC have been used in the cask body structural analysis which is presented in detail in Appendix 2.10.1. Planned testing programs on the TN-FSV wood filled limiters is discussed in Appendix 2.10.3. Test results to date indicate that ADOC predicts higher deceleration values, crush forces and crush depths.

FIGURE WITHHELD UNDER 10 CFR 2.390

FIGURE 2.10.2-1
IMPACT LIMITER

The dynamic analysis of the TN-FSV for the one foot normal condition free drop is presented in Section 2.10.2.6. The analysis of the impact limiter attachments is described in Section 2.10.2.7.

2.10.2.2. DESIGN DESCRIPTION

The impact limiters absorb energy during impact events by crushing of balsa and redwood. The site, locations and orientation of each wood block is selected to provide protection for the cask during all normal conditions of transport and hypothetical accident conditions.

The top and bottom impact limiters are almost identical. Each has a diameter of 78 inches and a height of 31.5 inches. The inner and outer shells are Type 304 stainless steel joined by radial gussets of the same material. The gussets limit the stresses in the 0.1875 in. thick steel outer cylinder and end plates due to pressure differentials caused by elevation and temperature changes during normal transport and provide wood confinement during impact. The metal structure positions, supports, confines and protects the wood energy absorption material. The metal structure does contribute to the energy absorbing capability of the impact limiter. However, the contribution for a side drop or oblique angles is negligible because contact starts at a single point with the unyielding surface (target) and initiates buckling of a single gusset. After the drop event is complete, relatively few gussets are buckled.

The region of the impact limiter which is backed-up by the cask body is filled with balsa wood and redwood oriented with the grain direction perpendicular to the end of the cylindrical cask (See Figure 2.10.2-1). The material and grain orientation are selected to provide acceptably low deceleration to prevent lead slump during impact after the thirty foot end drop. A 2.0 inch layer of balsa

wood with the grain parallel to the end of the cylindrical cask is provided on the outer face of the impact limiter to minimize decelerations under the one foot end drop.

A 6.5 inch wide ring of redwood and 4.12 inch wide ring of balsa wood (consisting of 6 segments or blocks of wood) are located in the sides of the pie shaped compartments which surround the end of the cylindrical surface of the cask with the grain direction oriented radially. This ring of redwood absorbs most of the kinetic energy during a side drop. A big portion of redwood was selected for this portion of the impact limiter because of its high crush strength and hence the ability of a small amount of wood to absorb a large amount of energy in a relatively short crush distance.

The corners of the pie shaped compartments are filled with redwood and balsa blocks. A 15.5 inch section of redwood is located next to the side redwood and a 4.62 inch block of balsa wood is located in the outer corner. The primary function of the redwood block is energy absorption during corner drop while the balsa wood limits the decelerations to acceptable levels during the one foot normal condition end drop.

All wood blocks used in the impact limiters are composed of individual boards glued together with a Phenol Resorcinol Adhesive. This adhesive was selected for its superior strength and moisture resistance. The glue is waterproof up to a temperature of 200°F. The adhesive used conforms to the requirements of Federal Specification MMM-A-188b. The wood blocks are assembled and glued together in accordance with an approved QA procedure. Minimum properties of the adhesive are listed in Table 2.10.2-1. Ranges of shear and tensile strengths of each type of wood are also listed. The adhesive is significantly stronger than any of the wood used in the limiter in terms of shear and tensile strength. Therefore the boards or blocks of wood will not fail along the glue joints.

The other mechanical properties of the wood used in the analysis of the impact limiters are shown in Table 2.10.2-2. The crush stress properties used cover the range of expected values for the density and moisture content specified in the procurement specification. These ranges also cover the expected variation in wood properties over the operating temperature range of interest; i.e., -20°F to 170°F.* During procurement, wood samples are tested for density, moisture content and crush stress in accordance with an approved sampling plan.

If the density, moisture content, and crush stress are not within the specified range, the wood blocks from which samples are taken would be rejected.

For the end drop, all of the wood in the central part of the impact limiter that is directly "backed-up" by the cask body will crush. The wood in the corner and side of the limiter will tend to slide around the side of the cask since it is not supported or backed-up by the body and it will not crush or absorb energy as effectively as the wood that is backed-up. During the side or oblique drop the wood backed up by the cask will crush, while the wood beyond the end of the cask body will have a tendency to slide around the end of the cask. The analyses assume that the effectiveness of the portion of the wood that is not backed-up would be 20%. Effectiveness is defined as the actual crush force developed at the target by this

* Von Riessman, W. A. and Guiss, T. R. The Effects of Temperature on the Energy-Absorbing Characteristics of Redwood, Sandia Laboratories SAND-77-1509, Aug. 1978

Knoell, A. C., Environmental and Physical Effects in the Response Balsa Wood in an Energy Dissipation, Jet Propulsion Laboratory, Technical Report No. 32-944, June 15, 1966

TABLE 2.10.2-1

MECHANICAL PROPERTIES OF WOOD AND WOOD ADHESIVE

Minimum Properties of Phenol Resorcinol Adhesive

Shear Strength by Compression Loading	2,800 lbs/in^2 (1)
Shear Strength by Tension Loading	340 lbs/in^2 (1)

Properties of Heavy Balsa (10-12 lb/ft^3)

Shear Strength Parallel to Grain	315-385 psi max. (2)
Tensile Strength Perpendicular to Grain	140-160 psi (2)

Properties of Redwood

Shear Strength Parallel to Grain	940 psi (3)
Tensile Strength Perpendicular to Grain	240 psi (3)

(1) Federal Specification MMM-A-188b

(2) Dreisback, J.F., Balsa Wood and Its Properties, Columbia Graphs, Columbia, CT 1952

(3) Marks Standard Handbook for Mechanical Engineers, Eighth Edition, pg. 6-124

material divided by the theoretical force required to deflect the material. The analysis also assumes a range of wood crush strengths. When determining maximum deceleration, the maximum crush strengths are used and the non backed-up material is assumed to be 20% effective. When determining crush depth, the minimum wood crush strengths are used and the non backed-up wood is considered to be 20% effective.

The impact limiter is attached to the cask by using six high strength bolts. The attachments have been sized to withstand the loads transmitted during a side drop. This analysis is described in Section 2.10.2.7 of this Appendix.

2.10.2.3 DESIGN CRITERIA

The outside dimensions of the impact limiter are sized to be well within federal and state highway height and width restrictions. The balsa and redwood distribution and densities have been selected to limit the maximum cask body inertia loads due to the one foot normal condition drop and the thirty foot hypothetical accident drop so that the design criteria specified for the containment boundary, the non containment structure and shielding (See Section 2.1) are met.

The welded stainless steel structure of the impact limiter is designed so that the wood is maintained in position and is confined during crushing of the impact limiters. The outer shell and gussets are designed to buckle and crush during impact. Local failure of the shell is allowed during impact limiter crushing. The welded stainless steel shell and its internal gussets are designed to withstand pressure differences and normal handling and transport loads with stresses limited to the material yield strength.

The impact limiters are designed to remain attached to the cask body during all normal and hypothetical accident conditions.

2.10.2.4 ANALYSIS FOR 30 FT FREE DROP ACCIDENT CONDITIONS

2.10.2.4.1 Approach

The kinetic energy due to the hypothetical 30 ft drop accident is absorbed by crushing of the impact limiters on the ends of the packaging. The limiters contain materials, i.e. balsa and redwood, which provide controlled deceleration of the packaging by crushing between the target surface and the cask body.

The applicable regulation, 10CFR71.73, requires that the packaging be oriented for the drop so that it strikes the target in a position for which maximum damage is expected. Dynamic impact analyses were performed for different packaging orientations using the ADOC computer code described in Section 2.10.2.5. This computer code has been validated by comparing its dynamic results with those from hand calculations for relatively simple problems, comparing its calculated force-deflection curves with those obtained from static crush tests, and by correlating dynamic results with actual measured cask behavior on other programs.

2.10.2.4.2 Assumptions and Boundary Conditions

The assumptions and boundary conditions are as follows:

1. The cask body is assumed to be rigid and absorbs no energy. This assumption is realistic since the design criteria of Section 2.1.2 limit metal deformations to small values. All of the impact energy is therefore assumed to be absorbed by the impact limiters.

2. The crushable material is one or several anisotropic materials. The different wood regions are modeled individually.

3. The crush strengths of the wood sections are obtained from the properties parallel to and perpendicular to the grain based on the orientation of the cask at impact.

4. Each wood region is modeled as a one dimensional elastic, perfectly plastic material up to a specific locking strain. After reaching the locking strain, the stress increases linearly with the additional strain. The wood properties (modulus of elasticity, average crush strength, locking modulus, and locking strain) are taken from force-deflection curves of sample blocks of wood. Typical force-deflection curves for balsa and redwood are shown in Figures 2.10.2-1A and 2.10.2-1B. Since the locking strain varies from sample to sample, conservatively low locking strains of 80% for balsa and 60% for redwood are used.

5. The crush properties of the wood are varied with the initial angle of impact and do not change during the drop event being evaluated.

6. The cask and impact limiters are axisymmetric bodies.

7. The crushing resistances of the impact limiter shell and gussets have a negligible effect on the crush strength of the limiter and, therefore, a negligible effect on the impact forces and inertia loads.

2.10.2.4.3 Packaging Dynamic Computer Model

Figure 2.10.2-2 illustrates the computer model used for all packaging orientations. Regions I, II, and III in the model are used to delineate regions where different impact limiter materials are used. It should be noted that the properties of the three regions have been designed by choosing wood types and orientations to accommodate the crush requirements of the drop orientations. The crushable materials of Regions I, II, and III are selected to control the decelerations resulting from vertical, corner, and

SAMPLE SIZE : 2.0"DIA x 2.0" HT.
WOOD DENSITY : 6.03 lbs/FT^3

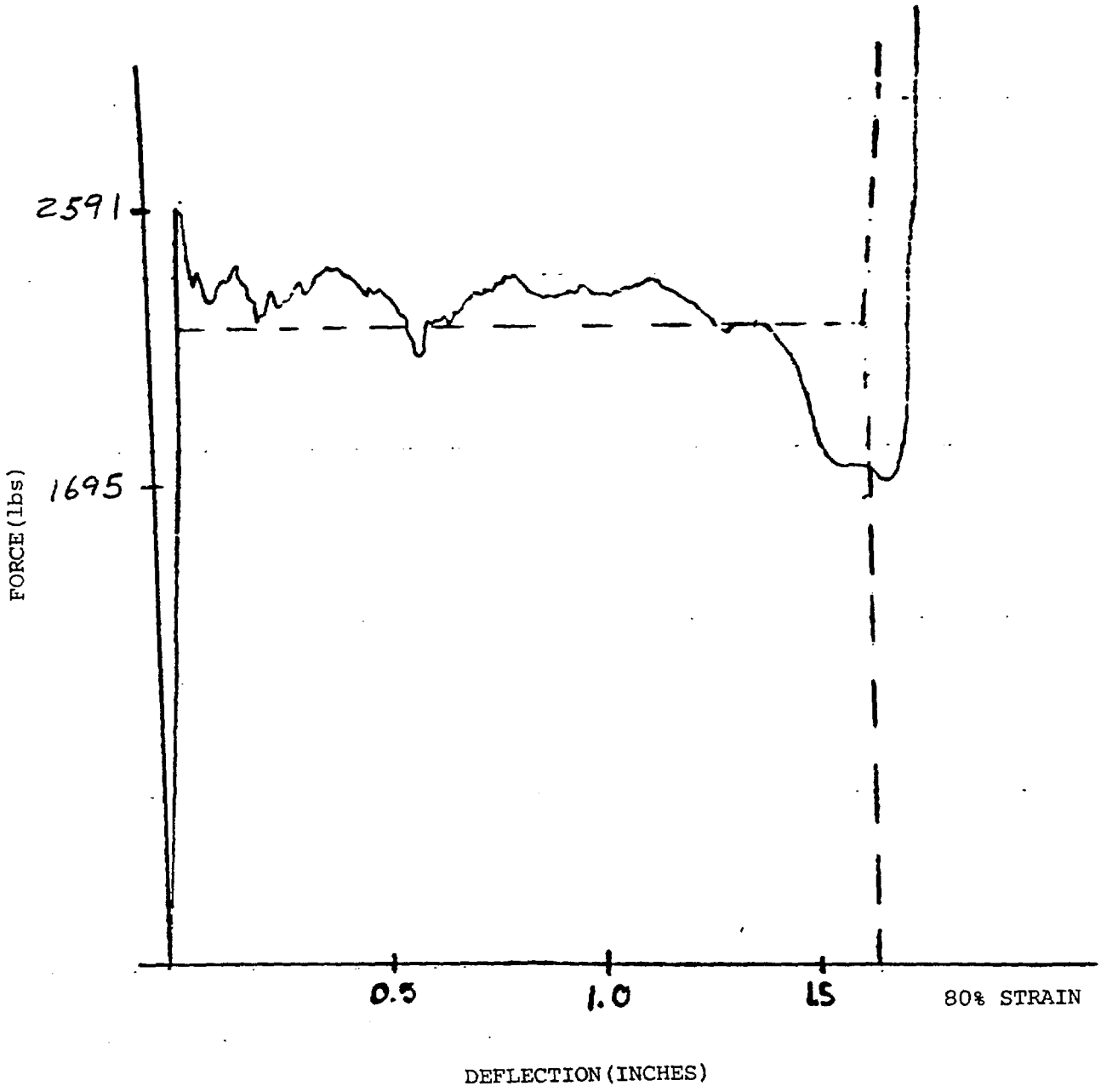

FIGURE 2.10.2-1A

SAMPLE FORCE-DEFLECTION CURVE FOR BALSA

NOTE:NOMINAL SAMPLE 1.625"DIA x 1.625" HT.

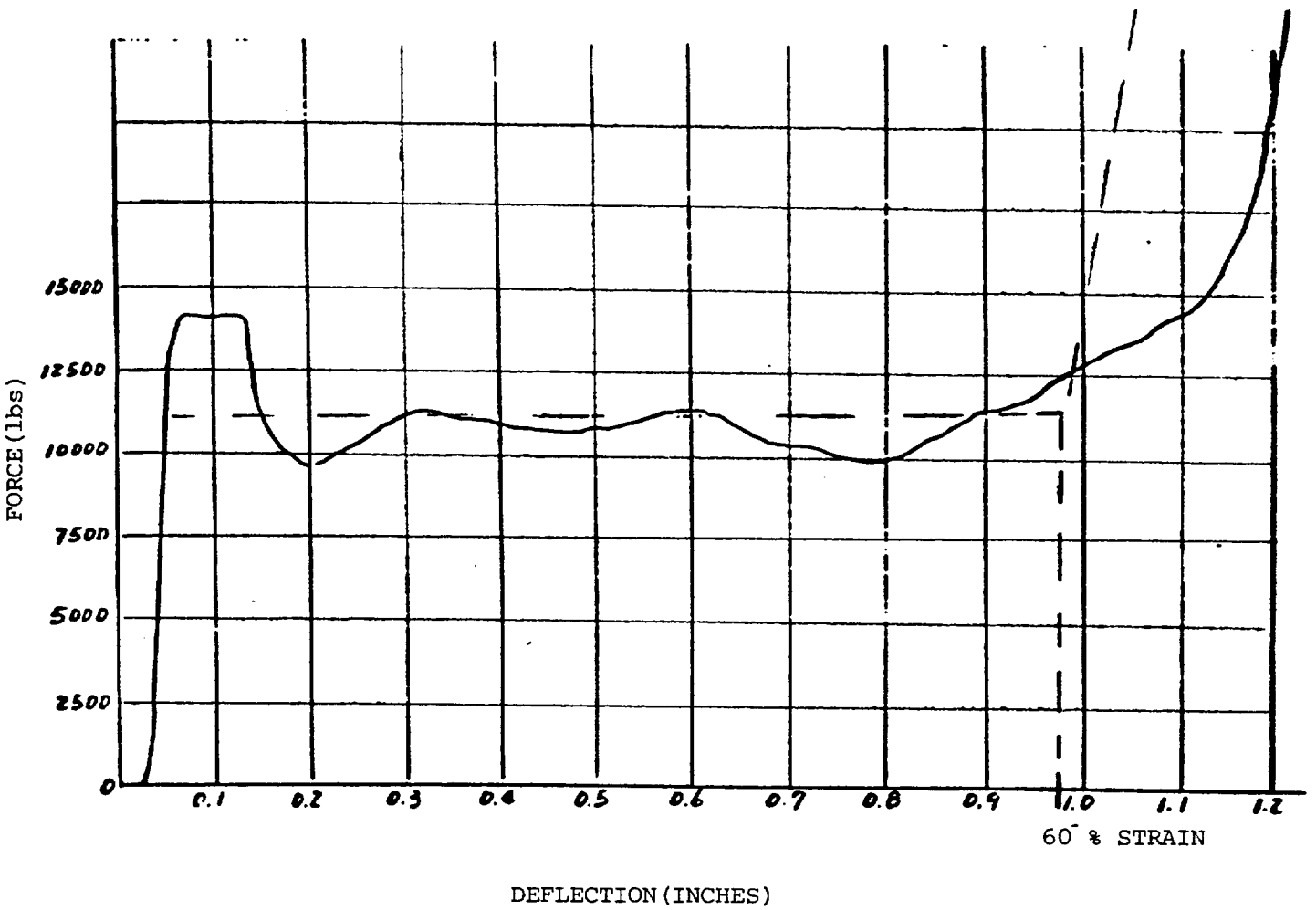

FIGURE 2.10.2-1B

SAMPLE FORCE-DEFLECTION CURVE FOR REDWOOD

side drop orientations, respectively. Table 2.10.2-2 tabulates the wood properties that were used to describe the wood stress-strain behavior in the analysis.

A portion of the impact limiter crushable material is backed up by the cask body as it crushes against the impact surface. The remaining material overhangs the cask body and is not backed up. Backed up regions project vertically from the target footprint to the cask body, while unbacked regions do not project vertically to the cask. The effectiveness of the energy absorbing crushable material varies depending on whether it is "backed up" by the cask or is unsupported. Two cases are analyzed to bound impact limiter performance. In one case the non backed up material is assumed to be 20% effective and maximum wood crush strength is used (maximum of the possible range based on specified density). In the other case the non-backed up material is also assumed to be 20% effective but the minimum wood strength is used. Evaluating impact limiter performance in this way results in a large range of deceleration values, crush forces and crush depth. This in combination with close control of wood properties during procurement assures that the effects of wood properties variation (including temperature effects) and the effectiveness (or lack of effectiveness) of the non backed-up portions of the limiter are covered.

2.10.2.4.4 Analysis Results Predicted by ADOC

The peak inertia loadings or cask body decelerations (in terms of g's) versus initial angle of impact are presented in Tables 2.10.2-3 and 2.10.2-4 for the 30 foot drop. (The 30 foot drop is measured from the impact surface to bottom of the impact limiter, the C.G. of the cask is much higher than 30 feet.) The depth of crush versus crush force is shown in Tables 2.10.2-5 to 2.10.2-16. Since the packaging CG is within a few inches of the center and the impact limiters are very similar, these tables are valid for impact on either end.

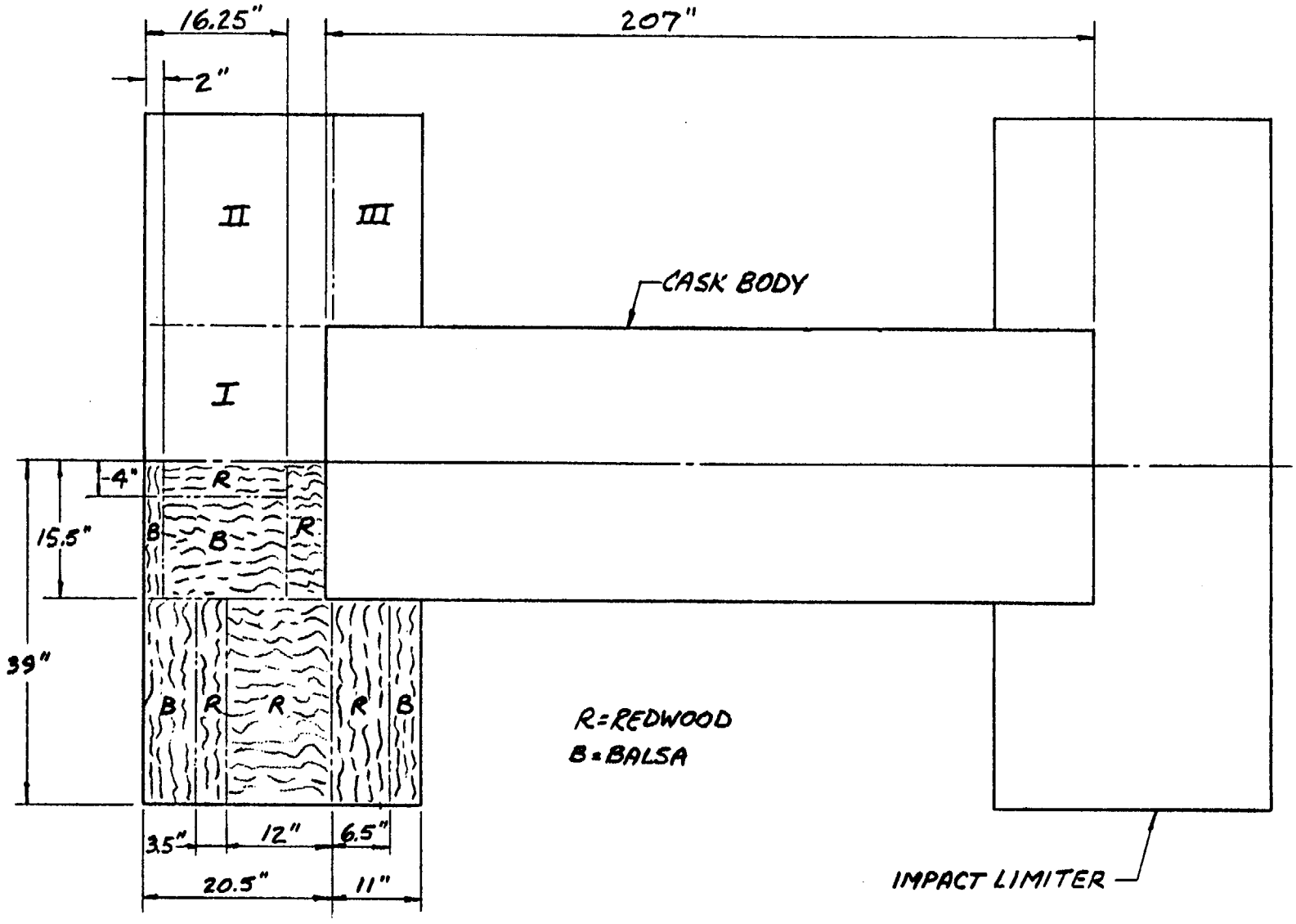

FIGURE 2.10.2-2

ADOC COMPUTER MODEL FOR TN-FSV PACKAGING

In order to determine the cask stresses, these maximum g loads are converted to forces and applied as quasistatic loadings on the outer cask body. A detailed ANSYS finite element model of the TN-FSV cask is used to perform this analysis. Cask body stress analyses are performed for the following drop orientations: end impact, side impact, CG over corner (80°) impact, 15° slap down, 45° impact on lid end, and 70° impact on lid end. The lid bolts are analyzed for the maximum axial g load of 54 which occurs at an angle of near perpendicular (90°). The full details of the stress analyses are presented in Section 2.10.1.

Based on the crush depths for the side drop from Tables 2.10.2-5 and 2.10.2-11, the trunnions would not hit the target. For the maximum wood properties and 20% effectiveness of non backed-up wood the clearance after the limiters crush would be approximately 12.71 inches. For the minimum wood properties and 20% effectiveness of non backed-up wood, the clearance after the limiter crush would be 10.17 inches. It is expected that the crush depth would be somewhere between the two bounding cases.

2.10.2.4.5 Results Based on Scans Calculations

The depth of crush versus crush force from the ADOC run was inputed into SCANS* for G load calculations. The results are presented in Table 2.10.2-17. As can be seen, the deceleration values calculated by scans agree well with the values predicted by ADOC.

*M.A. Gerhard, D.J. Trummer, G.L. Johnson, and G.C. Mok "SCANS (Shipping Cask Analysis System)" NUREG/CR-4554.

TABLE 2.10.2-2

TYPICAL WOOD MATERIAL PROPERTIES

PROPERTY	HIGH DENSITY BALSA	REDWOOD
Density	10-12 lb/ft^3	18.7-27.5 lb/ft^3
Parallel to Grain		
Crush Stress	1560-2010 psi	5000-6500 psi
Locking Strain	0.8	0.6
Unloading Modulus	32,000 psi	1,247,000 psi
Locking Modulus	3,400 psi	4,100 psi
Perpendicular to Grain		
Crush Stress	300-420 psi	750-975 psi
Locking Strain	0.8	0.6
Unloading Modulus	32,000 psi	1,247,000 psi
Locking Modulus	3,400 psi	4,100 psi

TABLE 2.10.2-3

MAXIMUM INERTIA G LOAD VERSUS INITIAL ANGLE OF IMPACT

FOR 30 FOOT DROP

MAXIMUM WOOD CRUSH STRESS

EFFECTIVENESS OF NON-BACKED UP WOOD: 20%

Initial Angle Of Impact	MAXIMUM G LOAD DURING FIRST IMPACT			
	Axial @ C.G.	TRANSVERSE Primary Impact End	TRANSVERSE @ C.G.	TRANSVERSE Opposite End
90°	54	0	0	0
80°	48	- 8	- 3	1
75°	46	-11	- 5	1
70°	43	-16	-7	2
60°	37	-35	-13	8
50°	31	-52	-19	14
45°	25	-52	-18	16
40°	17	-42	-15	12
30°	12	-45	-16	13 *
20°	11	-61	-21	20 *
15°	11	-75	-25	25 *
10°	10	-84	-28	29 *
5°	8	-95	-31	33 *
0°	0	-71	-71	-71
	MAXIMUM G LOAD DURING SECOND IMPACT			
30°	-2	42	-33	-107
20°	-1	47	-36	-120
15°	-1	47	-37	-120
10°	-1	47	-37	-120**
5°	-1	45	-37	-119

* MAXIMUM ACCELERATION OCCURRED DURING SECOND IMPACT

** MAXIMUM IMPACT FORCE 1,777,140 LB. AT DISTANCE OF 98.84 IN. FROM C.G.

TABLE 2.10.2-4

MAXIMUM INERTIA G LOAD VERSUS INITIAL ANGLE OF IMPACT
FOR 30 FOOT DROP
MINIMUM WOOD CRUSH STRESS
EFFECTIVENESS OF NON-BACKED UP WOOD: 20%

	MAXIMUM G LOAD DURING FIRST IMPACT			
		TRANSVERSE		
Initial Angle Of Impact	Axial @ C.G.	Primary Impact End	@ C.G.	Opposite End
90°	42	0	0	0
80°	54	- 9	- 4	1
70°	43	-15	- 7	1
60°	32	-30	-12	7
50°	28	-46	-16	13
45°	20	-40	-14	12
40°	15	-40	-15	11
30°	11	-42	-15	13 *
20°	9	-50	-17	16 *
15°	9	-60	-20	20
10°	8	-67	-22	23 *
5°	6	-75	-24	27 *
0	0	-56	-56	-56
	MAXIMUM G LOAD DURING SECOND IMPACT			
30°	-2	31	-24	-80
20°	-1	38	-29	-97
15°	-1	38	-29	-97
10°	-1	38	-29	-95
5°	-1	37	-29	-95

* MAXIMUM ACCELERATION OCCURRED DURING SECOND IMPACT

TABLE 2.10.2-5

DEPTH OF CRUSH VERSUS CRUSH FORCE

IMPACT ANGLE: 0°

WOOD PROPERTIES: MAXIMUM WOOD CRUSH STRESS

DISPLACEMENT (INCHES)	FORCE (KIPS)
0	0
2.516	943
4.676	1559
6.425	1635
8.60	1690

TABLE 2.10.2-6

DEPTH OF CRUSH VERSUS CRUSH FORCE

IMPACT ANGLE: 15°

WOOD PROPERTIES: MAXIMUM WOOD CRUSH STRESS

PRIMARY IMPACT		SECONDARY IMPACT	
DISPLACEMENT (INCHES)	FORCE (KIPS)	DISPLACEMENT (INCHES)	FORCE (KIPS)
2.64	1.2	0.44	1487
5.29	13	4.32	1632
7.95	956	7.38	1697
10.43	1051	9.62	1749
12.45	1118	11.01	1766
14.02	1143		
15.12	1172		
15.82	1320		

TABLE 2.10.2-7

DEPTH OF CRUSH VERSUS CRUSH FORCE

IMPACT ANGLE: 45°

WOOD PROPERTIES: MAXIMUM WOOD CRUSH STRESS

DISPLACEMENT (INCHES)	FORCE (KIPS)
0	0
2.63	57
5.26	269
7.86	370
10.4	519
12.83	771
15.05	966
18.76	1378
20.92	1479

TABLE 2.10.2-8

DEPTH OF CRUSH VERSUS CRUSH FORCE

IMPACT ANGLE: 70°

WOOD PROPERTIES: MAXIMUM WOOD CRUSH STRESS

DISPLACEMENT (INCHES)	FORCE (KIPS)
5.29	176
7.93	525
10.54	1016
13.05	1584
15.36	1874
17.36	1968
19.01	2027
20.25	2051
21.1	2056

TABLE 2.10.2-9

DEPTH OF CRUSH VERSUS CRUSH FORCE

IMPACT ANGLE: 80°

WOOD PROPERTIES: MAXIMUM WOOD CRUSH STRESS

DISPLACEMENT (INCHES)	FORCE (KIPS)
0	0
2.64	44
5.28	1448
7.83	1865
10.11	2008
12.05	2123
13.6	2263
14.75	2296

TABLE 2.10.2-10

DEPTH OF CRUSH VERSUS CRUSH FORCE

IMPACT ANGLE: 90°

WOOD PROPERTIES: MAXIMUM WOOD CRUSH STRESS

DISPLACEMENT (INCHES)	FORCE (KIPS)
0	0
2.6	2126
4.87	2126
6.73	2605
8.17	2605
9.6	2605

TABLE 2.10.2-11

DEPTH OF CRUSH VERSUS CRUSH FORCE

IMPACT ANGLE: 0°

WOOD PROPERTIES: MINIMUM WOOD CRUSH STRESS

DISPLACEMENT (INCHES)	FORCE (KIPS)
2.54	725
4.81	1199
6.77	1257
8.39	1305
9.66	1305
10.58	1344
11.14	1347

TABLE 2.10.2-12

DEPTH OF CRUSH VERSUS CRUSH FORCE

IMPACT ANGLE: 15°

WOOD PROPERTIES: MINIMUM WOOD CRUSH STRESS

PRIMARY IMPACT		SECONDARY IMPACT	
DISPLACEMENT (INCHES)	FORCE (KIPS)	DISPLACEMENT (INCHES)	FORCE (KIPS)
5.29	9.32	3.27	1217
7.95	733	7.08	1305
10.47	813	10.2	1359
12.64	867	12.8	1400
14.46	890	14.6	1431
15.96	920	15.8	1431
17.75	936		
18.04	1057		

TABLE 2.10.2-13

DEPTH OF CRUSH VERSUS CRUSH FORCE

IMPACT ANGLE: 45°

WOOD PROPERTIES: MINIMUM WOOD CRUSH STRESS

DISPLACEMENT (INCHES)	FORCE (KIPS)
2.64	43
5.28	205
7.88	284
10.43	395
12.9	601
15.3	815
17.5	993
19.38	1173

TABLE 2.10.2-14

DEPTH OF CRUSH VERSUS CRUSH FORCE

IMPACT ANGLE: 70°

WOOD PROPERTIES: MINIMUM WOOD CRUSH STRESS

DISPLACEMENT (INCHES)	FORCE (KIPS)
5.29	127
7.93	397
10.56	786
13.11	1238
15.55	1452
17.70	1538
19.56	1586
21.14	1823
22.4	2022
23.3	2042

TABLE 2.10.2-15

DEPTH OF CRUSH VERSUS CRUSH FORCE

IMPACT ANGLE: 80°

WOOD PROPERTIES: MINIMUM WOOD CRUSH STRESS

DISPLACEMENT (INCHES)	FORCE (KIPS)
2.6	32
5.3	1114
7.9	1430
10.4	1561
12.5	1731
14.3	1778
15.9	2024
17.1	2393
17.8	2572

TABLE 2.10.2-16

DEPTH OF CRUSH VERSUS CRUSH FORCE

IMPACT ANGLE: 90°

WOOD PROPERTIES: MINIMUM WOOD CRUSH STRESS

DISPLACEMENT (INCHES)	FORCE (KIPS)
2.6	1655
4.97	1655
7.03	2014
8.74	2014
10.06	2014
10.99	2014

TABLE 2.10.2-17

G LOAD PREDICTION - ADOC VERSUS SCANS

IMPACT ANGLE	VERTICAL G'S	
	ADOC	SCANS
0°	71	69.7
15° First Impact	27.09	22.7
15° Second Impact	36.58	35
30°	19.56	17
45°	30.48	26.9
60°	38.91	35.9
75°	45.75	44.5
C.G.	47.85	46.6
90°	54.4	54.4

2.10.2.5 SUMMARY DESCRIPTION OF ADOC COMPUTER CODE

One of the critical loadings which must be considered in the design of transport packagings to be used for the shipment or radioactive material is a free drop from thirty-foot height onto an unyielding surface (10CFR71). The packaging must be dropped at an orientation that results in the most severe damage. Impact limiters are usually provided on the packaging to cushion the effects of such impact on the containment portion of the packaging. The limiters are usually hollow cylindrical cups which encase each end of the containment and are filled with an energy absorbing material such as wood or foam.

A computer code, ADOC (Acceleration due to Drop On Covers), has been written to determine the response of a packaging during impact. The analysis upon which this code is based in discussed in this section. The overall analysis of the packaging response is discussed in Section 2.10.2.5.1, and the methods used to compute the forces in the limiters as they crush are presented in Section 2.10.2.5.2.

2.10.2.5.1 General Formulation

The general formulation used to compute the response of the packaging as it impacts with a rigid target is discussed in this section. The assumptions upon which the analysis is based are first presented followed by a detailed development of the equations of motion used to calculate the packaging dynamic behavior. This is followed by a discussion of the numerical methods and the computer code used to implement the analysis. A significant part of the development is concerned with the prediction of forces developed in the impact limiters as the impact occurs. This aspect of the problem is discussed in Section 2.10.2.5.2.

ASSUMPTIONS

The cask body is assumed to be rigid and axisymmetric. Therefore, all of the energy absorption occurs in the impact limiters which are also assumed to have an axisymmetric geometry. Several assumptions are made in calculating the forces which develop in the limiters as they crush. These are discussed in Section 2.10.2.5.2. Since the packaging is axisymmetric, its motion during impact will be planar. The vertical, horizontal, and rotational components of the motion of the packaging center of gravity (CG) are used to describe this planar motion.

EQUATIONS OF MOTION

A sketch of the packaging at the moment of impact is shown on Figure 2.10.2-3. The packaging is dropped from a height (H), measured from the lowest point on the packaging to the target. The packaging is oriented during the drop, and at impact, so that the centerline is at an angle (θ) with respect to the horizontal. At the instant of impact, the packaging has a vertical velocity of:

$$V_0 = \sqrt{2gH} \qquad (1)$$

Where,

g = gravitational constant

At some time (t) after first impact, the packaging has undergone vertical (u), horizontal (x), and rotational (ρ) displacements. The location of the packaging at this time is shown on Figure 2.10.2-4. One or both of the limiters have been crushed as shown. The resulting deformations (and strains) in the limiters result in forces which the limiters exert on the packaging, thereby decelerating it. These forces, and their points of application on the packaging, are shown on Figure 2.10.2-4 as F_{v1}, F_{v2} and F_h. The method used to calculate these forces and the points of application is given in Section 2.10.2.5.2, below.

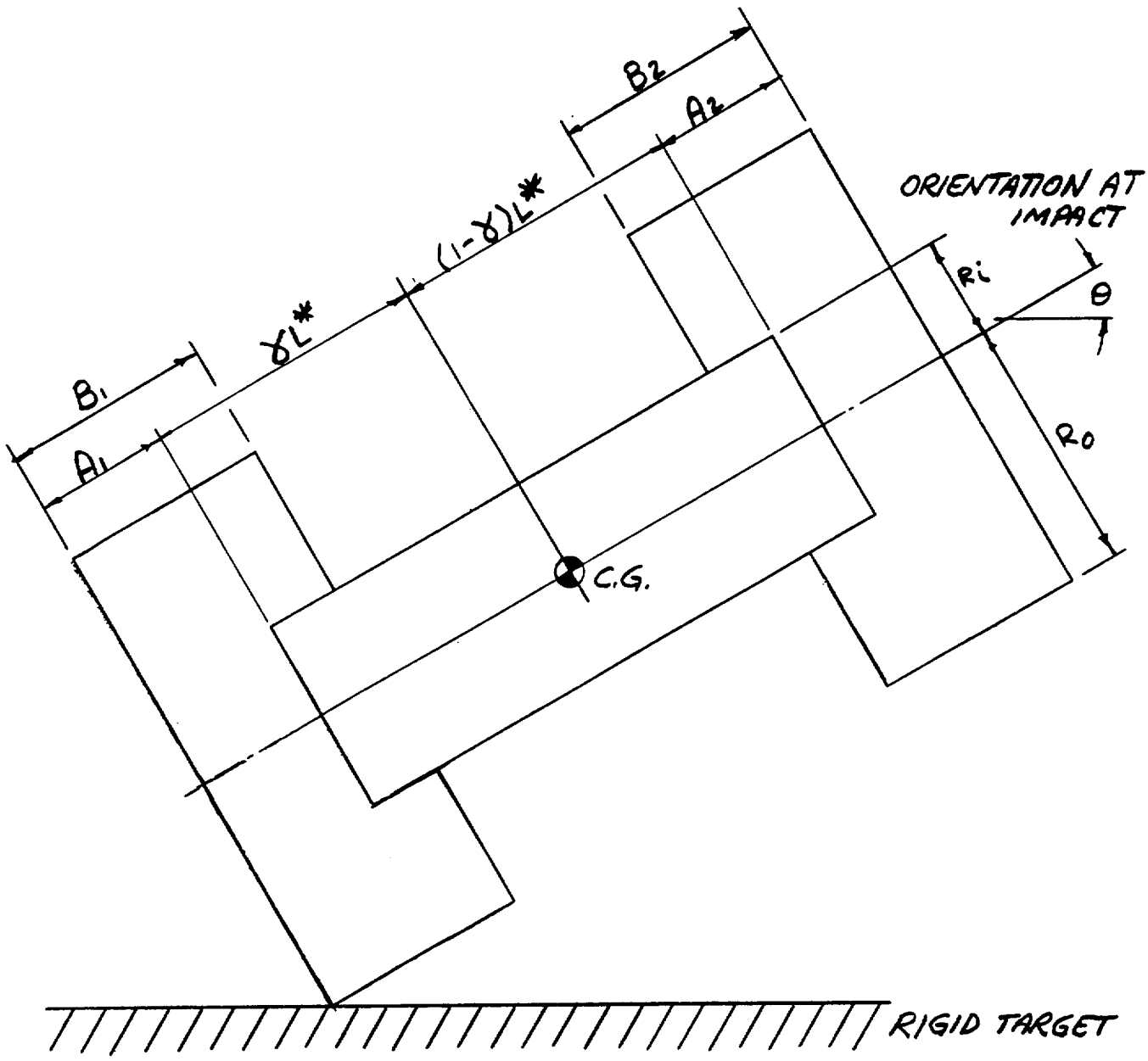

FIGURE 2.10.2-3
GEOMETRY OF PACKAGING

The three equations of motion describing the motion of the cask are:

$$M\ddot{u} + F_{v1} + F_{v2} - W = 0 \quad (2)$$

$$M\ddot{x} - F_h = 0 \quad (3)$$

$$J\ddot{\rho} - F_{v1} X_{v1} + F_{v2} X_{v2} + F_h Y_h = 0 \quad (4)$$

Where,

M = mass of packaging

J = polar moment of inertia of the packaging about its CG

W = packaging weight

($\ddot{}$) = acceleration

At impact (t = 0), all of the initial conditions are zero except that $\dot{u}$ = the vertical velocity,

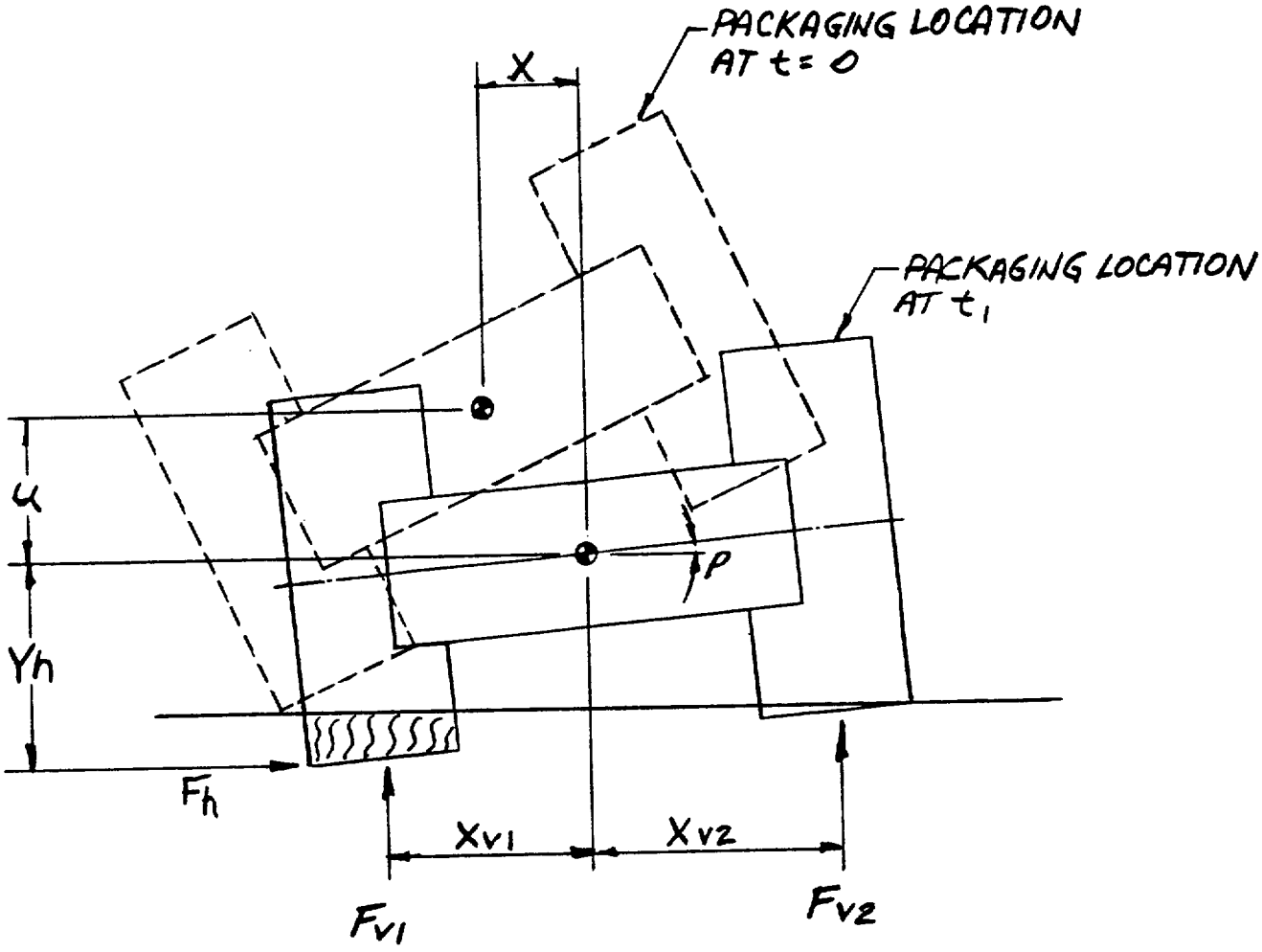

FIGURE 2.10.2-4

PACKAGING LOCATION AT TIME (t)

COMPUTER SOLUTION

The computer code is written to compute the motion of the packaging during impact. The solution is obtained by numerically integrating the equations of motion (equations 2, 3, and 4) from the time of impact (t = 0) to a specified maximum time (t_{max}). The integrations are carried forward in time at a specified time increment (Δt). Parametric studies indicate that a time increment of 1 msec is sufficiently small so that further reduction of the time increment does not affect the results. Solutions are usually carried out to about 150 msec for the near horizontal drops and to about 50 msec for the near vertical drops. The significant motions of the packaging normally occur within these time periods.

A standard fourth order Runge Kutta numerical integration method is used to perform the numerical integrations. The following procedure is used to carry the solution from time (t_i) to time (t_{i+1}). Note that at time (t_i) the displacements and velocities of the three degrees of freedom describing the motion of the CG of the packaging are known.

(1) Calculate the deformation of each of the limiters based on the packaging geometry and the motion of the packaging's CG (see Section 2.10.2.5.2 for details).

(2) Calculate the forces which the limiters exert on the packaging body using the deformation of the limiters and their stress-strain characteristics (see Section 2.10.2.5.2 for details).

(3) Use Equations 2, 3, and 4 to calculate the accelerations during the time interval.

(4) Use the Runge Kutta equations to calculate the location and velocity of the cask CG at time (t_{i+1}).

(5) Go to step (1) to repeat the process until time = t_{max}.

(6) Generate the output.

Output from the code consists of:

Problem title, packaging geometry, drop conditions, and integration data.

Limiter geometric and material property data.

History of packaging CG motion and amount of crushing in each of the limiters.

Force history data.

Plot of acceleration histories.

Plot of maximum limiter deformations.

2.10.2.5.2 Forces in Limiters

The methods used to calculate the forces (F_{v1}, F_{v2}, and F_h) in the limiter caused by a given crush depth are discussed in this section. These calculations are used to perform steps (1) and (2) above. The limiter geometry and material specification is discussed first. The general methodology used to calculate the forces are then presented which is followed with a detailed development of the equations used to calculate the force-displacement relationships.

LIMITER GEOMETRY

A sketch of the model of a limiter is shown on Figure 2.10.2-5. Regions I, II and III are used to delineate regions where different materials are used. It should be noted that the properties of the three regions are designed to accommodate the crush requirements of

the three significant drop orientations. The properties of regions I, II and III are selected to control the decelerations resulting from vertical, corner, and shallow drop orientations, respectively. The properties used to describe the stress-strain behavior of each of the three materials are discussed below. The dimensions (A) and (B) may vary for the limiters at each end of the packaging, but (R_o) and (R_i) are taken to be the same for both limiters. The same material properties are used for each of the limiters.

GENERAL APPROACH

The ideal energy absorbing material is one that has a stress-strain curve that has a large strain region where the stress is constant. Such a materials absorbs the maximum energy while minimizing force (which determines the magnitude of the deceleration). Wood, foam, and honeycomb materials exhibit such behavior and are prime candidates for impact limiter crushable material. If the constant

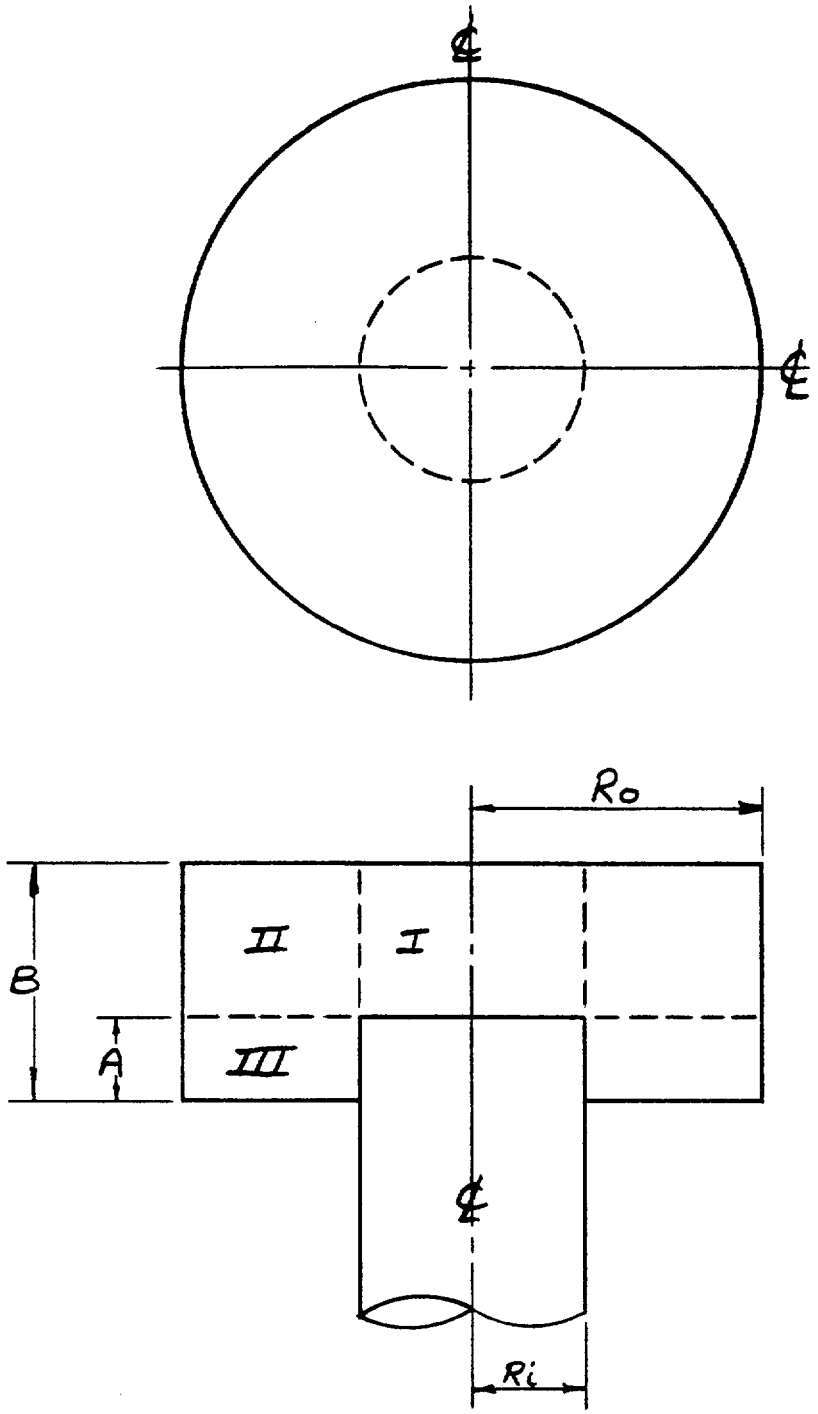

FIGURE 2.10.2-5
GEOMETRY OF LIMITER

stress region of the stress-strain curve is of primary interest, the forces may be calculated as the crush stress times the area of the surface defined by the intersection of the target with the doughnut shape of the impact limiter. This approach assumes that the crush stress, which acts normal to the crush surface, is not influenced by stresses acting in directions parallel to the crush surface (i.e., the confining stresses). This assumption is made in the computer code. The crush stress used as input to the code is selected to represent that value which is consistent with the degree of confinement afforded by the impact limiter geometry for the drop orientation considered. Therefore, the crushable material is modeled in the code with a one dimensional (oriented normal to the crush surface) stress-strain law. The properties of the stress-strain law are selected to represent the degree of confinement provided by stresses acting in the other two dimensions. The properties of the crushable material are not modified as the packaging rotates but are selected to represent the material properties for the initial crush direction of the material.

A portion of the "crushed" area of the limiter is often not backed up by the packaging body (i.e., a projection of a point in this non backed up area normal to the target (impact surface) does not intersect the cask body). The user must specify the percentage of these forces which are to be included in the calculation. The confinement provided by the overall construction of the limiter will determine the extent to which these non backed up forces are actually effective.
It should be emphasized that the computer code does not perform any computations which would allow the user to judge the adequacy of the selected percentage of non backed-up forces which are counted.

The evaluation of the impact area and its centroid (required to locate the impact forces) is computationally complicated because of the many variations possible in the manner in which the target intersects the limiter. This problem is resolved by dividing the surface of the limiter into many small segments. The segment is

located relative to the target at each computation. If the segment's original location is below the target, then it has crushed and it contributes a force equal to the stress times its area projected on the target. The location of this force is also known. The strain at the segment may also be evaluated so that the peak strains may be determined and stresses may be evaluated for strains which fall outside of the constant crush stress region of the stress-strain law.

The forces must be calculated at each time that the solution for the packaging response is computed. The problem, therefore, is to determine the forces acting on the limiters given the current location of the packaging center of gravity. The solution for the location of the packaging center of gravity is discussed in Section 2.10.2.5-1. The procedure used to perform these computations is as follows (each of the steps is detailed below).

(1) Define the location of the target relative to the limiters from the current location of the packaging center of gravity relative to the target.

(2) Divide the surface of the limiter into segments and calculate the strain in a one dimensional element spanning the distance between the center of the segment and the packaging body.

(3) Compute the stress in the element from the stress-strain relationship. Multiply the stress by the area of the element projected onto the target.

(4) After all of the segments on the limiter are evaluated, sum the segment forces and moments of the forces to find the total force and moment acting on the packaging.

(5) Calculate the horizontal force and moment of the horizontal force.

(6) Use equations 2, 3, and 4 to extend the solution to the next time step. The new solution consists of the location of the packaging CG at the new time. The above steps are then repeated. This process is continued until the specified maximum time is reached.

DETAILS OF FORCE COMPUTATIONS

Details of each of the six steps outlined above are given in this section. Note that the location of the packaging CG is known at the beginning of this computational sequence.

Deformation of the Limiter

The first step in the computation is to evaluate the location of the limiters relative to the target given the location of the packaging CG relative to the target. The limiter position relative to the target is defined by the six variables (D_1 through D_6) as shown on Figure 2.10.2-6. The location of the cask at first contact is shown on Figure 2.10.2-6a with the subscript (o) added to the D's indicating initial values. The initial values of these parameters (when the lowest corner of the packaging first contacts) are found from geometric considerations:

$$
\begin{aligned}
D_{10} &= 2R_0 \cos\theta \\
D_{20} &= 0 \\
D_{30} &= B_1 \sin\theta \\
D_{40} &= D_{30} + D_{10} + L^* \sin\theta + B_2 \sin\theta \\
D_{50} &= D_{40} - D_{10} \\
D_{60} &= D_{30} + L^* \sin\theta
\end{aligned}
\qquad (5)
$$

At a given time (t) the packaging CG has displaced vertically (u), horizontally (x), and has rotated (ρ) and reached the position shown in Figure 2.10.2-6b. Each of the six points have then fallen by an amount:

$$\Delta D = u+l(SIN\ \theta-SIN(\theta-\rho))+r(COS\ \theta-COS(\theta-\rho)) \quad (6)$$

Where,

l = axial distance CG to point (+CG to top)

r = radial distance CG to point (+CG to impact)

Then the corner deformation (D_2) at time (t + 1) becomes:

$$D_{2\ (t\ +\ 1)} = D_{2t} + \Delta D_2$$

Where,

$$l_1 = l_2 = -yL^* - B_1$$
$$l_3 = -yL^*$$
$$l_4 = l_5 = (1-y)L^* + B_2$$
$$l_6 = (1-y)L^*$$
$$r_1 = r_4 = -R_0$$
$$r_2 = r_3 = r_5 = r_6 = R_0$$

To facilitate the computation of strains in the limiter, the position of the limiter relative to the impact surface is classified as shown in Figure 2.10.2-7. There are three possible locations of the impact surface relative to the limiter. The task is therefore to define which of the three patterns apply, and to determine the parameters (ϕ) and (Δ) in terms of the variables D_1 through D_6, just determined.

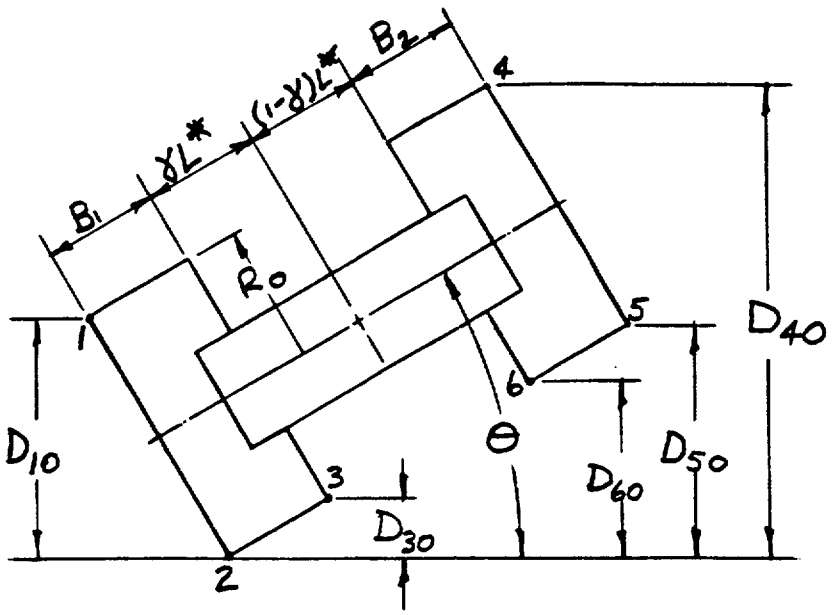

a) IMPACT LIMITER PARAMETERS AT FIRST IMPACT

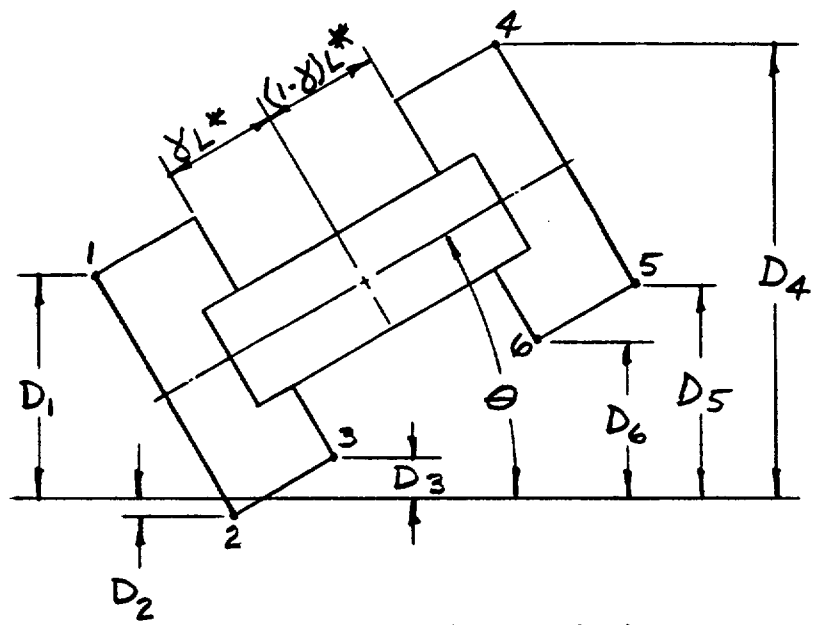

b) IMPACT LIMITER PARAMETER - GENERAL

FIGURE 2.10.2-6
DEFINITION OF LIMITER DEFORMATION

These deformations are next related to the three types of crush patterns for the bottom limiter shown on Figure 2.10.2-7. Crush pattern I applies when:

$$D_1 < 0;\ D_2 < 0;\ D_3 > 0 \tag{8}$$

Then,

$$\Delta = -D_2/\cos\phi \tag{9}$$

$$\phi = \cos^{-1}\left((D_3-D_2)/B_1\right)$$

Crush pattern II applies when:

$$D_1 > 0;\ D_2 < 0;\ D_3 > 0 \tag{10}$$

Then,

$$\Delta = -D_2/\cos\phi \tag{11}$$

$$\phi = \cos^{-1}\left((D_3-D_2)/B_1\right)$$

Crush pattern III applies when:

$$D_1 > 0;\ D_2 < 0;\ D_3 < 0 \tag{12}$$

Then,

$$\Delta = D_2/\sin\phi \tag{13}$$

$$\phi = \sin^{-1}\left((D_1-D_2)/2R_0\right)$$

The same set of equations apply to the top limiter if (D_1, D_2, D_3, B_1) are replaced with (D_4, D_5, D_6, B_2) in equations (8) through (13).

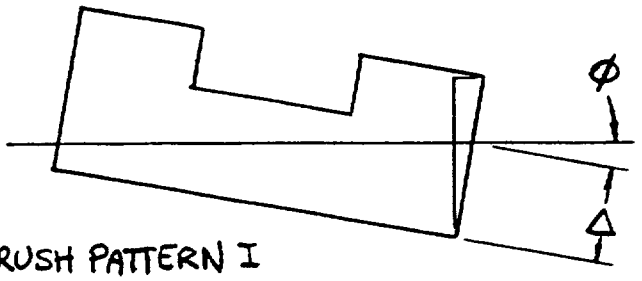

a) CRUSH PATTERN I

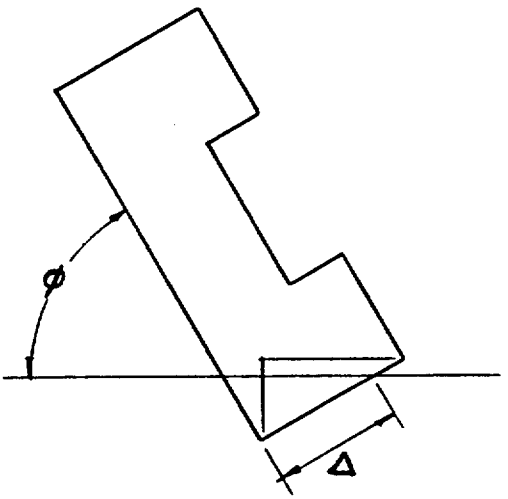

b) CRUSH PATTERN II

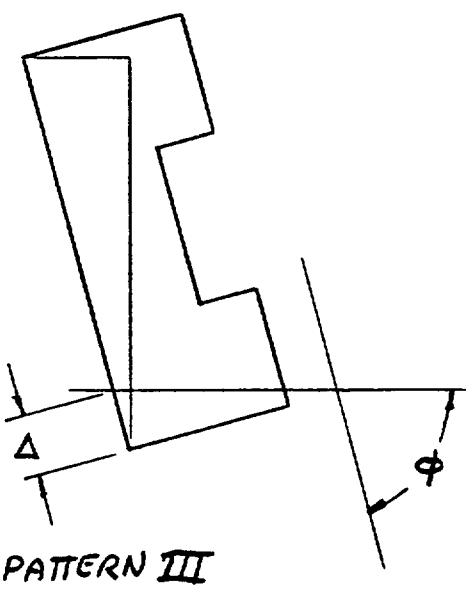

c) CRUSH PATTERN III

FIGURE 2.10.2-7
CRUSH PATTERN IN LIMITER

Strains in Limiters

The next step in the computation is to calculate strains in the limiters given the deformation defined above. The limiters are first divided into segments as shown in Figure 2.10.2-8. The number of segments used for the bottom (NB) and the sides (NS) are input by the user. Locations on the surface of the limiters are described in terms of the (R,Z,β) coordinate systems shown on the figure. Strains in the segments along the sides of the limiters are calculated based on the location of the center of the segment (R_0,Z,β). The segments at the bottom are divided into two pieces: one for $R < R_i$ (i.e. in Region 1) and the second for $R > R_i$. A strain is calculated for each of these two pieces for each segment along the bottom surface.

The strains (ε) are calculated as the deformation of the point normal to the crush surface (δ) divided by the undeformed distance of the point from the surface of the limiter to the outer container (q), again measured normal to the crush surface. Therefore:

$$\varepsilon = \delta/q \qquad (14)$$

Different equations govern each of these parameters for each of the three crush patterns as shown on Figure 2.10.2-7.

The geometry for crush pattern I is shown on Figure 2.10.2-9. Forces resulting from deformation of the side elements are neglected for this crush pattern. It may be shown that the deformation is:

$$\delta = \Delta \text{ COS } \phi + (R \text{ COS } \beta - R_0) \text{ SIN } \phi \qquad (15)$$

The undeformed length of the element is taken measured to the plane of the packaging bottom so that:

$$q = A_1 \text{COS } \phi \qquad (16)$$

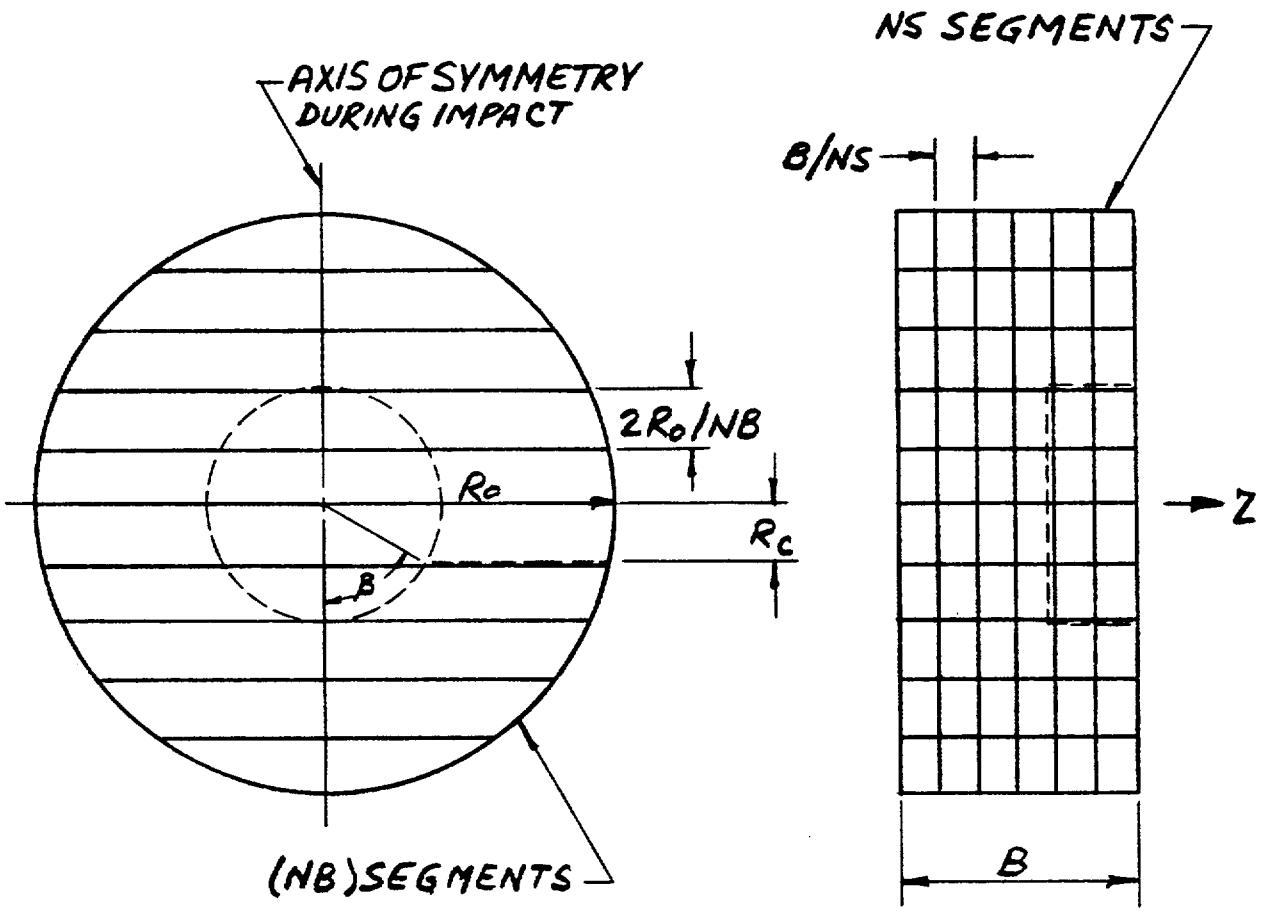

FIGURE 2.10.2-8
SEGMENTED LIMITER

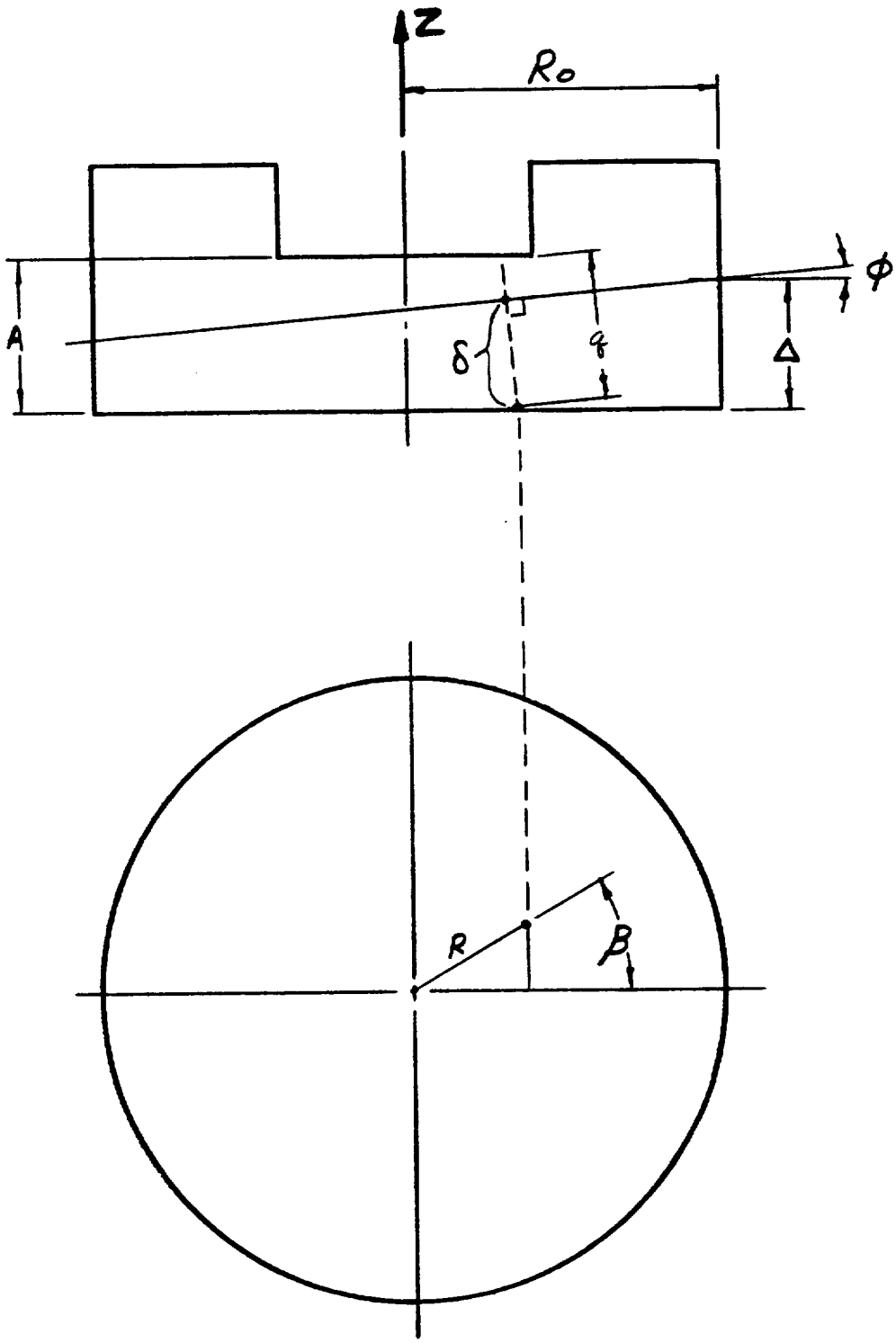

FIGURE 2.10.2-9
STRAIN COMPUTATION FOR CRUSH PATTERN I

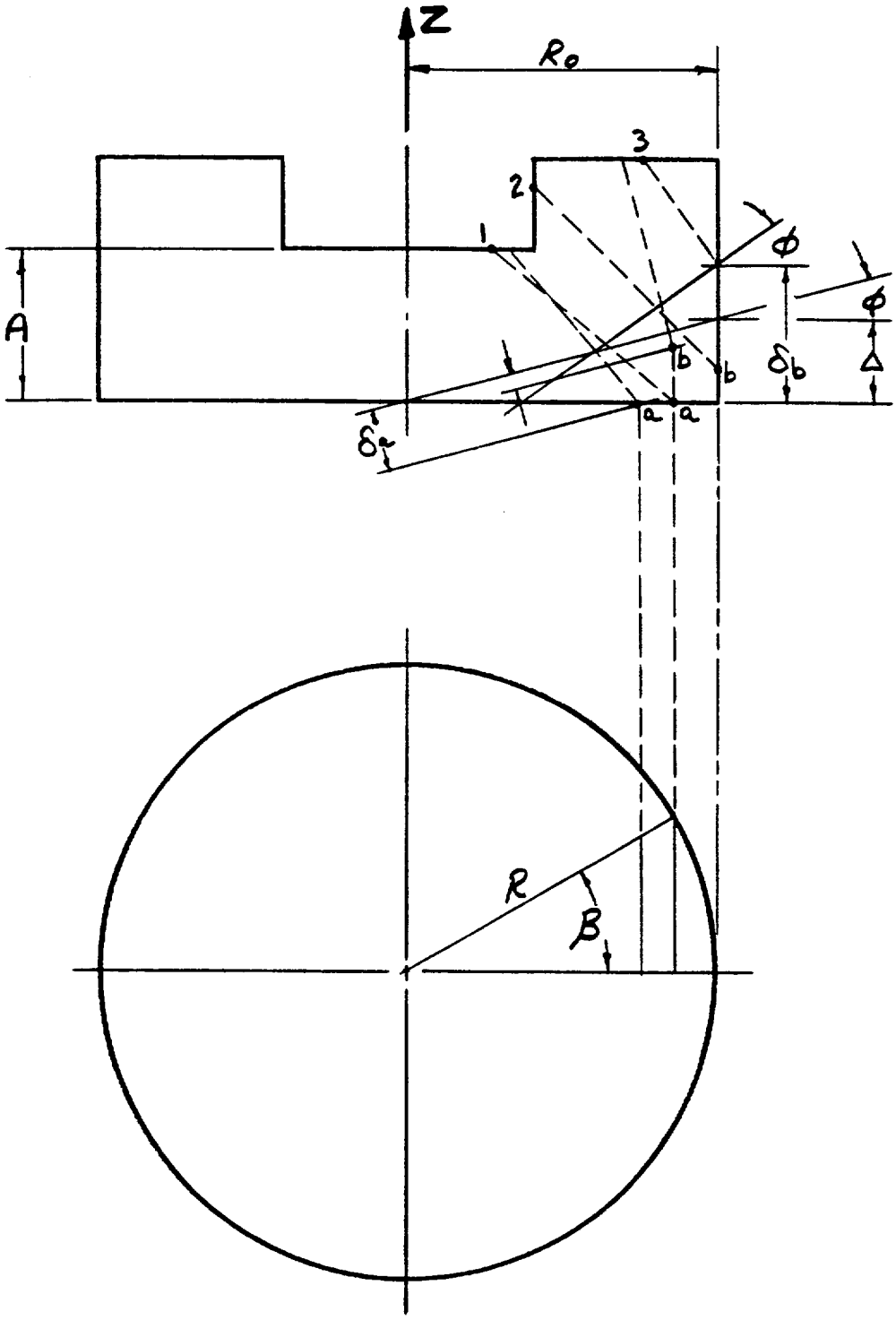

FIGURE 2.10.2-10
STRAIN COMPUTATION FOR CRUSH PATTERN II

The geometry for crush pattern II is shown on Figure 2.10.2-10. The deformation of the points on the bottom (a) and along the side (b) may be represented with the same equation:

$$\delta = \Delta \text{ COS } \phi + (R \text{ COS } \beta - R_0) \text{ SIN } \phi - Z/\text{COS } \phi \quad (17)$$

The original length of the element depends on the intersection of the projection of the point on the impact surface with the outline of the limiter. Four points are identified as shown on Figure 2.10.2-10. The lengths are:

$$\begin{aligned} q_1 &= (A-Z)/\text{COS } \phi \\ q_2 &= X/\text{SIN } \phi \\ q_3 &= (B-Z)/\text{COS } \phi \\ q_4 &= ((R_0^2 - R^2\text{SIN}^2 \beta)^{1/2} + R \text{ COS } \beta)\text{SIN } \phi \end{aligned} \quad (18)$$

Where,

$$X = R \text{ COS } \beta + (R^2\text{COS}^2 \beta - R_2 + R_1^2)^{1/2}$$

The deformation for crush pattern III is shown on Figure 2.10.2-11. Deformations of points on the bottom of the limiter are neglected for this crush pattern. The deformation is:

$$\delta = (\Delta - Z/\text{TAN } \phi - R_0(1 - \text{COS } \beta))/\text{SIN } \phi$$

The original length is measured to (R_i) so that:

$$q = (R_0 - R_i)/\text{SIN } \phi \quad (20)$$

Segment Stress

The stresses in the elements are calculated from the above strains. As mentioned above, three sets of stress-strain laws are input to the code, one for each of the regions defined in Figure 2.10.2-5.

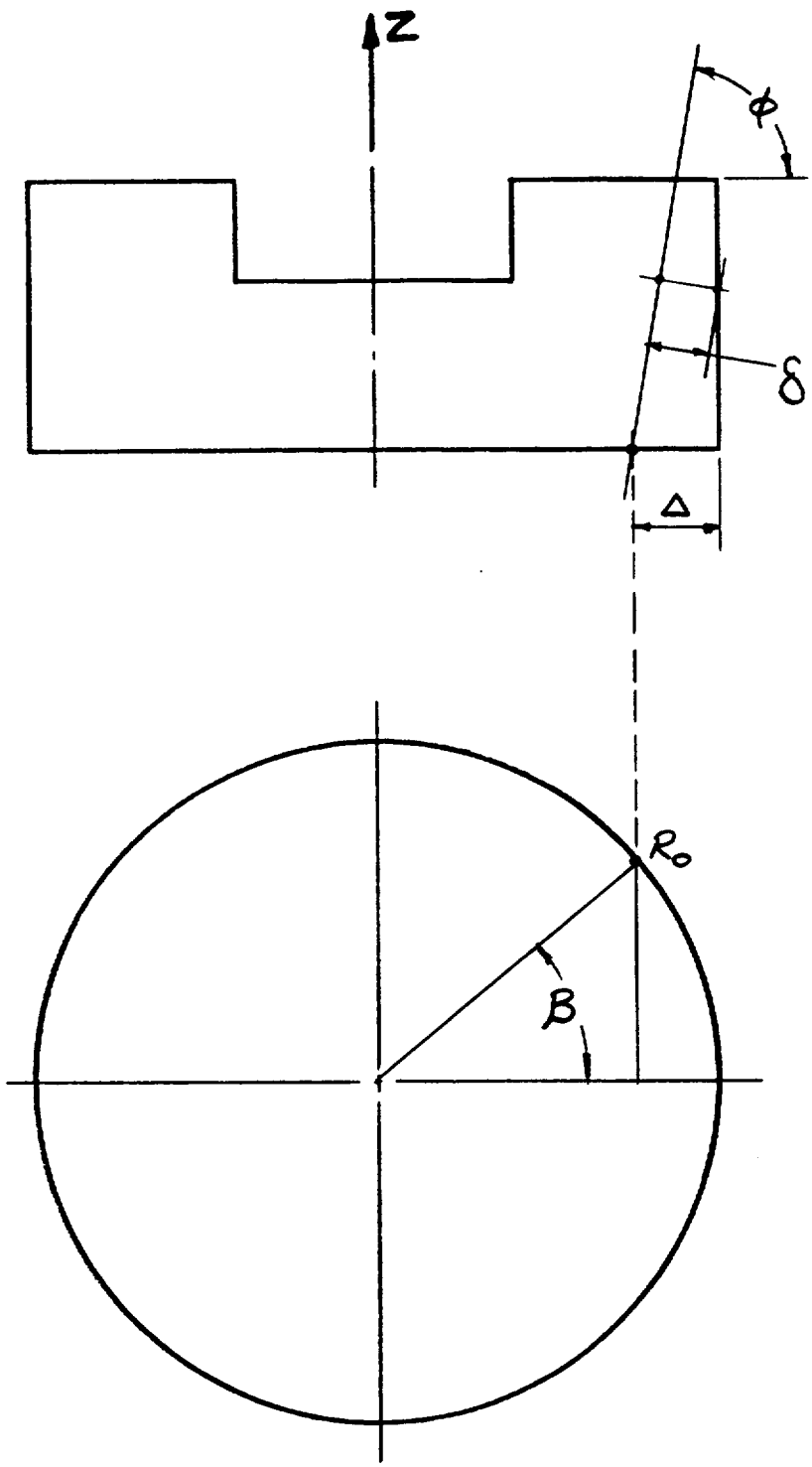

FIGURE 2.10.2-11
STRAIN COMPUTATION FOR CRUSH PATTERN III

The location of the center of the segment on the surface of the limiter is used to determine which of the three stress-strain laws is to be used. The model may be viewed as a set of one dimensional rods which run from the center of the segment, normal to the target, to another boundary of the limiter. The entire rod is given the properties which the limiter material has at the beginning point of the rod (i.e., the intersection with the target).

The stress-strain law used for the materials is shown on Figure 2.10.2-12. Each of the seven parameters shown on the figure is input to the code for each of the three regions of the limiter. The arrows on the figure indicate the load-unload paths used in the model. The step in the crush strength is built into the stress-strain law so that two crushable materials in series may be modeled. The two crush strengths should be specified as the actual crush strengths of the two materials. The first locking strain (ε_1) should be specified as the locking strain of the weaker material times the length of the weaker material divided by the total specimen length. The higher locking strain (ε_L) should be specified as the first locking strain plus the locking strain of the stronger material times its length and divided by the specimen length.

As stated above, the properties of the limiter material are not varied as the limiter crushes and the packaging rotates. Limiter materials such as wood exhibit anisotropic material properties. This must be accounted for when the properties are input to the code based on the anticipated direction of crushing. Most of the anisotropic wood data is based on tests performed in the elastic range. The following relationship has been used to represent wood properties for a loading which is applied at an angle (α) with respect to the wood grain:

$$P = (P_1 COS^4\alpha + P_2 SIN^4\ \alpha)/(COS^4\alpha + SIN^4\ \alpha) \qquad (21)$$

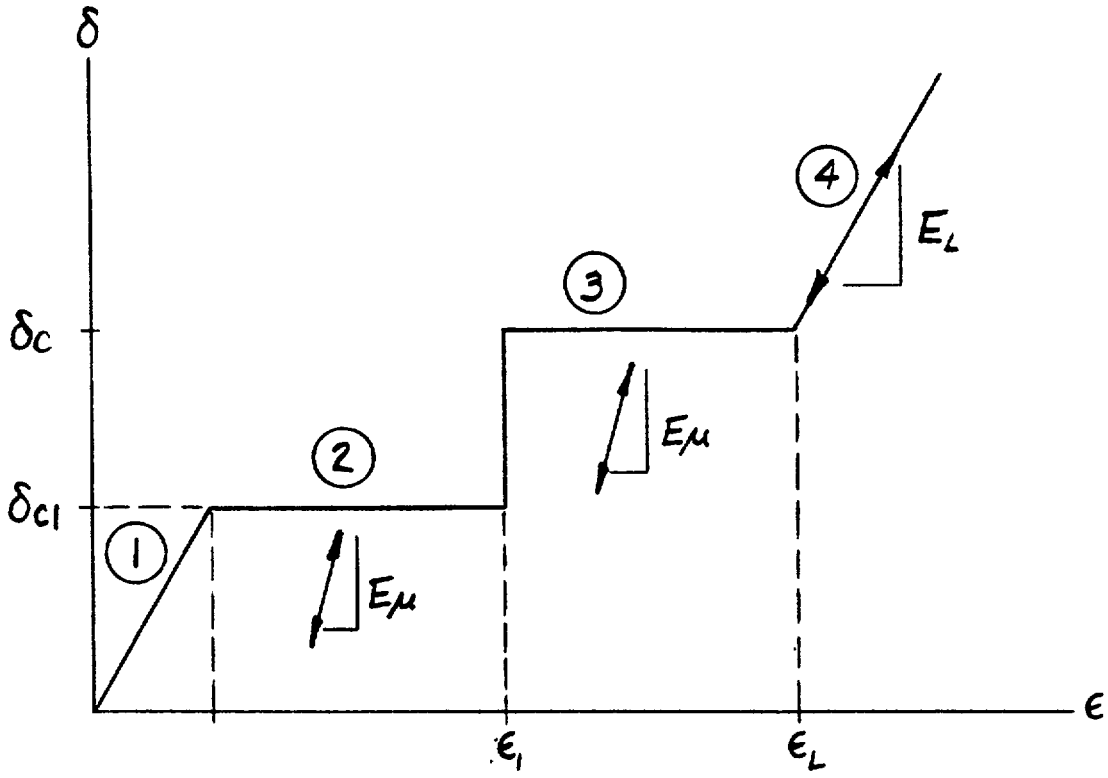

FIGURE 2.10.2-12
WOOD STRESS - STRAIN CURVE

Where,

P = property of interest at angle α

P_1, P_2 = properties parallel and perpendicular to grain

Evaluation of Forces

The stresses determined above are multiplied by the area of the segment projected onto the crush surface. The areas of the sidewall segments are (see Figure 2.10.2-8):

$$A_s = 2R_0 \, B \, COS(\theta - \rho)/(NB \, NS \, TAN \, \beta) \quad (22)$$

The area of the bottom segments is divided into two parts, one in region I and the other in region II. These areas are:

$$A_b = 4R_0 L_b SIN(\theta - \rho)/NB \quad (23)$$

Where,

$$L_b = (R_i^{\,2} - R_c^{\,2})^{1/2}; \text{ region I}$$

$$= (R_0^{\,2} - R_c^{\,2})^{1/2} - (R_i^{\,2} - R_c^{\,2})^{1/2}; \text{ region II}$$

These forces are summed for all of the elements to determine the total force acting on the packaging. The forces are also multiplied by their moment arms about the packaging CG to calculate the total moment acting on the packaging. The point on the segment is first projected, normal to the target, to evaluate whether or not it intersects the packaging body. If the projection does not intersect the packaging body, only a percentage of the force is included in the summation. The user specifies the percentage to be used.

Horizontal Force

A horizontal force develops at the limiter/target interface. This force is only considered for the bottom limiter (i.e., the first to impact) since the packaging is always close to horizontal when the top impact limiter is in contact.

The horizontal force (F_h) is first calculated as that required to restrain horizontal motion of the tip of the limiter.

The horizontal acceleration ($\ddot{\Delta}_H$) at the tip of the bottom limiter (point 2 on Figure 2.10.2-6) may be related to the CG motion of the packaging by:

$$\ddot{\Delta}_H = \ddot{x} - \ddot{\rho}[(\gamma L^* + B_1)\ \text{COS}\ \phi + R_0\ \text{SIN}\ \phi] \qquad (24)$$

Where,

$$\phi = \pi/_2 - \theta + \rho$$

Equating Δ_H to zero would result in no acceleration of the tip in the horizontal direction and provides the solution of x in terms of ρ.

Substituting this solution for x into Equation (3) results in an expression for the horizontal force (F_h), required to restrict horizontal acceleration of the tip, in terms of the rotational acceleration (ρ). Finally, equation 4 is used to eliminate (ρ) with the result,

$$F_h = \frac{M_v W[\gamma L^* + B_1)\text{COS}\phi + R_0\text{SIN}\phi]}{J_g + W[(\gamma L^* + B_1)\text{COS}\phi + R_0\text{SIN}\phi]^2} \qquad (25)$$

Where,

M_v = moment due to vertical forces = $F_{v1}x_{v1}-F_{v2}x_{v2}$
W = packaging weight

This force is restricted to:

$$F_h < \mu F_{v1} \quad (26)$$

Where,

μ = coefficient of friction specified by user

2.10.2.6 ANALYSIS FOR ONE FOOT DROP NORMAL CONDITION

This section describes the analysis of the TN-FSV for the one foot normal drop condition. The TN-FSV is lifted vertically and is transported horizontally. End and side drop orientations are therefore considered to be credible normal drop events. Any other drop orientation will cause the cask to tip over onto its side, clearly an accident. The accident analyses in Section 2.10.2.4 bound any possible tipping accident. Therefore, the one foot drop analysis is performed only for the end and side drop orientations.

The packaging kinetic energy is again assumed to be absorbed by crushing of the impact limiters. The dynamic system model of Section 2.10.2.4 was used to perform the side drop (0°) analysis using the ADOC computer program described in Section 2.10.2.5. The end drop analysis was performed assuming that the energy would be absorbed by the soft balsa wood (oriented in the weak direction) in the outer end of the limiter. This is a very accurate way to determine g loads on an end drop since the g values can be calculated by the expression F = Ma where F = crush stress times the area and M = package weight divided by the acceleration of gravity g.

The inertial load results of these one foot drop analyses are presented in Table 2.10.2-18. Again, two extreme cases are considered. The upper bound stiffness case assumes maximum wood crush strength and 20% effectiveness of non backed-up wood. The lower stiffness case assumes minimum wood strength and 20% effectiveness of non backed-up wood. The actual case will be between these upper and lower bounds. Stress analyses in Section 2.10.1 are performed for the case(s) with maximum inertia loads.

2.10.2.7 IMPACT LIMITER ATTACHMENT ANALYSIS

The impact limiter attachments are designed to keep the impact limiters attached to the cask body during all normal and hypothetical accident conditions. The loading which has the highest potential for detaching the impact limiter is the slapdown or secondary impact after a shallow angle 30 foot drop. During this impact, the crushing force on the portion of the impact limiter beyond the cask body (the non backed-up area) tends to pull the limiter away from the cask. The end and corner drops are not critical cases for the impact limiter attachments since the impact force tends to push the impact limiter onto the cask in these orientations.

For the attachment bolt analysis, maximum effectiveness of the non-backed up wood and maximum wood crush strengths of 2010 psi for balsa and 6500 psi for redwood are assumed. The maximum wood properties produce the highest overturning moment on the limiter. Based on the dynamic analysis performed using the ADOC code, the most severe slapdown impact occurs after a shallow angle oblique impact at 10° initial angle. The peak contact force at the end of the cask body subjected to secondary impact (slapdown) are maximum for this case. The peak force is 1,777,140 lb. as indicated in Table 2.10.2-3.

TABLE 2.10.2-18

MAXIMUM INERTIAL G LOAD DURING ONE FOOT DROP

	INITIAL ANGLE OF IMPACT	MAXIMUM G LOAD	
		AXIAL (ALL LOCATIONS)	TRANSVERSE (ALL LOCATIONS)
MAXIMUM WOOD CRUSH STRESS AND 20% EFFECTIVENESS OF NON-BACKED UP WOOD	90° (End Drop)	-14	0
	0° (Side Drop)	0	-17
MINIMUM WOOD CRUSH STRESS AND 20% EFFECTIVENESS OF NON-BACKED UP WOOD	90° (End Drop)	-10	0
	0° (Side Drop)	0	-13

The maximum moment applied to the impact limiter attachments is conservatively determined ignoring the mass of the impact limiter which tends to reduce the attachment forces. The center of the external impact force on the limiter is 0.59 in. from the center of the cask reaction force. Therefore, the net moment applied to the limiter by the impact force couple is $1.777 \times 10^6 \times 0.59$ or 1.048×10^6 in. lb. There is also a frictional force which acts to pull the impact limiter away from the cask. Assuming a frictional coefficient of 0.12 between the cask and limiter and between the limiter and impact surface, the magnitude of this force is

$$F_f = \mu R = (0.12)(1777 \times 10^3) = 213.24 \text{ kips}$$

The crush depth on the side is 9.8 inches. The resultant moment due to friction is

$$M_f = (213{,}240)(23.5-9.8) = 2.921 \times 10^6 \text{ in lbs.}$$

The total moment is therefore 3.969×10^6 in lbs.

These moment is reacted by the six impact limiter attachment bolts.

A free body diagram of the impact limiter is shown in Figure 2.10.2-13. It is conservatively assumed that the impact limiter pivots on the edge of the cask end. The maximum force, F, occurs in the bolt farthest from the pivot point, and the bolt force varies linearly with distance from the pivot point.

$$M_B = F_B(28.7) + \frac{2(22.1)^2}{28.7} FB + \frac{2(8.9)^2}{28.7} FB + \frac{(2.3)^2}{28.7} FB$$

$$M_B = 68.44 \, F_B$$

Therefore the maximum tensile force in an attachment bolt is

$$F_B = \frac{3.969 \times 10^6}{68.44} = 57,992 \text{ lbs.}$$

The tensile area of a 1-1/4 inch bolt is 0.969 in^2. The tensile stress in the most highly stressed bolt is therefore

$$\frac{57992}{0.969} = 59,847 \text{ psi}$$

This conservatively calculated stress is well below the minimum attachment bolt ultimate tensile strength of 140,000 psi. The factor of safety against bolt failure is 2.34. Therefore, the bolt will not yield and will hold the limiter on the cask.

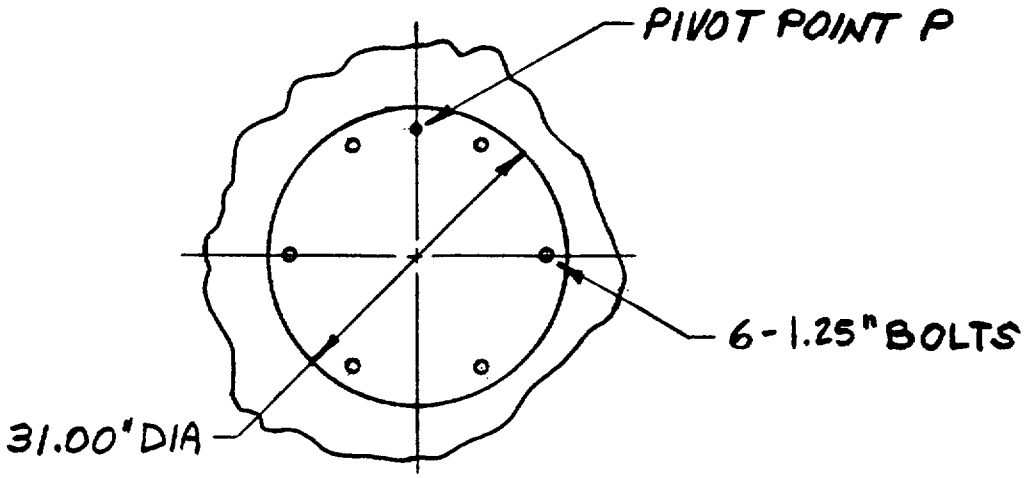

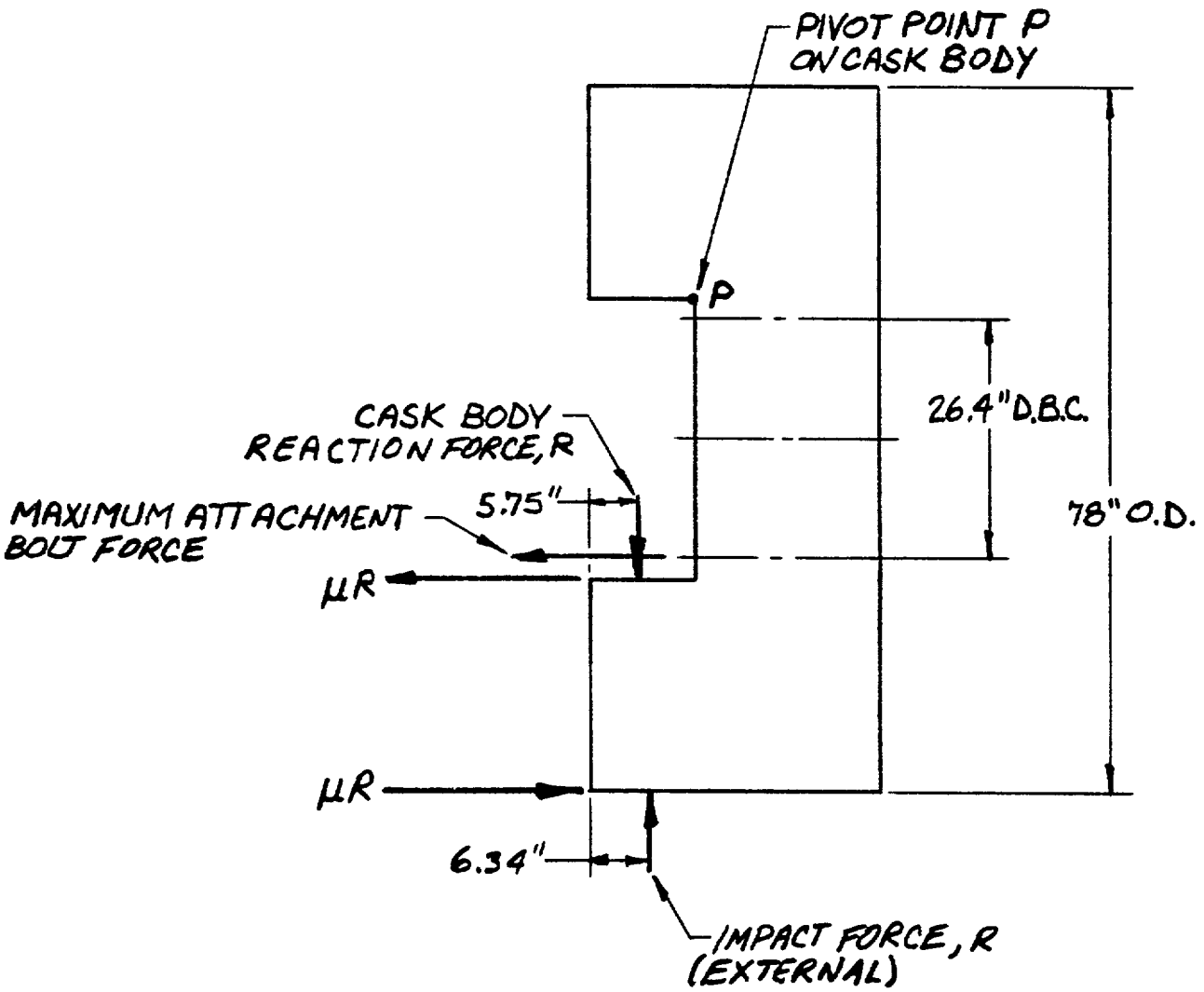

FIGURE 2.10.2-13

FREE BODY DIAGRAM OF IMPACT LIMITER FOR DETERMINING ATTACHMENT BOLT LOADS

APPENDIX 2.10.3
IMPACT LIMITER TESTING

This Appendix describes the impact limiter testing plans and test results (to be provided later).

APPENDIX 2.10.4
LIST OF FIGURES

LIST OF TABLES

APPENDIX 2.10.4
BUCKLING ANALYSIS OF INNER CONTAINMENT CYLINDER

The TN-FSV containment boundary is defined as the cask body inner shell (both cylinder and head), the closure flange and the lid outer plate. The subject of this analysis is the cylindrical portion of the inner shell. The length of this cylinder is 178.32 in., the inside diameter is 18.00 in. and the thickness is 1.125 in. The cylinder is welded to and supported by the closure flange at the lid end and to the bottom plate. The cylindrical region around the inner containment cylinder within the outer shell is filled with lead.

The inner containment cylinder is subjected to various loadings during fabrication and operation. The stresses in the cylinder have been conservatively evaluated and are shown to be acceptable in Sections 2.6 and 2.7 of this SAR. The purpose of this section is to show that the compressive stresses that may occur in the cylinder meet the selected buckling criteria.

2.10.4.1 Loadings

The inner containment cylinder is subjected to various loads during cask fabrication and operation. The first significant loading during the fabrication process is an external pressurization of the cylinder produced by the hydrostatic head of molten lead created during the pouring process. The column of molten lead is 184.76 in. long. This head causes a hydrostatic loading of 184.76 in. x .410 lb/in^3 or 76.0 psi on the cylinder. The hoop stress in the cylinder is $p \times R_o/t$ or $-76.0 \times 10.125/1.125$ which equals -684 psi. It will be shown below that this stress is well below any cylinder buckling limit.

The next significant loading on the cylinder occurs during cooldown to room temperature after freezing of the molten lead. The assembly of concentric steel-lead-steel cylinders is stress free and void free at the lead freezing temperature (620°F). This state occurs since the frozen lead has little strength at this temperature and molten lead is added continuously to fill voids that occur as the lead freezes. When the composite steel-lead-steel assembly begins to cool the lead shrinks radially against the inner steel cylinder (but away from the outer cylinder). This occurs since the thermal contraction of the lead is higher than that of the steel cylinders.

This differential contraction induced loading is minimized by cooling very slowly to permit time for the lead to creep so that residual fabrication stresses relax. The analysis of this condition is provided below.

The outer shell is not welded to the bottom of the plate until after the lead pour. Therefore, the inner and outer shell are free to contract at different rates during the cooldown process.

During Normal Conditions of Transport and Hypothetical Accident Conditions, the inner cylinder is subjected to additional loadings. When the temperature changes, thermal stresses occur primarily due to these same differential expansion effects between lead and steel rather than due to temperature differences in the cask body. As described above and in Appendix 2.10.1 the magnitudes of these stresses have been conservatively determined and evaluated in Sections 2.6 and 2.7 and are shown to be acceptable. However, temperature changes in the insulated cask body require appreciable time allowing lead creep and relaxation effects to occur. The analysis below includes these inelastic effects for the strain controlled differential expansion induced loadings.

Additional loadings applied to the cylinder during Normal Transport Conditions and Hypothetical Accident Conditions include those due to pressure differences applied to the cask wall and inertial loadings from the cargo or contents and the lead shielding. The analysis below conservatively uses as input the combined membrane stress components from Sections 2.6 and 2.7. These stresses include those caused by lead motion relative to the steel shells during end impact.

2.10.4.2 Analysis

a) Fabrication

The inner containment cylinder is subjected to a relatively mild hoop compressive stress during the lead pouring operation due to the hydrostatic head in the liquid lead of 76.0 psi. The hoop stress in the cylinder at that time is -684 psi.

During cooldown from the lead freezing temperature of 620°F to room temperature the lead shrinks radially more than the inner containment cylinder. The differential expansion is equal to:

$$\Delta R_{Lead-Steel} = R\ \Delta\alpha\ \Delta T$$

$$\Delta R = (10.125\text{ in})(17.88-9.53)10^{-6}{}^{\circ}F^{-1}(620-70)^{\circ}F$$

$$\Delta R = .0465\text{ in.}$$

Therefore the lead cylinder, if it were free, would shrink .0465 in. more radially than the inner containment cylinder. If all of this differential contraction is accommodated in the lead, the lead strain equals:

$$\varepsilon_{lead} = \frac{\Delta R}{R} = \frac{.0465\text{ in.}}{10.125\text{ in.}} = .00459\text{ in/in.}$$

This is .459% strain in the lead. If the lead remained a linear elastic material, the residual stress in the lead would be equal to:

$$\sigma_{lead} = E_{lead} \times \varepsilon_{lead}$$

$$= (2 \times 10^6 \text{ psi})\ (.00459) = 9180 \text{ psi}$$

If the lead cylinder remained elastic at this stress level, significant loads with corresponding high stresses and strains would be applied to the inner containment cylinder. However, the lead is actually quite soft, and the stress level in the lead remains low because of its inelastic behavior. Figure 2.10.4-1 shows typical short time low strain rate lead stress vs strain curves for various temperatures obtained by *Tietz. Note that the lead stress corresponding to .46% strain is on the order of 450 psi for essentially pure lead, even for very rapid straining (curve A strain rate produces .46% strain in about 6 seconds).

Additional insight to the possible magnitude of lead stresses for slow loading rates can be obtained from the stress relaxation and creep data (also by *Tietz) in Figures 2.10.4-2 and 3. From Figure 2.10.4-2 it can be seen that .5% strain rapidly applied at 100°F produces a stress of about 500 psi which relaxes to 300 psi in 100 hrs., 290 psi in 168 hrs. (1 week), and continues to relax with time. Also note that Figure 2.10.4-3 indicates that a constant stress of 280 psi in the lead would produce a strain of .5% in about 200 hrs. at 100°F.

*T.E. Tietz, "Mechanical Properties of a High Purity Lead and a 0.058 Percent Copper-Lead Alloy ...", Presented at the Sixty Second Annual Meeting of the Society, June 1959, ASTM 59, 1052.

These data indicate that the lead stress will not exceed about 300 psi if the cooldown is accomplished slowly (about 1 week). The interface pressure between the lead cylinder and inner containment cylinder required to exert an average hoop stress in the lead of 300 psi can be readily determined:

$$p_{interface} = \frac{\sigma_{lead} \times t_{lead}}{R_{interface}}$$

$$= \frac{300 \text{ psi} \times 3.44 \text{ in}}{10.125 \text{ in.}} = 101.9 \text{ psi}$$

The hoop stress in the inner containment cylinder is then:

$$\sigma_{\theta \text{ inner cyl}} = \frac{p_{interface} \times R_{interface}}{t_{cyl}}$$

$$= \frac{-101.9 \text{ psi} \times 10.125 \text{ in}}{1.125 \text{ in.}} = -917 \text{ psi}$$

If the cooldown occurred quite rapidly, a conservative upper bound stress in the lead would be 500 psi based on the lead data described above. At this value of lead stress the inner containment cylinder hoop stress could reach -917 x 500/300 or -1528 psi. If this sudden cooldown occurred, the cylinder stress would decrease as the lead stress relaxed, dropping below -1528 psi in about a week and becoming negligible with increasing time.

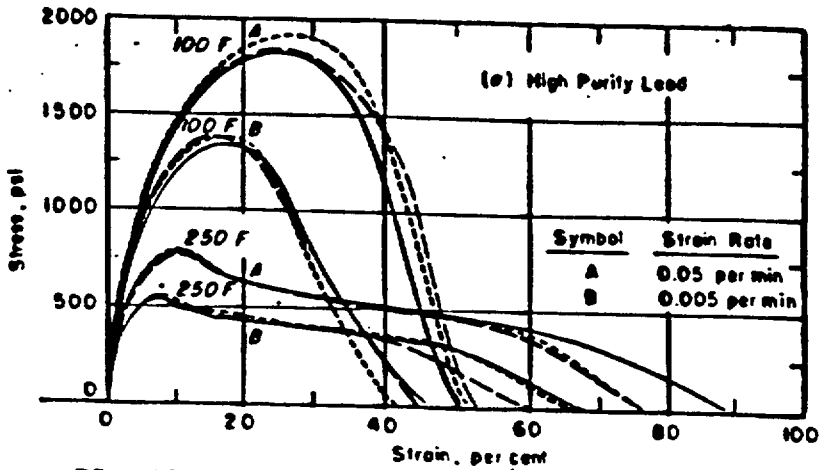

—Effect of Strain Rate on the Tensile Stress-Strain Curves at 100 and 250 F.

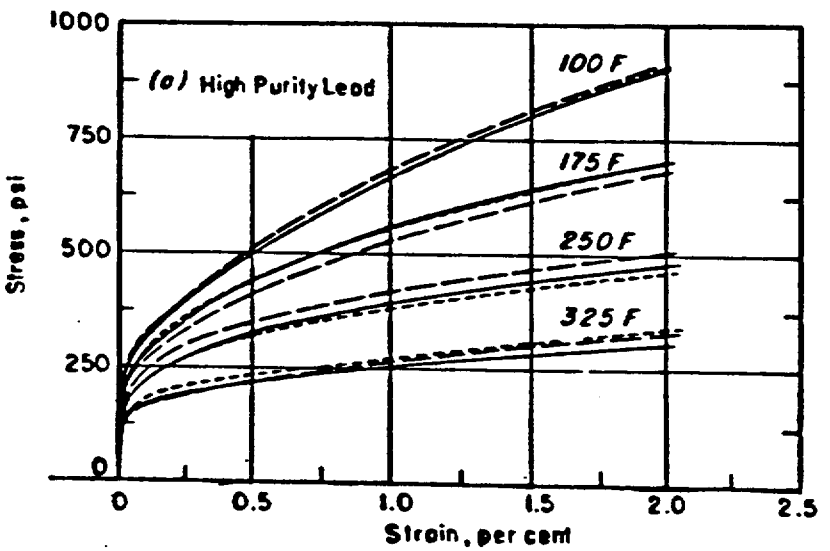

—Tensile Stress-Strain Curves to 2 per cent Strain at a Strain Rate of 0.005 per min.

FIGURE 2.10.4-1

TYPICAL STRESS VS STRAIN CURVE FOR PURE LEAD

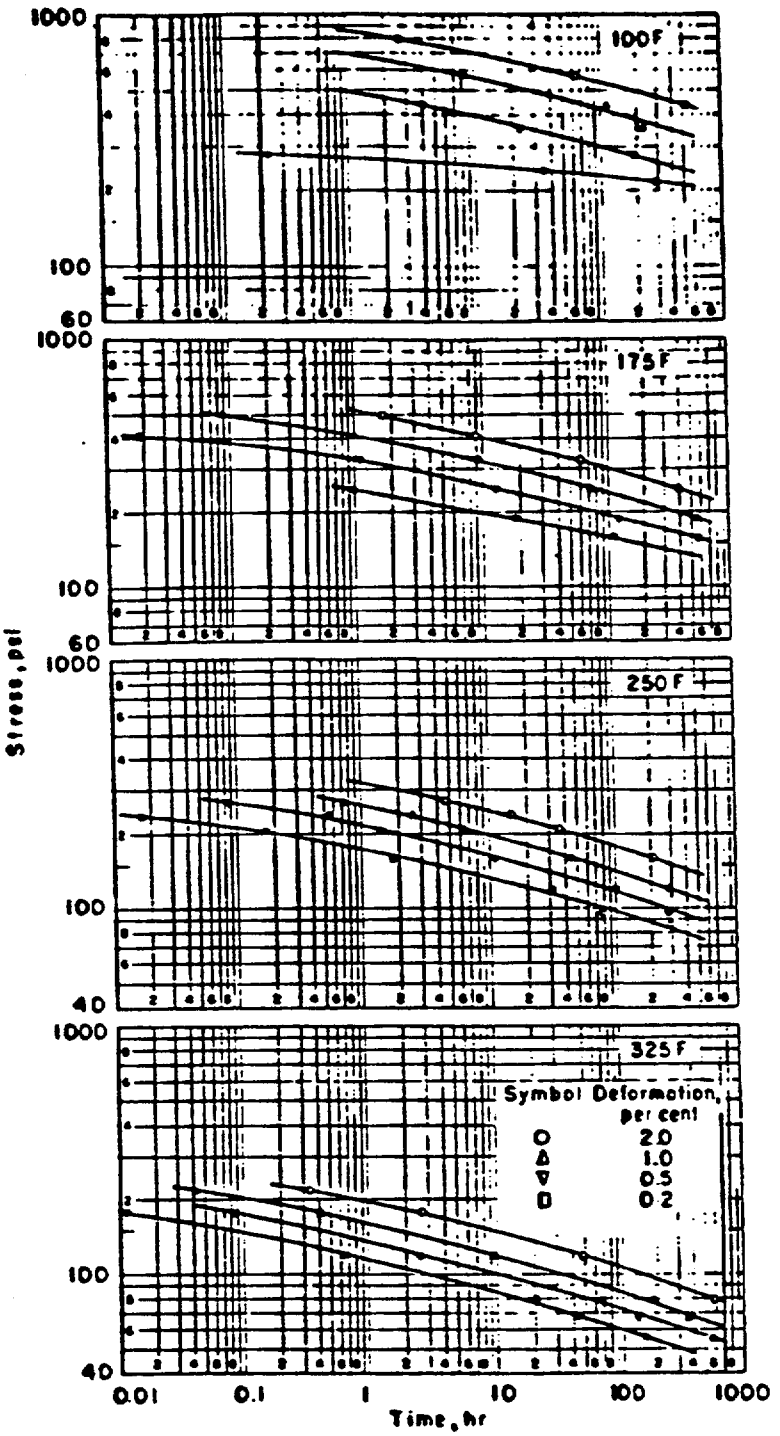

Stress *versus* Creep Time at Constant Strain Values of 0.2, 0.5, 1.0, and 2.0 per cent for High-Purity Lead.

FIGURE 2.10.4-2

STRESS RELAXATION VS TIME AT CONSTANT STRAIN VALUES OF 0.2, 0.5, 1.0 and 2.0% FOR PURE LEAD

TIETZ ON PROPERTIES OF LEAD AT ELEVATED TEMPERATURES

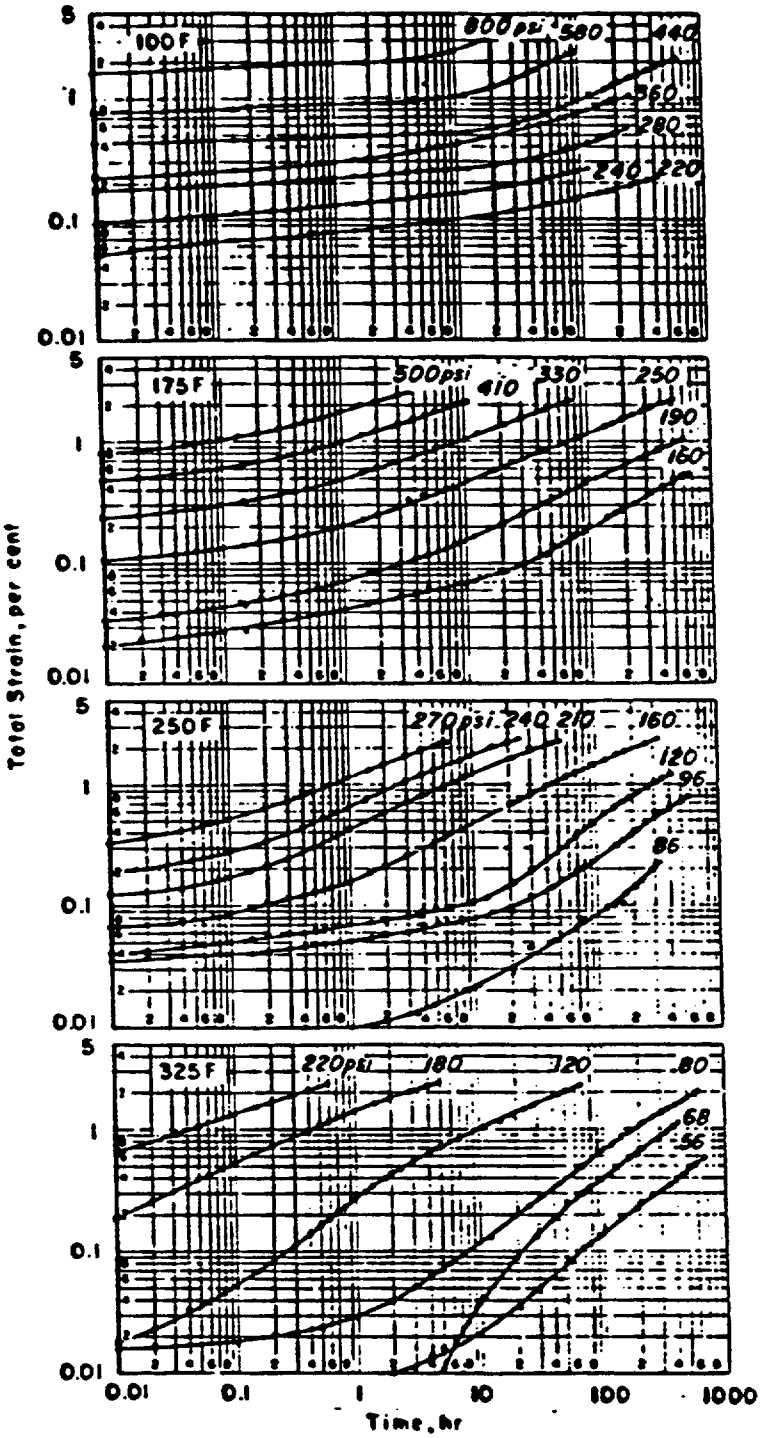

—Total Strain *versus* Creep Time for High-Purity Lead.

FIGURE 2.10.4-3

TOTAL STRAIN VS CREEP TIME FOR PURE LEAD

b) Normal Conditions of Transport

As described above, the annulus between the inner containment cylinder and outer shell is filled with lead that has frozen in the annulus, completely filling it at a temperature of about 620°F. The lead contracts more than the volume of the annulus decreases during cooldown after the lead pour. Finally, lead creep occurs with time under stress so that the lead cylinder exerts only negligible residual loading on the inner containment cylinder in the "as fabricated" condition.

When the cask body assembly temperature increases to the 160-170°F range expected during the hot environment condition, the lead cylinder expands away from the inner containment cylinder, but its volume increase will not fill the annulus between the shells. Therefore differential expansion induced loadings of the inner cylinder only occur for cases where the temperature is below room temperature.

If the cask body assembly is subjected to the -40°F cold environment, the lead cylinder will shrink radially more than the inner containment cylinder. The differential expansion is equal to:

$$\Delta R_{\text{Lead-Steel}} = R\ \Delta\alpha\ \Delta T$$

$$\Delta R = (10.125\text{ in})\ (15.55\text{-}8.55)\ \text{x}\ 10^{-6}\ °F^{-1}\ (70\text{+}40)°F$$

$$= .0078\text{ in.}$$

Therefore the lead cylinder, if it were free, would shrink .0078 in. more radially than the inner containment cylinder. If the differential contraction is accommodated in the lead, the lead strain would equal:

$$\varepsilon_{\text{lead}} = \frac{\Delta R}{R} = \frac{.0078\text{ in}}{10.125\text{ in.}} = .00077\text{ in/in}$$

This is a strain of .077%. If the lead remained a linear elastic material the residual stress in the lead would be on the order of ($2x10^6$) (.00077) or 1540 psi, and the hoop stress in the inner containment cylinder would be approximately -4,710 psi. Figure 2.10.4-1 shows that the lead stress will not exceed 300 psi at a strain level of .077%, even if the strain is rapidly applied.

The lead cools down to -40°F. Extrapolating slightly from the creep and relaxation data in Figures 2.10.4-2 and 2.10.4-3, and assuming it takes only six hours to cool, the lead cannot have a stress above about 500 psi for a strain of .077%. Therefore the actual hoop stress in the inner containment cylinder due to differential contraction (thermal stress) during the first cooldown will not exceed -917 x 500/300 or -1528 psi, and even this stress will relax with time.

The worst loading for buckling of the inner containment shell under normal conditions is the one foot end drop under cold conditions. (Table 2.6-8).

The maximum hoop compressive stress in the inner containment cylinder (locations 4 through 8) under the one foot drop is -5060 psi. This stress occurs at location 8. The maximum meridional membrane stress in the inner containment cylinder is -2,177 psi. This stress also occurs at location 8 under cold conditions.

c) Hypothetical Accident Conditions

Again, as described under Normal Conditions of Transport, the differential expansion induced stress (thermal stress) in the inner containment cylinder is small and, since the lead creeps during the slow cooldown, this stress decays away with time. The hoop and meridional compressive stresses in the inner containment cylinder during the hypothetical accident cases are obtained from the combined load tables of Chapter 2, Section 2.7. The worst cases for buckling are the 30 foot end drops and corner drops. The maximum

hoop compressive stress in the inner containment cylinder (locations 4 through 8) is -19578 x 1.04 or -20361 psi, which occurs at location 4 during the 30 foot corner through c.g. drop under cold conditions on the side opposite contact (Table 2.7-12). The maximum compressive meridional stress is -10428 x 1.04 or -10845 psi which also occurs at location 4 during the 30 foot corner drop under cold conditions on the side opposite contact. (Table 2.7-12). The stresses reported in Chapter 2 are based on a packaging weight of 47,000 lbs. As noted in Section 2.2, the stresses in Tables 2.7-9 through 2.7-12 should be multiplied by a factor of 1.04 to account for fabrication tolerances. This factor is included in this analysis.

Evaluation of Results

The above compressive stresses in the inner containment cylinder are acceptable based on the criteria presented in the ASME B&PV Code Case N-284 titled "Metal Containment Shell Buckling Design Methods." The evaluation is presented below:

a) Factors of Safety, Paragraph 1400:
A Factor of Safety of 2.0 is used for Fabrication and Normal Conditions of Transport. A Factor of Safety of 1.34 is used for Hypothetical Accident Conditions.

b) Capacity Reduction Factors, Paragraph 1511(a) and (b):

$R/t = 10.125/1.125$ in. $= 9$

$M_{\phi} = L/\sqrt{Rt} = 178.32/\sqrt{10.125 \times 1.125} = 52.8$

Using Figures 1511-1 and 1511-2, $\alpha_{\theta L} = 0.8$ and $\alpha_{\phi L} = 0.32$

It should be noted that these parameters are insensitive to the geometry and they will not increase with changes in R, t and L that are within a factor of 2.

c) Plasticity Reduction Factors, Paragraph -1600:
The highest individual values of hoop compression, σ_θ, during Fabrication, Normal Conditions of Transport and Hypothetical Accident Conditions listed above are 1528 psi, 5060 psi, and 20361 psi, respectively. The corresponding values of σ_ϕ x FS/σ_y for these stresses (with FS = 2 and 1.34; σ_y = 30000 psi) are 0.102, .337 and .910. The plasticity reduction factors in the hoop direction, η_θ, is 1.0 for the normal case and 0.446 for the accident case.

The highest individual values of axial compression, σ_ϕ, during Normal Conditions of Transport and Hypothetical Accident Conditions are 2177 psi and 10,845 psi. The corresponding values of σ_ϕ x FS/σ_y are .145 and 0.484. The applicable plasticity reduction factor in the axial direction is 1.0 for both the normal case and for the accident case.

d) Amplified Stress Components (Elastic and Plastic):
Next, the amplified stress components are calculated. The elastic amplified stresses are determined as:

$$\sigma_{is} = \sigma_i \times FS/\alpha_i$$

Then the plastic amplified stresses are determined:

$$\sigma_{ip} = \sigma_{is}/\eta_i$$

The results of these computations using the highest individual stress components are provided in Table 2.10.4-1.

e) Theoretical Buckling Values, Paragraph 1712:

In order to complete the analysis, it is necessary to determine $\sigma_{\phi el}$ and $\sigma_{\theta el}$ (both σ_{rel} and σ_{hel}). C_ϕ is 0.605 since M_ϕ is 52.8.

$$C_{\theta r} = 0.275\left(\frac{t}{r}\right) + \frac{2.1}{M_\phi^4}\left(\frac{R}{t}\right)^{3.0} \quad \text{since } M_\phi > 1.65\left(\frac{R}{t}\right)$$

$$C_{\theta r} = 0.0305$$

Then $\sigma_{\phi eL} = C_\phi \, Et/R$ and $\sigma_{\theta eL} = C_{\theta r} \, Et/R$.

Substituting numbers in these formulas:

$$\sigma_{\phi eL} = 0.605 \times 28.3 \times 10^6 \times 1.125/10.125 = 1.9 \times 10^6 \text{ psi}$$

$$\sigma_{\theta el} = \sigma_{rel} = \sigma_{hel} = 0.0305 \times 28.3 \times 10^6 \times 1.125/10.125$$

$$= 95{,}905 \text{ psi}$$

These theoretical buckling stresses are well above both the plastic and elastic amplified stress components in Table 2.10.4-1. Therefore, the individual stress components meet the limits of Code Case N-284.

f) Interaction Equations, Paragraph 1713:

Code Case N-284, paragraph 1713.2, states that it is conservative to ignore interaction of the meridional and hoop compression when buckling is inelastic. Therefore the elastic interaction equation 1713.1.1(b) is used ($\sigma_{\phi s} \geq 0.5\sigma_{\theta s}$):

$$\frac{\sigma_{\phi s} - 0.5\,\sigma_{heL}}{\sigma_{\phi eL} - 0.5\,\sigma_{heL}} + \left(\frac{\sigma_{\theta s}}{\sigma_{\theta heL}}\right)^2 \leq 1.0$$

The amplified elastic stresses in Table 2.10.4-1 are maxima and do not occur at the same location. It is conservative to evaluate the interaction of these maxima since all other combinations will have a lower interaction total.

During fabrication, no interaction check is required since

$\sigma_{\theta s} = 3820 < \sigma_{hel} = 95905$ (Ref. N284, paragraph 1713.1.1(a)).

During normal conditions of transport, no interaction check is required since $\sigma_{\phi s} = 13605$ psi $> 0.5\ \sigma_{\theta s} = 0.5\ (12650) = 6325$ psi and $\sigma_{\phi s} = 13605$ psi $< 0.5\ \sigma_{hel} = 47952$ psi. (See N284, paragraph 1713.1.1(b)).

During hypothetical accident conditions, no interaction check is required since $\sigma_{\phi s} = 45413$ psi $> 0.5\ \sigma_{\theta s} = 0.5\ (34105) = 17053$ psi and $\sigma_{\phi s} = 45413$ psi $< 0.5\ \sigma_{hel} = 47952$ psi (Reference N284, paragraph 1713.1.1(b)).

Conclusions

Therefore the compressive stresses in the inner containment cylinder during fabrication and operation are acceptable based on the buckling requirements of Code Case N-284.

Table 2.10.4-1

INNER CONTAINMENT CYLINDER AMPLIFIED STRESS COMPONENTS

	Stress Component	
	Hoop (θ) (psi)	Meridional (ϕ) (psi)
Fabrication		
($\alpha_{\theta L}$=0.8, $\alpha_{\phi L}$=0.32, FS=2.0)		
Calculated Stress (σ_θ, σ_ϕ)	1528	---
Amplified Stress (Elastic)	3820	---
Plasticity Reduction Factor	1.0	---
Amplified Stress (Plastic)	3820	---
Normal Conditions of Transport		
(α_i as above, FS = 2.0)		
Calculated Stress (σ_θ, σ_ϕ)	5,060	2,177
Amplified Stress (Elastic)	12,650	13,606
Plasticity Reduction Factor	1.0	1.0
Amplified Stress (Plastic)	12,650	13,606
Hypothetical Accident Conditions		
(α_i as above, FS = 1.34)		
Calculated Stress (σ_θ, σ_ϕ)	20,361	10,845
Amplified Stress (Elastic)	34,105	45,413
Plasticity Reduction Factor	0.446	1.0
Amplified Stress (Plastic)	76,469	45,413
Limits on Above Amplified Stress	95,905	1.9×10^6